

The 8th International Conference on Magneto-Science Conference Manual

High Magnetic Field Laboratory, Hefei Institutes of Physical Science, Chinese Academy of Sciences Key Laboratory of High Magnetic Field and Ion Beam Physical Biology, Chinese Academy of Sciences School of Physics and Materials Science, Anhui University

Key Laboratory for Space Bioscience and Biotechnology, School of Life Sciences, Northwestern Polytechnical University

Oct 11-14, 2019 Hefei, China

The Conference Committees

Local Organizing Committee

Chairs: Guangli Kuang & Xin Zhang

Vice Chairs: Peng Shang, Ning Gu, Zhigao Sheng, Dachuan Yin, Yi Lv

Local Scientific Committee

Youwei Du, Yuheng Zhang, Baogen Shen, Bingjun Gao, Yuping Sun, Mingliang Tian, Junfeng Wang, Lijun Wu, An Xu

International Organizing Committee

Eric Beaugnon (Grenoble, France)—Chair

Andreas Bund (Dresden, Germany)

Richard J. A. Hill (Nottingham, UK)

Tsunehisa Kimura (Kyoto, Japan)

Zhongming Ren (Shanghai, China)

Peng Shang (Xi'an, China)

James M. Valles, Jr. (Providence, USA)

Noriyuki Hirota (Tsukuba, Japan)—Vice Chair

Peter C. M. Christianen (Nijmegen, Netherlands)

Peter J. Hore (Oxford, UK)

Sumio Ozeki (Matsumoto, Japan)

Justin Schwartz (PSU, USA)

Dmitri V. Stass (Novosibirsk, Russia)

The Conference Topics

The International Conference on Magneto-Science 2019 (ICMS 2019) will be held on October 11-14, 2019, Hefei, Anhui province, China. The first conference on Magneto-Science was held in 2005 (Yokohama). The success at Yokohama was followed by conferences at Hiroshima in 2007 (Japan), Nijimegen in 2009 (Netherlands), Shanghai and Xi'an in 2011 (China), Bordeaux in 2013 (France), Matsumoto in 2015 (Japan) and Reims in 2017 (France). ICMS 2019 will cover magnetic field effects on materials and processes in physics, chemistry, biology and health science. Topics include:

- · Magnetic processing of materials
- · Magnetic control of structures, properties, and functions
- · Biological effects of magnetic fields
- · Magnetic surgery
- · Magnetic nanoparticles
- · Chemical reactions and processes under magnetic fields
- · Analytical aspect of magnetic fields
- · Magnetic separation science and technology
- · Interactions between water systems and magnetic fields
- · Colloids and interface science under magnetic fields
- · Magnetic levitation and microgravity
- · Generation and application of various magnetic fields
- · Others relating to magnetics and magnetic fields





第八届国际磁科学会议

The 8th International Conference on Magneto-Science (ICMS2019)

强磁场条件下的科学研究涉及物理学、化学、材料科学、地球科学、生命科学与医学等众多学科。国际磁科学会议(ICMS, International Conference of Magneto-science)是国际上关于磁场下的材料和生命科学研究最有影响力的国际会议之一,吸引了全世界众多专家学者参与。该会议从 2005 年起首先在日本横滨举办,之后每两年一届定期召开,先后由日本、荷兰和法国稳态强磁场中心等单位承办。

我国稳态强磁场大科学装置于 2017 年正式通过国家验收后,取得了 2019 年第八届国际磁科学会议的举办权。这也是我国稳态强磁场中心建成后首次承办的国际磁科学会议,有助于国际学者了解我国磁科学领域的最新技术和研究进展,搭建起强磁场下多学科前沿科学研究和学术交流的国际化桥梁,并促进和提升我国磁科学领域的学科发展和核心竞争力。

本次会议主要包括磁场下的物理、材料、生命科学与医学等。参加会议的国际学者来自 美国、德国、荷兰、日本、法国、韩国、捷克、波兰等十几个国家;国内学者来自中科院多 个研究所、北京大学、西北工业大学、东南大学、浙江大学、同济大学、华中科技大学等多 家单位。本次会议由中国科学院合肥物质科学研究院强磁场科学中心、中国科学院强磁场与 离子束物理生物学重点实验室和西北工业大学生命学院空间生物实验模拟技术国防重点学科 实验室主办,安徽大学物理与材料科学学院协办,得到了中科院国际合作局国际会议资助, 和也健康科技、上海渊兮医疗科技、西安聚能超导磁体科技有限公司和北京原力辰超导技术 有限公司等多家企业的赞助。

会议网站: www.icms2019hf.org

日期: 10月11-14日

地点: 合肥皇冠假日酒店 & 中科院合肥物质科学研究院(科学岛)

组委会主席: 匡光力、张欣

组委会副主席:商澎、顾宁、盛志高、尹大川、吕毅

学术委员会:都有为、张裕恒、沈保根、高秉钧、孙玉平、田明亮、王俊峰、吴李君、许安

会议协议酒店: 合肥皇冠假日酒店&合肥贝斯特韦斯特精品酒店

会议秘书: 李志元、黄肖敏、纪新苗、吕悦

会议日程安排:

10月11日	9: 00AM - 10: 00PM	报到	合肥贝斯特韦斯特精品酒店
10月12日	8: 30AM - 6: 00PM	大会报告	合肥皇冠假日酒店翠海厅
10月13日	9: 00AM - 6: 00PM	分会场报告	合肥科学岛,交叉科研楼
10月14日	9: 00AM - 11: 45AM	中文报告	合肥科学岛,交叉科研楼

Routes

Hefei Xinqiao International Airport — Hefei Best Western Premier Hotel and Crowne Plaza Hotel



Taxi: about 40 min, ~70-80 RMB Bus Route#4: 1.5 hours, 25 RMB

Hefeinan Railway Station — Hefei Best Western Premier Hotel and Crowne Plaza Hotel



Taxi: about 25 min, ~30-40 RMB Bus Route#156: 1.5 hours, 2 RMB

Hefei Railway Station — > Hefei Best Western Premier Hotel and Crowne Plaza Hotel



Taxi: about 30 min, ~30-40 RMB Bus Route#10: 1.5 hours, 2 RMB

Hefei Best Western Premier Hotal and Crowne Plaza Hotal ----- Science Island



Taxi: about 20 min, ~25-35 RMB

Bus Route#156 - #903: 1.5 hours, 4 RMB

The 8th International Conference on Magneto-Science

The Conference Program

Date	Activity	Location
Oct 11 th	9 AM-10 PM, Registration	Best Western Premier Hotel Lobby (Building E, 598 Huangshan Road)
Oct 12 th	Plenary talks	Crowne Plaza Hefei, 1st floor, Cuihai Hall (Building A, 598 Huangshan Road)
Oct 13 th	Parallel sessions	Science Island (Interdisciplinary Research Building, 350 Shushanhu Road)
Oct 14 th	9AM-12 AM, Chinese sessions	Science Island (Interdisciplinary Research Building, 350 Shushanhu Road)

ICMS2019 Staff Contact List				
Name Cell Phone(+86) Duties				
Xiaomin Huang	15855131147	Accommodation		
Zhiyuan Li	18919699703	Coordination/Exhibit		
Xinmiao Ji	15255131756	Registration and receipt		
Yue Lv	18298265313	Volunteers contact person		
Qingping Tao	18356518353	Front deals and Transportation		
杨星星	18110956464	Front desk and Transportation		
Biao Yu	18019944646	Posters		
Xin Zhang	18656012500	Emergency		

High Magnetic Field Laboratory, Chinese Academy of Sciences

Hefei, China October 2019

October 11, 2019

Registration/Sign in

Hefei Best Western Premier Hotel Lobby

(注册/签到处: 贝斯特韦斯特一楼大厅)

Note: On-site registration and sign in information:

9AM-10PM on Oct 11th, Hefei Best Western Premier Hotel Lobby 8AM-6PM on Oct 12th, Hefei Crowne Plaza hotel, Cuihai Hall.

9AM-5PM on Oct 13th, Hefei Science Island (Hefei Institutes of Physical Sciences, Chinese Academy of Sciences), Interdisciplinary Research Building.

Banquet

By invitation or banquet ticket purchase only

Time: Oct 11th 6:15-8:30 PM

Location: Xueji mountain villa (Xueji Shanzhuang, 雪霁山庄),

Hefei Shushan District, Yulan Avenue #8.

Transportation is provided between Best Western/Crowne Plaza Hotel and Xueji mountain villa. Bus will take off from the hotel at **5 PM.** Please follow the volunteers with blue vest for instructions.

If you have any questions, please contact: Qingping Tao (18356518353) or Yue Lv (18298265313).

	Oct	12 th , Plenary talks. C	uihai Hall, Crowne Plaza Hotel	
Chair	Name	Institute	Торіс	Time
	Guangli Kuang	High Magnetic Field Laboratory, CAS, China	Welcome and Introduction to Chinese High Magnetic Field Laboratory	8:30-8:45AM
Mingliang	Xianhui Chen	University of Science and Technology of China, China Technology of China, China Technology of China, China Phase Diagram and Evolution of Magnetic Ordering State Driven by Field Effect Transistor in (Li,Fe)OHFeSe/S Thin Flakes		8:45-9:10AM
Tian	Alois Loidl	University of Augsburg, Germany	Quantum Magnetism (Kitaev Spin Liquids, Bethe Strings)	9:10-9:35AM
	Jiangfeng Du	University of Science and Technology of China, China	Harnessing the Power of Quantum Systems Based on Single-spin Magnetic Resonance	9:35-10:00AM
		Coffee Brea	k and Group Photo	
	Theo Rasing	Radboud University, Netherlands	All-Optical Control of Magnetism: From Fundamentals to Nanoscale Engineering	10:30-10:55AM
Ning Gu	Shojiro Takeyama	University of Tokyo, Japan	Exploding Magnetic Fields up to 1200 T under Control and Its Possible Applications	10:55-11:20AM
	Atsuko Kobayashi	Tokyo Tech, Japan	Interactions Between Water Systems and Magnetic Fields: Magnetite Controls Ice Nucleation	11:20-11:45AM
			Lunch	
	Yi Lv	The First Affiliated Hospital of Xi'an Jiaotong University, China	Magnetic Surgery	1:30-1:55PM
Xin Zhang	James Lin	University of Illinois at Chicago, USA	Power Deposition and Safety Considerations for Human Subjects in High-Field Magnetic Resonance Image Scanning Systems	1:55-2:20PM
	James Valles	Brown University, USA	Learning About Life with Intense Magnetic Fields	2:20-2:45PM
	Vitalii Zablotskii	Czech Academy of Sciences, Czech	Biological Effects of High-Gradient Magnetic Fields	2:45-3:10PM
		Co	ffee Break	
	Yongxin Pan	Institute of Geology and Geophysics, CAS, China	Magnetosome, Magnetoferritin and Their Potential Applications	3:30-3:55PM
Junfeng Wang	Peter Hore	University of Oxford, UK	Chemical Magnetoreception: Navigation Using Cryptochrome Photoreceptors	3:55-4:20PM
Jameny Wally	Joseph Kirschvink	California Institute of Technology, USA	Human Magnetoreception: Tests of Magnetite- based Magnetoreception	4:20-4:55PM
	Can Xie	Peking University, China	MagR, a Putative Magnetoreceptor Protein Binds Cryptochrome	4:55-5:20PM
		Po	ster Time	
	R	eception dinner at Cro	owne Plaza Hotel	6:30-8:30 PM

Chair	Name	Institute	Торіс	Time
	Eric Beaugnon	Univ. Grenoble Alpes, France	Magnetic Field Effect on Water Wetting	9:00-9:25AM
Noriyuki Hirota	Xuegeng Yang	Institute of Fluid Dynamics, Helmholtz-Zentrum Dresden-Rossendorf, Germany	Effects of Magnetic Field on Hydrogen Bubble Detachment during Water Electrolysis	9:25-9:45AM
	Yasuhiro Ikezoe	Nippon Institute of Technology, Department of Applied Chemistry, Japan	The Easiest Way to Levitate Water by Magnetic Field	9:45-10:05AM
		Co	ffee Break	
	Jinlin Han	National Astronomical Obseratories, CAS, China	Cosmic Magnetic Fields	10:30-10:55AN
Eric Beaugnon	Tsunehisa Kimura	Kyoto University, Japan	Diamagnetism Induced by Atomic-Level Eddy Current	10:55-11:15AM
	Eizo Ushijima	Aisin Cosmos R&D Co., Ltd. Japan	Improvement in the Efficiency of the Microbead- arrangement Method Using Magnetic Field	11:15-11:35AM
		Lunch, Poster	rs and Scientific Tour	
	Qingyou Lu	High Magnetic Field Laboratory, CAS, China	Direct observation of topological magnetic structures	2:00-2:25PM
Xuegeng Yang	Sanne J.C. Granneman	High Field Magnet Laboratory (HFML-EMFL), Radboud University, Netherlands	Dark-field Microscopy in High Magnetic Field	2:25-2:45PM
	Hao Wen	Chongqing University, China	Detection of Gravitational Waves by Use of Magnetic Fields	2:45-3:05PM
		Со	ffee Break	
	Noriyuki Hirota	Tsukuba, NIMS, Japan	Development of High Gradient Magnetic Separation System for the Removal of Scales from Boiler Feed Water in Thermal Power Plant	3:30-3:55PM
Qingyou Lu	Barbara Fritzsche	Institute of Processing Engineering and Environmental Technology, Germany	Magnetic Separation of Diverse Rare Earth Ions	3:55-4:15PM
	Zhe Lei	Institute of Fluid Dynamics, Germany	Magnetic Separation of Dy(III) from Solution, Stability Issue and Transport Process	4:15-4:35PM

Chair	Name	Institute	Торіс	Time
	Yukako Fujishiro	University of Tokyo, Japan	Emergent Transport Phenomena in Topological Spin Textures Revealed by High Magnetic Field Measurements	9:00-9:25AM
Zhigao Sheng	Max Hirschberger	RIKEN Center for Emergent Matter Science (CEMS), Japan	Effects of Berry Curvature Studied through Thermal Hall Conductivity Measurements in 35 Tesla: Electrons in a Canted Ferromagnet and Bogolyubov Quasiparticles in a Cuprate Superconductor	9:25-9:50AM
	Haosu Luo	Shanghai Institute of Ceramics, CAS, China	ME Composite PMNT/Metglas and Magnetic Sensor	9:50-10:10AM
		Со	ffee Break	
	Xuebin Zhu	Institute of Solid State Physics, CAS, China	Magneto-Hydrothermal Synthesis of MX2 Nanosheets as Electrodes for Supercapacitors	10:25-10:50AM
	Fapei Zhang	High Magnetic Field Laboratory (HMFL), CAS, China	Solvent-assisted Magnetic Manipulation of Molecular Orientation, Film Structure and Charge Transport of Semiconducting Polymers	10:50-11:10AM
Max Hirschberger	Sergei Barilo	Institute of Solid State and Semiconductor Physics, Belarusian Academy of Science, Belarus	Comparison of Crystal Growth Approaches and Novel Properties of Pure and Mixed Rare Earth Orthoferrites	11:10-11:30AM
	Mengyuan Huang	Institute of Fluid Dynamics, Helmholtz-Zentrum Dresden-Rossendorf, Germany	Numerical Simulation of Mass Transfer and Flow Near Conically Shaped Electrodes under the Influence of a Magnetic Field	11:30-11:50AM
		Lunch, Poster	rs and Scientific Tour	
	Isao Yamamoto	Yokohama National University , Japan	Control of Crystallization by Magnetic Field	2:00-2:20PM
Yunbo Zhong	Jun Wang	Northwestern Polytechnical University, China	Tailoring the Microstructure and Properties of CoCrFeNi-Based High-entropy Alloys Using High Magnetic Field	2:20-2:40PM
	Kohki Takahashi	Institute for Materials Research, Tohoku University, Japan	In-situ Observation of Solidification Process of Organic Materials in Magnetic Fields and Magnetic Force Fields	2:40-3:00PM
		Со	ffee Break	
	Fumiko Kimura	Kyoto University, Japan	Magnetically Oriented Microcrystal Array and Suspension of Microcrystalline Lysozyme for Crystal Structure Analysis	3:30-3:50PM
Xuebin Zhu	Guodong Tang	Nanjing University of Science and Technology, China	Nanostructured SnSe Integrated with Se Quantum Dots with Ultrahigh Power Factor and Thermoelectric Performance from High Magnetic Field Assisted Hydrothermal Synthesis	3:50-4:10PM
	Yunbo Zhong	Shanghai University	Effects of Super High Static Magnetic Field on the Microstructures of Binary Alloys during the Bulk Solidification Process	4:10-4:30PM
	Yixuan He	Northwestern Polytechnical University, China	On the Eutectoid Decomposition of Co3B→Co2B+α- Co in a Co-B Eutectic Alloy	4:30-4:50PM

Oct 13 th , Session 3. Room 208, Interdisciplinary Research Building, Science Island				
Chair	Name	Institute	Topic Time	
	Xin Zhang	High Magnetic Field Laboratory, CAS, China	Progresses of Bioeffect Studies of Static Magnetic Field in China	9:00-9:25AM
Peng Shang	Peng Shang	Northwestern Polytechnical University, China	Effects of Space Hypomagnetical Fileds on Skeletal System and Related Mechanisms	9:25-9:50AM
	Weidong Pan	Institute of Electrical Engineering, CAS, China	Biological Effects of Magnetic Fields and Magnetoreception in Insects	9:50-10:15AM
		Со	ffee Break	
	Jianfei Sun	Southeast University, China	Magnetic Nanodrug Mediated Precise Magnetic Stimulation for Brain Regulation	10:30-10:55AM
Guizhi Xu	An Xu	Hefei Institutes of Physical Sciences, CAS, China	Biological Effects of High Static Magnetic Fields on Caenorhabditis Elegans and Their Offspring	10:55-11:15AM
	Ying Liu	Beijing University of Chinese Medicine/Institute of Biophysics, CAS, China	Multiple Pathways Involve in the Bio-response to the Hypomagnetic Field	11:15-11:35AM
		Lunch, Poster	rs and Scientific Tour	
	Dongki Lee	Gangnam Severance Hospital, Yonsei University, Korea	Application of Magnetic Pressing Anastomosis in Benign Biliary Stricture	2:00-2:25PM
Jianfei Sun	Dachuan Yin	Northwestern Polytechnical University, China	Utilization of Gradient Magnetic Field for Merging Dense-liquid during Liquid-liquid Phase Separation	2:25-2:50PM
	Long-Fei Wu	Aix Marseille University, CNRS, France	Photosensitive Magnetoreception of Marine Bacteria	2:50-3:10PM
		Со	ffee Break	
	Guizhi Xu	Hebei University of Technology, China	TMS-EEG Experiments and Analysis on Brain Connectivity	3:30-3:50PM
Daahaaa Via	Chunxiao Xu	Institute of Electrical Engineering, CAS, China	Arabidopsis Flowering Is Affected by Near-Null Magnetic Field	3:50-4:10PM
Dachuan Yin	Juan He	Shanxi Normal University, China	Magnetobiology Based on External Magnetic Radiation and Internal Magnetism Detection on Sitobion Avenae	4:10-4:30PM
	Yanwen Fang	Heye Health Technology, China	Magnet, Health, and Happiness	4:30-4:50PM
Conc	luding remai	rks for the English sess	ions/poster awards, in Room 208	5:00-5:20PM

Oct 13 th , Session 4. Room 520, Interdisciplinary Research Building, Science Island				
Chair	Name	Institute	Topic Time	
	Ning Gu	Southeast University, China	High Performance Magnetic Nanomaterials for Biomedicine	9:00-9:25AM
Haiming Fan	Wenzhong Liu	Huazhong University of Science and Technology, China	0.05°C Resolution Thermometry by Using T2 Relaxation of Magnetic Nanoparticles in NMR	9:25-9:50AM
	Yu Cheng	Tongji University, China	Magnetic Nanomaterials for Developing Novel Cancer Therapies	9:50-10:15AM
		Co	ffee Break	
	Haiming Fan	Northwest University, China	Engineered Magnetic Nanoparticle for Advanced Nanothermotherapy and Magnetic Resonance Imaging	10:30-10:55AM
Ning Gu	Yao Cai	Institute of Geology and Geophysics, CAS, China	Positive Magnetic Resonance Angiography by Ultrafine Ferritin-based Iron Oxide Nanoparticles	10:55-11:15AM
	Wei Zhang	Dalian University of Technology, China	Magnetic Nanoparticles for Self-regulating Temperature Hyperthermia	11:15-11:35AM
		Lunch, Poste	rs and Scientific Tour	
	Hitoshi Watarai	Osaka University, Japan	Magneto-Optical Detection of Agglomeration and Deagglomeration of Magnetic Nanoparticles in Aqueous Solutions	2:00-2:20PM
Yu Cheng	Silin Guo	Huazhong University of Science and Technology, China	Magnetic Susceptibility to Measure Magnetic Nanoparticle Concentration from NMR Spectroscopy	2:20-2:40PM
	Hui Wang	High Magnetic Field Laboratory, CAS, China	Bifunctional Magnetic Nanoparticles for Multi-modal Bioimaging and Cancer Therapy	2:40-3:00PM
Conc	Concluding remarks for the English sessions/poster awards, <u>in Room 208</u> 5:00-5:20PM			

Oct 14 th , Chinese Session Room 208, Interdisciplinary Research Building, Science Island				
Name	Institute	Торіс	Time	
张小云 (Xiaoyun Zhang)	深圳大学	磁场对外伤性植物人康复效应	9:00-9:30AM	
王健 (Jian Wang)	浙江大学运动科学与健康工程 研究所	Effect of Static Magnetic Field Type and Exposure Time on Whole Blood Viscosity in Vitro (静态永磁磁 场类型和暴磁时间对离体人体血液粘度的影响)	9:30-10:00AM	
姚陈果 (Chenguo Yao)	重庆大学	高压超短脉冲电场消融肿瘤关键技术及临床应用 10:00-10:3		
	Co	offee Break		
刘仕琪 (Shiqi Liu)	西北妇女儿童医院	Magnetic Compression for the Management of Pediatric Digestive Tract Diseases (磁吻合在小儿外 科消化道疾病中的应用)	10:50-11:20AM	
杨军 (Jun Yang)	空军特色医学中心	旋转磁场的临床试用观察	11:20-11:50AM	

The 8th International Conference on Magneto-Science

Posters

Poster #	Authors	Affiliation	Title
1	Fumiko Kimura ^{1,2*} , Shigeru Horii ^{1,2} , Hayato Kashiwagi ¹ , Daisuke Notsu ¹ , Toshiya Doi ¹ , Masahisa Wada ^{3,4} , Tsunehisa Kimura	¹ Graduate School of Energy Science, Kyoto University, Yoshida-Honmachi, Kyoto 606-8501, Japan; ² Nagamori Institute of Actuators, Kyoto University of Advanced Science, Kyoto 615-8577, Japan; ³ Division of Forestry and Biomaterials, Kyoto University, Kitashirakawa, Kyoto 606-8502, Japan; ⁴ College of Life Sciences, Kyung Hee University, Yongin-si 446-701, Republic of Korea. ⁵ Fukui University of Technology, 3-6-1 Gakuen, Fukui 910-8505, Japan	Determination of Anisotropic Magnetic Susceptibility of High Temperature Superconducting Particles
2	Ewa Miękoś*, Marek Zieliński	University of Lodz, Faculty of Chemistry, Department of Inorganic and Analytical Chemistry	The effects of constant magnetic field on the properties of polymers, biopolymers and their composites
3	Zhe Shen, Jiale Zhu, Lang Ren, Tianxiang Zheng, Yunbo Zhong*	State Key Laboratory of Advanced Special Steel & School of Materials Science and Engineering, Shanghai University, Shanghai 200072, China	Influence of electromagnetic stirring frequency on the grain refinement of Cu-15Ni-8Sn alloy during horizontal continuous casting
4	Tianxiang Zheng, Zhe Shen, Bangfei Zhou, Wenhao Lin, Xu Chen, Yunbo Zhong*	State Key Laboratory of Advanced Special Steel & Shanghai Key Laboratory of Advanced Ferrometallurgy & School of Materials Science and Engineering, Shanghai University, Shanghai 200444, China	Effect of high static magnetic field on the microstructural evolution and mechanical enhancement of Al-20wt.%Si ribbon during the annealing process
5	B.F. Zhou, T.X. Zheng, Y.B. Zhong*, Z.M. Ren	State Key Laboratory of Advanced Special Steel, Shanghai University Shanghai, PR China	Morphological Evolution of Solid-Liquid Interface during the Directional Solidification of Zn-2wt.%Bi Monotectic Alloy under a Vertical Static Magnetic Field
6	Ganpei Tang, Zhongze Lin, Zhe Shen, Jiale Zhu, Tianxiang Zheng, Yunbo Zhong*	State Key Laboratory of Advanced Special Steel & School of Materials Science and Engineering, Shanghai University, Shanghai 200072, China	Aixal magnetic field induced the columnar-to-equiaxed transition during the directionally solidified Cu-15Ni-8Sn alloy
7	Licheng Dong, Yunbo Zhong*, Tianxiang Zheng, Zhe Shen, Bangfei Zhou	State Key Laboratory of Advanced Special Steels, Shanghai University Shanghai 200072, China	Preparation of Co-doped ZnO diluted magnetic semiconductor via hydrothermal method under a static magnetic field
8	N.Liubachko* and S.Barilo	SSPA "Scientific-practical materials research centre of NAS of Belarus", Minsk, Belarus	Growth of single crystals of the weak ferromagnet Fe3BO6
9	Sen Chen 1, 3, Hong-zhang Wang ² , Jing Liu 1,2, 3*	¹ Technical Institute of Physics and Chemistry, Zhongguancun East Rd.29, Haidian District, Beijing, China; ² University of Chinese Academy of Sciences, Yuquan Rd.19(A), Shijingshan District, Beijing, China; ³ Tsinghua University, Shuangqing Rd.30, Haidian District, Beijing, China	Magnetic Fluid Based on Liquid Metal
10	Ali Hassan ^{1,2} , Wei Ding ^{2,3} , Yuecheng Bian ^{1,2} , Adnan Aslam ^{1,2} , Zhigao	¹ Anhui Province Key Laboratory of Condensed Matter Physics at Extreme Conditions, High Magnetic Field Laboratory, Chinese Academy of Sciences, Hefei 230031, China; ² University of Science and Technology of China,	MnFe2O4/Coffee Waste biocarbon composites dominated by size dependent magnetic component for microwave

	Sheng ^{1*}	Hefei 230026, China; ³ Key Laboratory of Materials	absorption materials
		Physics, Institute of Solid State Physics, Chinese Academy of Sciences, Hefei 230031, China	
11	Muhammad Adnan Aslam ^{1,2} , Ali Hassan ^{1,2} , Ding Wei ³ , Yuecheng Bian ^{1,2} , Caixing ^{1,2} , Qiangchun liu ⁴ , Zhigao Sheng ^{1*}	¹ Anhui Province Key Laboratory of Condensed Matter Physics at Extreme Conditions, High Magnetic Field Laboratory, Chinese Academy of Sciences, Hefei 230031, China; ² University of Science and Technology of China, Hefei 230026, China; ³ Key Laboratory of Materials Physics, Institute of Solid State Physics, Chinese Academy of Sciences, Hefei 230031, China; ⁴ School of Physics and Electronics Information, Huaibei Normal University, Huabei 235000, China	Low density and efficacious EM wave absorption material based on bio-carbon obtained from Wheat straw
12	Caixing Liu 1,2, Yang Yang 1, Yuecheng Bian 1,2, Zongwei Ma 1, Chun Zhou 1, Qianwang Chen 1,2, Yuping Sun 1,3, and Zhigao Sheng 1*	¹ Anhui Province Key Laboratory of Condensed Matter Physics at Extreme Conditions, High Magnetic Field Laboratory, Chinese Academy of Science, Hefei 230031, China; ² University of Science and Technology of China, Hefei 230026, China; ³ Key Laboratory of Materials Physics, Institute of Solid State Physics, Chinese Academy of Sciences, Hefei 230031, China	Acceleration of Liquid-Solid Reaction with a Magneto-Catalyzed Method
13	Zongwei Ma, Chun Zhou, Zhigao Sheng*	Anhui Key Laboratory of Condensed Matter Physics at Extreme Conditions, High Magnetic Field Laboratory, Chinese Academy of Sciences, Hefei 230031, China	Magneto-Optical Systems Built in High Magnetic Field Laboratory
14	Yuecheng Bian ^{1,2,3} , Wei Ding ⁴ , Lin Hu ¹ , Zongwei Ma ¹ , Long Cheng ¹ , Ranran Zhang ¹ , Xuebin Zhu ⁴ , Xianwu Tang ⁴ , Jianming Dai ⁴ , Jin Bai ⁴ , Yuping Sun ^{1,3} , Zhigao Sheng ^{1,3*}	¹ Anhui Province Key Laboratory of Condensed Matter Physics at Extreme Conditions, High Magnetic Field Laboratory, Chinese Academy of Science, Hefei 230031, China; ² University of Science and Technology of China, Hefei 230026, China; ³ Key Laboratory of Materials Physics, Institute of Solid State Physics, Chinese Academy of Sciences, Hefei 230031, China.	Acceleration of Kirkendall Effect process in silicon nanospheres using magnetic fields
15	Xuhua Xiao ^{1, 2} , Guoxing Pan ¹ , Songlin Su ^{1, 2} , Xuebin Zhu ³ , Fapei Zhang ¹	¹ Anhui Province Key Laboratory of Condensed Matter Physics at Extreme Conditions, High Magnetic Field Laboratory (HMFL), Chinese Academy of Sciences, Hefei, China; ² University of Science and Technology of China Hefei China; ³ Key Laboratory of Materials Physics Institute of Solid State Physics Chinese Academy of Science Hefei, China	Enhanced backbone alignment and charge transport of a semiconducting diketopyrrolopyrrole copolymer by solvent vapor annealing under high magnetic field
16	Peilin Yang ¹ , Tiantian Cai ¹ , Yuebin Zhang ² , Qiu-Yun Tan ³ , Kedong Wang ³ , Zhen Guo ¹ , Guohui Li ² , Bing-Wu Wang ⁴ , & Can Xie ^{1,5}	¹ State Key Laboratory of Membrane Biology, Laboratory of Molecular Biophysics, School of Life Sciences, Peking University, Beijing 100871, China; ² State Key Laboratory of Molecular Reaction Dynamics, Dalian Institute of Chemical Physics, Chinese Academy of Sciences, 457 Zhongshan Rd, Dalian 116023, China; ³ State Key Laboratory of Nuclear Physics and Technology, Peking University, Beijing 100871, China; ⁴ College of Chemistry and Molecular Engineering, Peking University, Beijing 100871, China; ⁵ Beijing Computational Science Research Center, The Chinese Academy of Engineering Physics, Beijing 100084, China	Magnetic features of the magnetoreceptor MagR revealed via its tetramer

17	Zhen Guo ¹ , Can Xie ^{1,2}	¹ State Key Laboratory of Membrane Biology, Laboratory of Molecular Biophysics, School of Life Sciences, Peking University, Beijing 100871, China; ² Beijing Computational Science Research Center, The Chinese Academy of Engineering Physics, Beijing 100084, China	The Iron-Sulfur Cluster Binding of MagR: An Updated Model
18	<u>Liyuan Liu,</u> <u>Guirong Ding</u> *	Department of Radiation Protection Medicine, AirForce Medical University,Xi' an, Shaanxi, PRC, 710032, China	Effects of Power Frequency Magnetic Field on Cell Behaviour in MCF-7 Cells
19	Lanxiang Tian ^{1, 2*} , Yingying Zhang ^{1, 2} , Bingfang Zhang ^{1, 2} , Yongxin Pan ^{1, 2}	¹ Biogeomagnetism Group, Key Laboratory of Earth and Planetary Physics, Institute of Geology and Geophysics, Chinese Academy of Sciences, Beijing, 100029; ² France-China International Laboratory of Evolution and Development of Magnetotactic Multicellular Organisms, Beijing 100029, China	Effects of hypomagnetic field on neurotransmitter, hormone and blood parameters in laboratory rodents
20	<u>Chong Ding,</u> Haijun Zhu, Guizhi Xu*	Hebei University of Technology, Tianjin, China	The Effects of High-frequency Repetitive Transcranial Magnetic Stimulation on Cognition and Neuronal Excitability in Neonatal Mice
21	Haijun Zhu, Chong Ding, Guizhi Xu*	Hebei University of Technology, Tianjin, China	The Effects of Repetitive Transcranial Magnetic Stimulation on the Cognition and Neuronal Excitability of Mice
22	Shenghang Wang ^{1,2,3} , Zhihao Zhang ^{1,2,3} , Dandan Dong ^{1,2,3} , Peng Shang ^{2,3} *	¹ School of Life Sciences, Northwestern Polytechnical University, Xi'an Shaanxi, 710072, China; ² Key Laboratory for Space Biosciences and Biotechnology, Northwestern Polytechnical University, Xi'an Shaanxi, 710072, China; ³ Research & Development Institute of Northwestern Polytechnical University in Shenzhen, Shenzhen, China	High static magnetic field inhibit osteosarcoma growth by promoting intracellular iron accumulation and increasing ROS
23	YR Xue ^{1,2,3} , JC Yang ^{1,3,4} , SJ Zhou ^{1,2,3} ,P Shang ^{1,3*}	¹ Research & Development Institute of Northwestern Polytechnical University in Shenzhen, Shenzhen, China; ² School of Life Sciences, Northwestern Polytechnical University, Xi'an, China; ³ Key Laboratory for Space Bioscience and Biotechnology, Northwestern Polytechnical University, Xi'an, China; ⁴ Department of Spinal Surgery, People's Hospital of Longhua Shenzhen, Shenzhen, China	Effects of high static magnetic fields on the recovery of microgravity-induced bone loss in mice
24	Jiancheng Yang ^{1, 2,} ⁴ , Gejing Zhang ^{3, 4} , Dandan Dong ^{3, 4} , Hao Zhang ¹ , Peng Shang ^{2, 3, 4*}	¹ Department of Spinal Surgery, People's Hospital of Longhua Shenzhen, Shenzhen, China; ² Research & Development Institute of Northwestern Polytechnical University in Shenzhen, Shenzhen, China; ³ School of Life Sciences, Northwestern Polytechnical University, Xi'an, China; ⁴ Key Laboratory for Space Bioscience and Biotechnology, Northwestern Polytechnical University, Xi'an, China	Investigating the physiological effects of 2–12T high static magnetic field exposure on bone in mice
25	Gejing Zhang ^{1, 4} , Jiancheng Yang ^{1, 3,} ⁴ , Zheyuan Zhang ^{1,} ⁴ , Peng Shang ^{1, 2, 4*}	¹ School of Life Sciences, Northwestern Polytechnical University, Xi'an, China; ² Research & Development Institute of Northwestern Polytechnical University in Shenzhen, Shenzhen, China; ³ Department of Spinal Surgery, People's Hospital of Longhua Shenzhen, Shenzhen, China; ⁴ Key Laboratory for Space Bioscience and Biotechnology, Northwestern Polytechnical University, Xi'an, China	The effects of iron oxide nanoparticles combined with static magnetic field on osteoblasts and osteoclasts in vitro and on unloading-induced bone loss in vivo

26	Yue Jin ^{1#} , <u>Wei</u> <u>Guo</u> ^{1#} , Xupeng Hu ^{2#} , Mengmeng Liu ¹ , Xiang Xu ¹ , Fenhong Hu ¹ , Yiheng Lan ³ , Chenkai Lv ³ , Yanwen Fang ⁴ , Mengyu Liu ⁴ , Tieliu Shi ³ , Shisong Ma ⁵ , Zhicai Fang ⁴ , Jirong Huang ^{1*}	¹ Shanghai Key Laboratory of Plant Molecular Sciences, College of Life Sciences, Shanghai Normal University, Shanghai 200234, China; ² Institute of Plant Physiology and Ecology, Chinese Academy of Sciences, Shanghai 200032, China; ³ Shanghai Key Laboratory of Regulatory Biology, School of Life Sciences, East China Normal University, Shanghai, 200241, China; ⁴ Heye Health Industrial Research Institute of Zhejiang Heye Health Technology, Anji Zhejiang 313300, China; ⁵ School of Life Sciences, University of Science and Technology of China, Hefei 230026, China	Static magnetic field regulates Arabidopsis root growth via auxin signaling
27	<u>Jiaojiao Wu</u> , Yu Cheng*	The Institute for Biomedical Engineering and Nano Science, School of Medicine, Tongji University, Shanghai, P.R. China	Alternating Magnetic Fields Coupled with Magnetic Nanocubes Can Turn on the Force and the Heat for Synergistic Cancer Treatment
28	Jiacheng Yu ^{1,2} , Tongwei Zhang ^{1,2} , Huangtao Xu ^{1,2} , Yao Cai ^{1,2} , Yongxin Pan ^{1,2} , and Changqian Cao ^{1,2*}	¹ Key Laboratory of Earth and Planetary Physics, Institute of Geology and Geophysics, Chinese Academy of Sciences, Beijing 100029, P. R. China; ² France-China Joint Laboratory for Evolution and Development of Magnetotactic Multicellular Organisms, Chinese Academy of Sciences, Beijing 100029, China	Thermostable iron oxide nanoparticle synthesis within recombinant ferritins from the Piezophilic Hyperthermophile Pyrococcus CH1
29	Yingze Li ¹ , Chang chen ^{1*} , Yu Cheng ^{2*}	¹ Department of Thoracic Surgery, Shanghai Pulmonary Hospital, Tongji University School of Medicine, Shanghai, China; ² The Institute for Biomedical Engineering & Nano Science, Tongji University School of Medicine, Shanghai, China	MNPs Promote the M2 Subtype towards M1-like Subtype Macrophages and Microglias
30	Feng Tao, Yao Qin, Yu Cheng*	The Institute for Biomedical Engineering and Nano Science, School of Medicine, Tongji University, Shanghai 200092, P.R. China	Micro-Therapeutic System Enhanced Nitric Oxide Release for Gas Therapy
31	Ya-Li Liu ¹ , Fiaz Ahmad ¹ , Jing-Jie Chen ¹ , Tuo-Di Zhang ¹ , Ya-Jing Ye ¹ , Wei-Hong Guo ¹ , Peng Shang ^{1,2} , Da-Chuan Yin	¹ Institute for Special Environmental Biophysics, Key Laboratory for Space Bioscience and Biotechnology, School of Life Sciences, Northwestern Polytechnical University, Xi'an 710072, PR China; ² Shenzhen Research Institute of Northwestern Polytechnical University, Shenzhen 518057, Guangzhou, PR China	Focusing Fe3O4 particles using time-varying magnetic field
32	Huangtao Xu ^{1,2} , Yongxin Pan ^{1,2*}	¹ Biogeomagnetism Group, Key Laboratory of Earth and Planetary Physics, Institute of Geology and Geophysics, Chinese Academy of Sciences, Beijing 100029, China. ² University of Chinese Academy of Sciences, Beijing 100049, China	Effects on the heating efficiency of magnetoferritin nanoparticles in an alternating magnetic field
33	Zi-Qing Wu ¹ , Yong-Ming Liu ^{1,2} , Da-Chuan Yin ^{1*}	¹ Institute for Special Environmental Biophysics, Key Laboratory for Space Bioscience and Space Biotechnology, School of Life Sciences, Northwestern Polytechnical University, Xi'an 710072, Shaanxi, PR China; ² School of Biological Engineering, Sichuan University of Science and Engineering, Zigong 643000, Sichuan, PR China	Magnetic Confinement of Diamagnetic Objects for Space Utilization
34	Mikihide Hirota *, Ryota Motoki, Ryuichi Fujikawa,	Department of Physics, Graduate School of Engineering Science, Yokohama National University. 79-5 Tokiwadai, Hodogaya-ku, Yokohama 240-8501, Japan	New detection method for diagnosis of cancer metastasis by using pulsed magnetic field

	and Isao Yamamoto		
35	Fu Rui, Xu Guizhi, Zhu Haijun, Yin Xiaonan, Xu Baohong and Ding Chong*	State Key Laboratory of Reliability and Intelligence of Electrical Equipment, Hebei University of Technology, Tianjin, 300130, China	Effects of different frequency repetitive transcranial magnetic stimulation on memory ability and excitability of hippocampal DG neuronal in mice
36	<u>Lei Zhang,</u> Qingping Tao, Xin Zhang*	High Magnetic Field Laboratory, Key Laboratory of High Magnetic Field and Ion Bean Physical Biology, Hefei Institutes of Physical Science, Chinese Academy of Sciences, Hefei 230031, China	Cell biological effects of high static magnetic field and mechanism study
37	Qingping Tao ^{1,2} , Lei Zhang ¹ , Xuyao Han ³ , Hanxiao Chen ^{1,2} , Xinmiao Ji ¹ , Xin Zhang ^{1,2} , ^{4*}	¹ High Magnetic Field Laboratory, Key Laboratory of High Magnetic Field and Ion Bean Physical Biology, Hefei Institutes of Physical Science, Chinese Academy of Sciences, Hefei 230031, China; ² Science Island Branch of Graduate School, University of Science and Technology of China, Hefei 230026, China; ³ School of Pharmacy, Anhui Medical University, Hefei 230032, Anhui Province, China; ⁴ Institutes of Physical Science and Information Technology, Anhui University, Hefei 230601, China	Magnetic susceptibility difference-induced nucleus positioning in gradient ultra-high magnetic field
38	Xiaofei Tian, Dongmei Wang, Shuang Feng, Lei Zhang, Xinmiao Ji, Ze Wang, Qingyou Lu, Chuanying Xi, Li Pi, Xin Zhang*	High Magnetic Field Laboratory, Hefei Institutes of Physical Science, Chinese Academy of Sciences, Hefei, Anhui, 230031, PR China	Effects of 3.5–23.0T static magnetic fields on mice: A safety study
39	Lei Cheng ^{1,2} , An Xu ^{1,2*}	¹ University of Science and Technology of China, Hefei, Anhui 230026, PR China; ² Key Laboratory of High Magnetic Field and Ion Beam Physical Biology, Chinese Academy of Sciences, Anhui Province Key Laboratory of Environmental Toxicology and Pollution Control Technology, Hefei Institutes of Physical Science, Chinese Academy of Sciences, Hefei, China	1T Static Magnetic Field Regulated Serotonin Secretion and Behavior in <i>Caenorhabditis</i> elegans via TRPV1 Receptor
40	Tianying Zhan*, Xiaomei Wang*, Zijun Ouyang, Youli Yao, Jiangyao Xu, Shikang Liu, Kan Liu, Qiyu Deng, Yushu Wang, Yingying Zhao#	Base for International Science & Technology Cooperation: Carson Cancer Stem Cell Vaccines R&D Center, Department of Physiology, School of Basic Medical Sciences, Xili campus of Shenzhen University, Keyuan Ave 1066, Shenzhen, Guangdong, China	Rotating Magnetic Field Ameliorates Experimental Autoimmune Encephalomyelitis by Promoting T cell Peripheral Accumulation and Regulating the Balance of Treg and TH1/TH17
41	Jiangyao Xu ¹ , Xiaoyun Zhang ² , Xiaomei Wang ^{1*}	¹ Department of Physiology, School of Basic Medical Sciences, Shenzhen University, Shenzhen 518060, P. R. China; ² College of Life Science and Oceanography, Shenzhen University, Shenzhen 518060, People's Republic of China	Effects on longevity extension and mechanism of action of 4Hz rotating magnetic field in <i>C. elegans</i> and HUVEC
42	Kan Liu ¹ , Jiangyao Xu ¹ , Peng Zhai ¹ , Xiaoyun Zhang ² , Xiaomei Wang ^{1*}	¹ Department of Physiology, School of Basic Medical Sciences, Shenzhen University, Shenzhen 518060, P. R. China; ² College of Life Science and Oceanography, Shenzhen University, Shenzhen 518060, People's Republic of China	Vascular Remodelling of Veins is Suppressed by Low Frequency Rotating Magnetic Field

The 8th International Conference on Magneto-Science

Abstracts

October 12th, 2019

Excitations in Quantum Spin Systems

Zhe Wang¹ and Alois Loidl²*

¹ Institute of Physics II, University of Cologne, 50937 Cologne, Germany; ² Center for Electronic Correlations and Magnetism, University of Augsburg, 86135 Augsburg, Germany *Corresponding author: alois.loidl@physik.uni-augsburg.de

In quantum magnets, emergent states of matter are characterized by their elementary excitations that can be induced and tuned in external longitudinal and transverse magnetic fields. Due to enhanced quantum fluctuations, reduced dimensionality, and frustration effects, quantum magnets often host exotic and fractionalized excitations. Here we report on recent experiments on quantum spin systems,

where these unconventional magnetic excitations have been observed, were characterized and analyzed in full detail.

In the first part of the talk, we will review recent experiments on the one-dimensional quantum spin systems SrCo₂V₂O₈ and BaCo₂V₂O₈ in high magnetic fields. In one-dimensional (1D) spin $S = \frac{1}{2}$ systems, the elementary magnetic excitations are spinons with fractional spin quantum numbers. We report on THz spectroscopy on the antiferromagnetic spin-chain compound SrCo₂V₂O₈, which is a paradigmatic representative of the 1D Heisenberg-Ising (XXZ) model: In the magnetically ordered state and in transverse fields confined spinons are identified, which can be described by a one-dimensional Schrödinger equation [1,2]. The spinon confinement is suppressed by moderate transverse fields, inducing a quantum-disordered phase [2] with emergent fermionic excitations. In strong longitudinal fields, we were able to observe string states, Bethe strings, which are accurately described by the Bethe ansatz [3]. Quantum criticality and the complex magnetic excitation spectrum close to the quantum critical point has also been observed in BaCo₂V₂O₈ as function of longitudinal [4] and transverse [5] fields up to 30 respectively 60 T. Near the critical field,

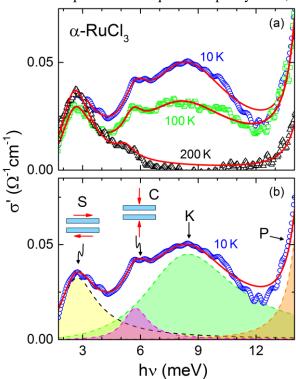


Fig. 1 Dynamic conductivity in α-RuCl₃ revealing a broad continuum of fractionalized excitations:

- (a) Conductivity for temperatures between 10 and 200 K.
- (b) Deconvolution of the conductivity spectrum using phonon excitations S, C, and P located at 2.5, 6, and 15 meV and a continuum of fractionalized excitations K close to 8.5 meV. The phonon modes at 2.5 and 6 meV represent sliding (S) and compression (C) modes of rigid molecular RuCl₃ layers, as schematically indicated. Taken from Ref. [6].

high-energy excitations dominate the spin dynamics as compared to much weaker fractional excitations.

Another illuminating example of exotic excitations in quantum matter is the observation of fractionalized excitations in quantum spin liquids, where quantum fluctuations and strongly frustrated magnetic exchange suppress long-range magnetic order. More than one decade ago, Kitaev proposed an exactly solvable model for $S = \frac{1}{2}$ Ising spins on a two-dimensional honeycomb lattice, with bonddirectional interactions resulting in a topological quantum spin liquid (QSL) and emergent Majorana fermions. α-RuCl₃ crystallizes in an almost ideal two-dimensional honeycomb lattice with weak interlayer coupling and is a prime candidate for the realization of Kitaev physics. However, due to further non-Kitaev interactions, the system undergoes spin ordering below 7 K. The antiferromagnetic order can easily be suppressed by moderate magnetic fields and fractionalized spin degrees of freedom, composed of itinerant and localized Majorana fermions are expected at temperatures above magnetic order and beyond quantum criticality. Here we report on thermodynamic [6] and time-domain THz transmission experiments [7,8,9] on α-RuCl₃ documenting the existence of fractionalized spin excitations. For the analysis of the heat-capacity experiments, the phonon background was determined using ab-initio calculations of the phonon density of states [6]. The THz experiments were performed for wave numbers from 1 to 10 meV, for external magnetic fields up to 30 T and for temperatures from 5 to 295 K. Figure 1 shows representative results of THz experiments in zero external magnetic fields documenting a broad continuum due to fractionalized spin excitations, which becomes fully suppressed at elevated temperatures [8]. In addition, we found clear evidence of rigid-plane shear and compression modes, which reveal a weak temperature dependence only. We also followed the evolution of the extended magnetic continuum, a fingerprint of fractionalized spin degrees of freedom, as function of external magnetic fields crossing quantum criticality [7,9] and we found significant enhancement of the continuum close to the quantum-critical point. For further increasing fields, in the field-polarized ferromagnetic phase, well-defined magnetic modes evolve out of this continuum [7,9].

References

- [1] Zhe Wang et al., Phys. Rev. B 91, (2015) 140404(R).
- [2] Zhe Wang et al., Phys. Rev. B **94**, (2016) 125130.
- [3] Zhe Wang et al., Nature **554**, (2018) 219.
- [4] Zhe Wang et al., Phys. Rev. Lett. 120, (2018) 207205.
- [5] Zhe Wang et al., Phys. Rev. Lett. **123**, (2019) 067202.
- [6] S. Widmann et al., Phys. Rev. B 99, (2019) 094415.
- [7] Zhe Wang et al., Phys. Rev. Lett. 119, (2017) 227202.
- [8] S. Reschke et al., Phys. Rev. B 100, (2019) 100403(R).
- [9] A. Sahasrabudhe, et al., preprint, (2019) arXiv:1908.11617.

ALL-OPTICAL CONTROL OF MAGNETISM:

from fundamentals to nanoscale engineering

Theo Rasing

Radboud University, Institute for Molecules and Materials, Heijendaalseweg 135,6525AJ Nijmegen, the Netherlands

th.rasing@science.ru.nl

The 21st century digital economy and technology is presently facing fundamental scaling limits (heating and the superparamagnetic limit) as well as societal challenges: the move to mobile devices and the increasing demand of cloud storage leads to an enormous increase in energy consumption of our ICT infrastructure. These developments require new strategies and paradigm shifts, such as photon- and spin-based technologies. Since the demonstration of magnetization reversal by a single 40 femtosecond laser pulse, the manipulation of spins by ultra-short laser pulses has become a fundamentally challenging topic with a potentially high impact for future spintronics, data storage, and quantum computation. The ability to control the macroscopic magnetic ordering by means of femtosecond laser pulses provides an alternative and energy efficient approach to magnetic recording. The realization that femtosecond laser induced all-optical switching (AOS) as observed in ferrimagnets exploits the exchange interaction between their sub-lattices, has opened the way to engineer new and rare-earth-free magnetic materials for AOS. Expansion to hybrid magnetic materials, multilayers, FePt and even magnetic garnets are ongoing efforts to expand AOS to future magnetic recording media technology. Recent developments using plasmonic antennas indicate the possibility to even scale the technique of AOS to the nanoscale, making AOS a potential candidate for fast and energy efficient data storage.

Recent References

A.Kirilyuk, et al, Rev. Mod. Phys. 82, 2731-2784 (2010)

I.Radu et al, **Nature 472**, 205 (2011)

T. Ostler et al, **Nature Comm. 3**, 666 (2012)

C. Graves et al, Nature Materials 12, 293 (2013)

Tian-Min Liu et al, Nano Letters, (2015)

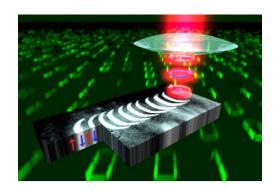
R. V. Mikhaylovskiy et al, Nature Comm. 2015

L. LeGuyader et al, Nature Comm. 2015

T. J. Huisman, et al, Nature Nanotechnology 11, 455 (2016)

A. Stupakiewicz et al, **Nature** 20807 (2017)

E. Iacocca et al, Nature Comm. 10, 2019



Interactions between water systems and magnetic fields: Magnetite Controls Ice Nucleation

Atsuko Kobayashi 1*

¹ Earth-Life Science Institute, Tokyo Institute of Technology, Meguro, 152-8550 Tokyo, Japan *Corresponding author: kobayashi.a.an@m.titech.ac.jp

Magnetic effects on the physical properties of water have been investigated for well over a century, largely at the high-field end where the diamagnetic properties of pure H_2O dominate. More mysterious are claims of weaker field effects on properties that cannot be explained easily thorough diamagnetic interactions. Here I will present my results identifying nanoparticles of magnetite that are commonly dispersed in aqueous media as a potential mechanism in at least one of these interactions.

In supercooled water, ice nucleation is a stochastic process that requires $\sim 250-300$ molecules to transiently achieve structural ordering before a seed crystal can nucleate; this happens most easily on crystalline surfaces, a process termed heterogeneous nucleation [1]. Recent experiments have shown that crystals of nanophase magnetite (Fe₃O₄) are powerful nucleation sites for this heterogeneous crystallization of ice, comparable to other materials like silver iodide and some cryobacterial peptides [2, 3]. In natural fluids containing magnetite particles (such as Aeolian dust, seawater, glacial ice, etc.), magnetite could well dominate the ice nucleation dynamics.

Trace levels (ppb – ppm) of nanoparticles of magnetite are also present in many plant and animal tissues (reviewed in [3]). These crystals originate both through controlled biomineralization processes as well as from environmental contamination during the life of the organisms. These particles are also effective at nucleating ice, causing 'freezer damage' to vegetables and meat from the formation of needle-like crystals of hexagonal ice that break cell membranes. We were able to show that the application of a weak, low-frequency (~1 mT @ 10 Hz) rotating magnetic field designed to overcome Brownian motion of these particles was able to inhibit ice crystallization and promote supercooling [3]. The smaller ice crystals formed from supercooled tissues cause less cellular damage, and can potentially minimize the loss of food between the farm and the kitchen table.

Finally, please note that ferromagnetic contaminants at ppb levels commonly leach out of laboratory glassware and disposable containers and can build up in solution to significant levels [4]. Experimenters must avoid such contamination in all studies of putative magnetic effects on water.

References

- [1] E. B.Moore, V.Molinero, Nature 479 (2011) 506-508.
- [2] A. Kobayashi, H. N. Golash and J. L. Kirschvink, Cryobiology 72(3) (2016) 216-224.
- [3] A. Kobayashi, M. Horikawa, J. L. Kirschvink and H. N. Golash, PNAS 115(21) (2018) 5383-5388.
- [4] A. Kobayashi, J. L. Kirschvink and M.H. Nesson, Nature 374 (1995) 123-123.

Biological Effects of High-Gradient Magnetic Fields

<u>Vitalii Zablotskii</u>^{1*}, Tatyana Polyakova¹, Alexandr Dejneka¹

¹ Institute of Physics of the Czech Academy of Sciences, Na Slovance 2, Prague, 18221 Czech Republic *Corresponding author: zablot@fzu.cz

As the fields of nanomedicine, magnetotherapy and magnetogenetics intensively grow, knowledge of the interactions between magnetic fields and living cells is of increasing importance. The exact

mechanisms of the interaction between magnetic fields and cells still elude our complete understanding. However, some of the fundamental mechanisms were recently identified for different types of cells exposed to a high-gradient magnetic field (HGMF).

In this report we aim at highlighting recent advances made in identifying fundamental mechanisms by which magnetic gradient forces act on cell fate specification and cell differentiation.

Let us imagine cells that are in a high-gradient magnetic field, which changes in the both magnitude and direction (Fig. 1). Through what mechanisms do the cells sense a non-uniform magnetic field and how such a field changes the cell fate? We show that

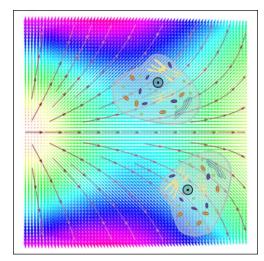


Fig. 1 Cells in a non-uniform magnetic field [1].

magnetic forces generated by high-gradient magnetic fields (∇B >10 kT/m) can be comparable to intracellular forces and therefore may be capable of altering the functionality of an individual cell and tissues in unprecedented ways.

We identify the cellular effectors of such fields and propose novel routes in cell biology predicting new biological effects such as magnetically induced differentiation of stem cells, magnetically assisted cell division or prevention of cells from dividing, magnetically induced cytoskeleton remodeling, magnetic control of the membrane potential and cell-to-cell communication as well as magnetic control of intracellular ROS levels [2,3].

We also provide a review of the currently available magnetic systems capable of generating magnetic fields with spatial gradients of up to 10 MT/m. On the basis of experimental facts and theoretical modeling we reveal timescales of cellular responses to high-gradient magnetic fields and suggest an explicit dependence of the cell response time on the magnitude of the magnetic field gradient. **Acknowledgments:** this work is supported by Operational Programme Research, Development and Education, financed by the European Structural and Investment Funds and the Czech Ministry of Education, Youth and Sports through Project No. SOLID21— CZ.02.1.01/0.0/0.0/16_019/0000760.

References

- [1] V. Zablotskii, T. Polyakova, and A. Dejneka, BioEssays 40(8) (2018) 1800017.
- [2] V. Zablotskii, O. Lunov, S. Kubinova, T. Polyakova, E. Sykova and A. Dejneka, J. Phys. D: Appl. Phys. 49 (2016) 493003.
- [3] V. Zablotskii, T. Polyakova, O. Lunov and A. Dejenka, Scientific Reports 6 (2016) 37407.

Human Magnetoreception: Tests of magnetite-based magnetoreception

<u>Joseph L. Kirschvink</u>^{1*}, Connie X. Wang², Isaac A. Hilburn¹, Daw-An Wu^{2,3}, Yovan Badal⁴, and Shinsuke Shimojo^{2,3}

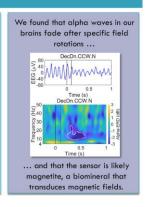
¹Division of Geological & Planetary Sciences, California Institute of Technology, Pasadena, CA, USA; ²Computation & Neural Systems, California Institute of Technology, Pasadena, CA, USA; ³Division of Biology & Biological Engineering, California Institute of Technology, Pasadena, CA, USA; ⁴Division of Physics, Math & Astronomy, California Institute of Technology, Pasadena, CA, USA *Corresponding author: kirschvink@caltech.edu

Although many migrating and homing organisms are sensitive to Earth's magnetic field as illustrated in the attached figure, most humans are not consciously aware of the geomagnetic stimuli that we encounter in everyday life. Either we have lost the magnetosensory system shared by many of our not-too-distant animal ancestors, or a system still exists with detectable neural activity but lacks potent output to elicit perceptual awareness in us. With initial support from the Human Frontiers Science Program, we now have strong support for the existence of a subconscious human magnetic sensory system [1]. We have found some brief, ecologically-relevant rotations of Earth-strength magnetic fields that produce strong, specific, and repeatable decreases in EEG alpha band (8-13 Hz) power in the few seconds following magnetic stimulation. Similar brainwave changes are known to arise from visual, auditory, and tactile stimuli and are termed alpha event-related desynchronization (alpha-ERD). To date, our data show that: (1) the human geomagnetic compass response is polar in nature (can distinguish North from South), (2) can operate in total darkness, and (3) is not based on any form of electrical induction (and hence is not an electrical artifact). These results rule out both a quantum compass and an induction sensor as the transduction mechanisms, leaving a system based on biologically-precipitated nanocrystals of magnetite (Fe₃O₄) as the most likely. We will discuss the effects of high-field exposure on the human magnetosensory system at this meeting.

Humans have a Geomagnetic Sensory System as do many other Animals







[1] C.X. Wang et al., 2019. Transduction of the Geomagnetic Field as Evidenced from Alphaband Activity in the Human Brain."



October 13, 2019, Session 1

Magnetic Field Effect on Water Wetting

Bao Chen ¹, Nicolas Glade ², <u>Eric Beaugnon</u> ^{1*}

¹ Univ. Grenoble Alpes, CNRS/LNCMI, BP166, 38042 Grenoble Cedex 9, France; ² Univ. Grenoble Alpes, TIMC-IMAG, Domaine de la Merci, 38706 La Tronche Cedex, France

*Corresponding author: eric.beaugnon@lncmi.cnrs.fr

Magnetic fields effects on water have been widely studied. In one of these studies [1], it has been demonstrated that under air or oxygen, a 6T field influences the contact angle of pure water with platinum, and that this effect depends on exposure time and is slowly relaxed after removal of the field.

We present new results of this effect, not only using pure water moved up and down in the magnetic field, but also using waters with different electrical conductivities, being moved or not in the magnetic field, with different magnetic field values and on different substrates, using copper and gold.

A flask of water is either maintained static in the maximum field of a superconducting or resistive magnet, or moved up and down from the maximum field to almost zero field, 20 times per minute. 12 L samples are deposited on a clean metallic substrate every 20 minutes and the contact angle is measured out of the field with a macro-camera using ImageJ free software. The field is shut down after 150 min, and some samples are then still measured.

In all experiments under magnetic field, a common behavior is observed: after switching on the field, the contact angle gradually decreases with time until reaching a saturation value. After switching off the field, the contact angle slowly recovers its initial value. Several parameters are tested:

- 1) Magnetic field intensity: the saturation value of the contact angle between water and gold decreases with field intensity up to maximum applied field (20 T).
- 2) Moving or not moving the water in the magnetic field: in both cases, a contact angle decrease is observed.
- 3) Water electrical conductivity: using three different waters, we observed that the field effect increases with the electrical conductivity of water (fig 1).

In a few experiments, the bad reproducibility of some results however suggests that a complex mechanism is still hidden and needs more investigations.

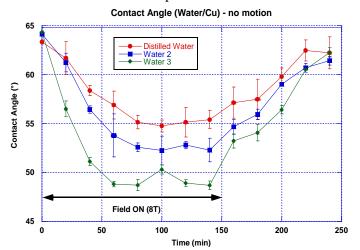


Fig 1. Contact angle between water and Cu, for 3 different waters with increasing electrical conductivities (Distilled Water, Water 2 and Water 3). Water container is static in the field.

Reference

[1] I. Otsuka, S. Ozeki, J. Phys. Chem. B, Vol. 110, No. 4, 2006

Effects of Magnetic Field on Hydrogen Bubble Detachment during Water Electrolysis

Xuegeng Yang ^{1*}, Gerd Mutschke¹, Margitta Uhlemann², Kerstin Eckert ^{1,3}

¹ Institute of Fluid Dynamics, Helmholtz-Zentrum Dresden-Rossendorf, 01314 Dresden, Germany; ²

IFW Dresden, Institute of Complex Materials, 01069 Dresden, Germany; ³ Institute of Process

Engineering and Environmental Technology, Technical University of Dresden,

01062 Dresden, Germany

*Corresponding author: x.yang@hzdr.de

Water electrolysis is a promising option for hydrogen production from renewable resources. One main challenge in making water electrolysis economically competitive is to raise its efficiency by decreasing the cell voltage. In this respect, electrode coverage by gas bubbles is one of the key sources which creates undesired overpotential.

Better understanding of the fundamentals of bubble nucleation, growth, and detachment in detail might bring new ideas in such effective manipulating of bubbles and substantially accelerate a way toward advanced electrolysis. Despite extensive efforts in the past, important aspects of bubble dynamics, such as the interaction/coalescence of bubbles significantly affecting their evolution or different growth modes of the bubbles themselves, are not yet fully understood. To provide that necessary information on the bubble shape profile, including the contact angle, the contact line the bubble forms with the electrode [1], the Marangoni convection [2], we use a micro electrode to produce single hydrogen bubbles. Water electrolysis was carried out under potentiostatic conditions in a 1 M H_2SO_4 solution in a small electrochemical cell ([2], [3]). The behavior of a single hydrogen bubble evolving on a microelectrode (100 μ m in diameter) was analyzed by measurements of the current transient as well as by microscopic high-speed imaging. Tracer particles were additionally added to the solution to measure the flow in the vicinity of the bubble.

The contribution will present experimental results of the hydrogen bubble release size and the bubble growing mechanism at two different magnetic field orientations and at different field intensities. As shown in Fig.1, the bubble departure size decreased with increase of the magnetic field intensity when the magnetic field was applied parallel to the electrode surface. However, an increase of the departure size was observed when the field was applied perpendicular to the electrode surface. The effects were further explained by the MHD convection around the bubble. A comparison of the flow field by measurements and numerical simulation will be presented.

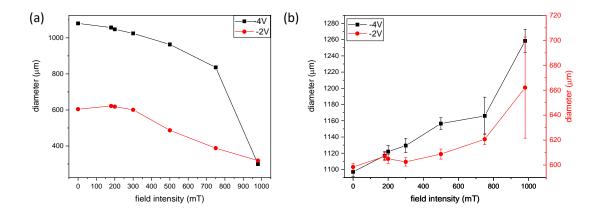


Fig. 1. Bubble departure size at two different potentials when the magnetic field was applied (a) parallel and (b) perpendicular to the electrode surface.

Reference

- [1] X. Yang, F. Karnbach, M. Uhlemann, S. Odenbach and K. Eckert, Langmuir 31 (2015), 8184-8193
- [2] X. Yang, D. Baczyzmalski, C. Cierpka, G. Mutschke and K. Eckert, Physical Chemistry Chemical Physics 20 (2018), 11542-11548
- [3] D. Baczyzmalski, F. Karnbach, G. Mutschke, X. Yang, K. Eckert, M. Uhlemann, and Ch. Cierpka. Physical Review Fluids 2, no. 9 (2017): 093701

The Easiest Way to Levitate Water by Magnetic Field

Yasuhiro Ikezoe* and Masayuki Sugaya

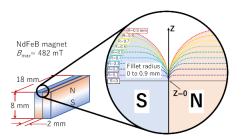
Nippon Institute of Technology, Department of Applied Chemistry, 4-1 Gakuendai, Miyashiro, Saitama, Japan 345-8501
y.ikezoe@nit.ac.jp

If the levitation of objects can be realized on the earth, it will be possible to carry out alternative experiments for those in space, and, at the same time, extreme reduction of cost and energy saving can be expected. In order to make a macroscopic object levitate in air, there is no method other than magnetic levitation. Generally, magnetic levitation of a paramagnetic or ferromagnetic object which is attracted by a magnet is impossible, and only diamagnetic object which receives a repulsive force from a magnet can be magnetically levitated. However, since the magnetic force that a diamagnetic material receives from a magnet is exceedingly weak, we must use one of the most powerful magnets specially established in the institute for strong magnetic field research, and the users, usage time, and application scope are limited. Therefore, it is expected to develop a new method capable of realizing magnetic levitation even with a small magnet such as a permanent magnet.

In previous studies, it was reported that, by creating a small gap between the magnetic poles, the magnetic force there could be increased, and substances with large diamagnetism such as carbon and bismuth could be magnetically levitated even with permanent magnets. In this study, we scrutinized the

magnetic field distribution around magnetic poles of two magnets which are adjacently aligned in the anti-parallel manner, and investigated the possibility of magnetic levitation of "water", instead of bismuth or carbon. Consequently we have successfully demonstrated the levitation of water only by using permanent magnets.

The lower left of Figure 1 shows the layout of two rectangular magnets used for simulating the magnetic field distribution, and the right side of Figure 1 shows an enlarged cross-sectional view of the ridge line of the two magnets which are in contact. We simulated ten different situations of the magnetic field using magnets with different fillet radius, from 0 to 0.9 mm. Here the z-axis is defined perpendicular to the horizontal plane and points vertically upwards. The direction of the magnetic moment of the two magnets is set along the z-axis, and is antiparallel to each other. The end of the contact surface of the two magnets is set to z = 0. Figure 2 shows how the magnetic force changes when the edge radius of the magnet is changed in increments of 0.1 mm. The smaller the edge radius, the greater the magnetic force.



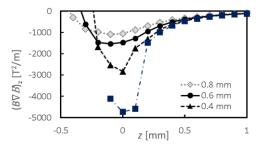


Fig. 1. layout of magnets

Fig. 2. $(B\nabla B)_z$ distribution under various conditions

When the fillet curvature edge radius was 0.6 mm or less, it was found that a region where water can levitate appears in the atmosphere. Magnets commercially available have the fillet radius of about 0.5 mm. This suggests that if a small amount of water is introduced to the space between two contacted magnets, it levitates in air.

In the experiments, we used four small magnets; two are same as the magnets shown in Figure 1 and other two are for modifying the magnetic field slightly and providing a minimal point of total potential energy for the stable levitation of water ball (Figure 3). Since making a small water ball with a diameter of less than 1 mm

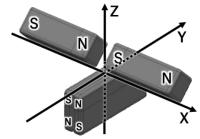


Fig. 3. Layout of magnets for magnetic levitation of water

is really difficult, we generated mist around magnets by using an ultrasonic atomizer. Figure 4 shows a time series of pictures of levitating water ball in the proximity of the ridge line of the magnets. The time we started generating mist is set 0 min. Thereafter, the tiny water droplets started getting together and they formed a water ball (Fig. 4b to e). During the experiments, we observed a layer of water droplets like the Milky Way. This is because the tiny water droplets were accumulated near the potential well before they collided the larger ball. The water ball kept growing up to 0.5 mm diameter, and then contacted the magnet wall in the last.

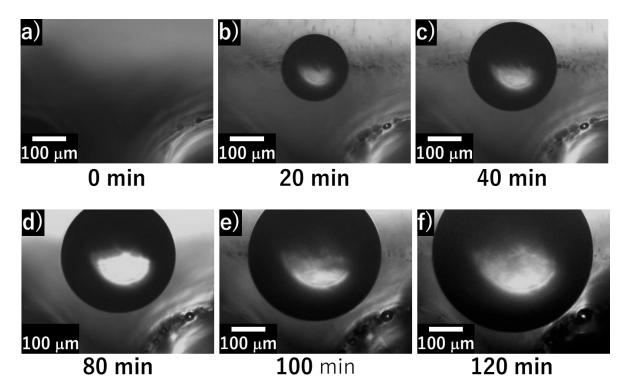


Fig. 4. A time series of pictures of levitating water ball

The method presented here is very easy and low-cost, and we are able to make many kinds of experiments under optical microscope. Therefore, we expect our method makes magnetic levitation more familiar to engineers or researchers and is not only used to a fundamental scientific experiments like crystallization of protein molecules, but is also applied to a variety of applications such as surface tensiometer, viscometer, seismometer, accelerometer, and so on.

References

- [1] Beaugnon, E. & Tournier, R. *Nature*, **349**, 470 (1991)
- [2] Lyuksyutov, I. F. et al., Appl. Phys. Lett. <u>65(10)</u>, 1817-1819 (2004)
- [3] Pigot C., et al., IEEE TRANS. MAG., 44(11), 4521-4524(2008)

Cosmic Magnetic Fields

Jinlin Han

National Astronomical Observatories, Chinese Academy of Sciences; A20 DaTun Road, ChaoYang District, Beijing 100101, China

e-mail: hjl@nao.cas.cn

A variety of approaches are used to investigate the magnetic fields in the Universe. Some are based on magnetic effects on radiation processes of celestial objects, including Zeeman splitting of emission lines from clouds or clumps, polarized thermal emission from aligned dust grains in magnetized clouds, and diffuse radio synchrotron emission from relativistic electrons in magnetic fields in the diffuse medium. The others stem from magnetic effects on the propagation of radiation in the intervening

medium, such as starlight polarization due to selective extinction by magnetically aligned dust grains, Zeeman splitting of absorption lines from foreground magnetized clouds, and Faraday rotation of linearly polarized emission in a magnetized medium.

Magnetic fields have been observed in extended diffuse Galactic interstellar objects, such as supernova remnants, HII regions and bubbles, and interstellar filaments. The field strengths and orientations can be partly derived from available observations, e.g., from starlight polarization, polarized thermal dust emission, polarized synchrotron emission, and Faraday rotation. The orientation of magnetic fields in nearby spiral galaxies follows the spiral arms as shown by starlight polarization and polarized synchrotron emission. Faraday RMs give hints for possible magnetic field onfigurations in only a few galaxies. Magnetic fields in the intracluster medium are revealed by radio halos and relics and RMs of background and embedded sources. The polarized relic emission indicates compressed anisotropic turbulent fields in the shock regions. The existence of magnetic fields in the intergalactic medium and the cosmic web is indicated by radio synchrotron emission, though evidence is sparse.

Future observations should aim at the 3D tomography of the large-scale coherent magnetic fields in our Galaxy and nearby galaxies, a better description of intracluster field properties, and firm detections of intergalactic magnetic fields in the cosmic web.

References

Han JL, et al. 1997, A&A 322, 98 Han JL, et al. 1999, MNRAS 306, 371

Diamagnetism Induced by Atomic-Level Eddy Current

Tsunehisa Kimura ^{1,2*}, Fumiko Kimura ¹, and Yosuke Kimura ¹

¹ Kyoto University, Sakyo-ku, Kyoto 606-8502, Japan; ² Fukui University of Technology, 3-6-1

Gakuen, Fukui 910-8505, Japan

*Corresponding author: tkimura@kais.kyoto-u.ac.jp

Langevin (or Larmor) diamagnetism results from an additional motion of bound electrons induced by an applied dc magnetic field. On the other hand, diamagnetism is also observed when an ac magnetic field is applied to free electrons in conducting material. This is due to the eddy current predicted by Faraday's law of induction. Then, a question may arise: does eddy current occur at the atomic level? The answer is "yes" and we call this diamagnetism Faraday diamagnetism [1].

Figure 1 shows schematic of the motion of a bound electron under dc and ac magnetic fields.

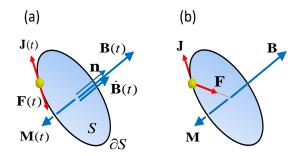


Fig. 1 Comparison of (a) Faraday diamagnetism under ac magnetic field and (b) Langevin diamagnetism under dc magnetic field. The direction of the force \mathbf{F} acting on bound electron is (a) (anti-) parallel to the electric current \mathbf{J} , while it is (b) perpendicular to \mathbf{J} . (reproduced from [1])

The electric current \mathbf{J} of the system (a) induced by the applied ac magnetic field $\dot{\mathbf{B}}(t)$ is described by an RL electric circuit composed of the self-inductance L due to a coil formed by the orbital motion of electron and the resistance R due to thermal noise. Then, the response \mathbf{J} and the resultant magnetization \mathbf{M} is derived. We obtained the diamagnetic susceptibility γ for Faraday diamagnetism as follows:

$$\gamma = 2K\chi$$

where χ is the Langevin susceptibility and K is Nagaoka constant ($0 \le K \le 1$). The total susceptibility measured experimentally is $\chi + \gamma$, indicating that diamagnetism is enhanced.

Due to this enhancement, the anisotropic susceptibility $\Delta \chi + \Delta \gamma$ might also increase under ac magnetic field. We performed magnetic orientation of microcrystals of L-alanine under rotating magnetic fields and obtained a result, $\Delta \gamma / \Delta \chi = 0.94$. This is consistent with the theoretical prediction above.

Reference

[1] T. Kimura, F. Kimura, and Y. Kimura, J. Magn. Magn. Mater. 451 (2018) 65-69.

Improvement in the efficiency of the microbead-arrangement method using magnetic field

Eizo Ushijima ^{1*}, Kenichi Mitsumori², Satoshi Fujimoto², Kazuo Nakazato³

¹ Aisin Cosmos R&D Co., Ltd. (2-36 Hachiken-cho, Kariya-shi, Aichi 448-8650, Japan); ² MEMS

CORE CO., Ltd (3-11-1 Akedori, izumi-ku, Sendai-shi, Miyagi 981-3206, Japan); ³ Nagoya University

(Furo-cho, Chikusa-ku, Nagoya-shi, Aichi 464-8603, Japan)

* ushijima@ai-c.aisin.co.jp,e_ushiji@nuee.nagoya-u.ac.jp

To mitigate the increase in national medical expenses due to the aging population, we are currently researching and developing the sensor for detecting infinitesimal amount substance using complementary metal oxide semiconductor (CMOS) integrated circuits, which is one of the basic technologies in preventive medicine. So far, the microbead-arrangement method using magnetic field was applied to improve the sensor sensitivity of this sensor [1]. In addition, a Halbach array magnet was prototyped as a portable device for generating a strong magnetic field [2]. According to the microbead-arrangement experiment under a strong magnetic field to evaluate the influence of the prototype Halbach array magnet, the arrangement accuracy of the microbeads was

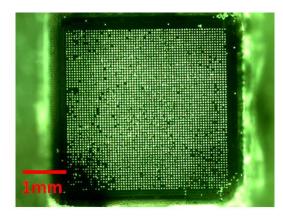


Fig. 1. Surface of the CMOS sensor array with the magnetic arrangement of microbeads observed using a fluorescent microscope camera.

approximately 89%. There is a possibility of improving the sensor sensitivity by increasing arrangement accuracy of the microbeads. In order to improve the arrangement accuracy of the microbeads, the structure on the sensor array and the microbead distribution method were examined. Figure 1 shows the state of the CMOS sensor array surface with the distribution state of microbeads after the experiment. We confirmed that each microbead was arranged in each channel without the surplus microbeads on the other region.

Keywords: microbead-arrangement, CMOS sensor array, Halbach array magnet

Acknowledgment

This work was supported by JST A-STEP Grant Number JPMJTS1514, Japan.

References

[1] E. Ushijima, S. Fujimoto, K. Niitsu, and K. Nakazato, in Proc. IEEE BioCAS2017, pp. 1-4, Oct.2017.

[2] E. Ushijima, K. Nakazato, Proc. MAP8, 2018.

Dark-field microscopy in high magnetic field

Sanne J.C. Granneman^{1*}, Hans Engelkamp¹, Peter C.M. Christianen¹

¹High Field Magnet Laboratory (HFML-EMFL), Radboud University, Toernooiveld 7, 6525 ED

Nijmegen, The Netherlands

*sanne.granneman@ru.nl

The fact that different polymorphs of the same compound can have distinct chemical and physical properties makes polymorphism a pressing problem in the pharmaceutical industry. Consequently, polymorph control during the crystallization process is highly sought after, but can be extremely difficult. An interesting new method recently presented itself with the discovery of a new polymorph of coronene grown inside the magnetic field [1]. To investigate the potentialities of using a (high) magnetic field to

influence polymorphism in pharmaceuticals, the Horizon 2020 project MagnaPharm was initiated. This multidisciplinary project combines experiments in (high) magnetic field with computational investigations as well as state-of-the art electron microscopy.

At the HFML in Nijmegen, we aim at elucidating the mechanism underlying the observed polymorph selection in the magnetic field, and the usually simultaneously observed suppression of nucleation. Initially we studied the crystallization process (caused by cooling of the solution) in high magnetic field with UV-VIS and light scattering techniques. Both techniques give some information about the onset of crystal growth, but they turned out to be not sensitive enough to precisely pinpoint nucleation. A more typical and sensitive method to study the crystallization process is optical microscopy. However, the noisy environment and limited space inside the magnets make this very challenging. Already existing optical microscopy inserts at the HFML were built to accommodate imaging with incident or transmitted light, Schlieren microscopy and shadowgraphy [2]. Unfortunately, these techniques have the disadvantage that the experiments have to be performed on static, already existing crystals, or have relatively low optical resolution.

To be able to pinpoint precisely the onset of nucleation, a new insert based on a Schwarzschild objective was designed and built in-house. With this type of objective, only light which is scattered by the sample is visualized, making this insert a dark-field microscope. By incorporating local heating and a thermometer, the temperature of the sample is accurately controlled. This dark-field microscopy insert is very versatile, allowing studying not only the onset of nucleation, but also for instance the effect of the magnetic field on already existing, mobile, crystals. This talk discusses the design of the dark-field microscopy insert and several applications in magnetic field.

Acknowledgments: This research is funded by the European Union's Horizon 2020 Research and Innovation programme under Grant Agreement Number 736899.

References

[1] J. Potticary, L. R. Terry, C. Bell, A. N. Papanikolopoulos, P. C. M. Christianen, H. Engelkamp, A. M. Collins, C. Fontanesi, G. Kociok-Köhn, S. Crampin, E. Da Como, and S. R. Hall, Nature Communications 7 (2016) 11555 [2] P. W. G. Poodt, Doctoral Thesis, Radboud University Nijmegen, (2008)

Detection of gravitational waves by use of magnetic fields

Hao Wen
Chongqing University, China

High-frequency Gravitational waves [HFGWs, e.g., in 10⁹Hz (GHz) or higher bands] can propagate through and interact with background high magnetic fields (static or quasi-static), leading to the perturbed electromagnetic waves (EMWs). In the past 20 years, our group in Chongqing University, have persistently investigated the scheme of gravitational wave (GW) detection by trying to capture such perturbed EMWs, based on use of high magnetic fields. From 2013, in cooperation with the High Magnetic Field Laboratory, Chinese Academy of Sciences (CHMFL), and other collaborators, we proposed the project to construct the first HFGW detector in the world for GHz or higher bands, as one of the most promising schemes so far. Therefore, in this presentation, we will briefly report the main

aspects and some new progresses of the detection of GWs by use of magnetic fields. In recent years, the LIGO and Virgo have successfully realized direct detections of GWs produced by binaries of compact astrophysical bodies (black holes or neutron stars), in the frequency band around some 10^1 to 10^2 Hz, but, the HFGWs (from the inflation, various cosmological models, high-energy astrophysical processes, braneworld, etc.) cannot be detected by LIGO or Virgo due to their specific detection mechanism. Actually, until now, such HFGWs have never been captured, though, they contain very rich and crucial cosmological and astrophysical information, related to many fundamental issues of the Universe and gravity, such as the big-bang, dimensions of the space, essence of the time, dark energy and dark matter. Thus, the scheme of GW detection by use of magnetic fields, should be a very important and interesting topic, and will also be complementary to the detections by LIGO, Virgo and other detectors, for different frequency bands.

Development of high gradient magnetic separation system for the removal of scales from boiler feed water in thermal power plant

Noriyuki Hirota¹, Hidehiko Okada¹, Fumihito Mishima², Shigehiro Nishijima², Yoko Akiyama³, Hideki Matsuura⁴, Seitoku Namba⁴, Tomokazu Sekine⁵

¹ National Institute for Materials Science, 3-13 Sakura, Tsukuba, 305-0003, Japan; ² Fukui University of Technology., 3-6-1 Gakuen, Fukui, 910-8505, Japan; ³ School of Engineering, 2-1 Yamadaoka, Osaka Univ., Suita 565-0871, Japan; ⁴ Shikoku Research Institute Inc. 2109-8 Yashimanishi, Takamatsu 761-0192, Japan; ⁵ Ebara Industrial Cleaning Co. Ltd., 1-4-1 Egawa, Kawasaki, 210-0823, Japan

*Corresponding author: <u>hirota.noriyuki@nims.go.jp</u>

The thermal power generation is one of the major ways to generate electricity, however, they discharge a large amount of carbon dioxide. Improvement of the energy conversion efficiency in thermal power plants is expected to contribute for reduction of fuel consumption and carbon dioxide emission. A thermal power plant consists of steam turbine generators, boilers and a system to feed water to boilers. Deposition of scale in the water circulation system and the boiler degenerates energy conversion efficiency. Therefore, reduction of scale seems to contribute to decrease fuel consumption and carbon dioxide emission.

Most of scales consist of iron oxides. Iron dissolved in boiler feed water from walls of pipes and devices at relatively lower temperature part, and then, flows into the boiler. When temperature of water excesses about 200 ℃, most of irons form magnetite (Fe₃O₄) and deposits on wall of pipes. Magnetite can be separated magnetically from the boiler feed water. Therefore, we are investigating the way to adopt the high gradient magnetic separation (HGMS) technique to this system. In case of HGMS, the matrix that consists of ferromagnetic wire meshes is set in the flow path located in a superconducting magnet bore. Magnetite particles attracted and deposited to magnetized wires due to the magnetic force. Preferable position to set the magnetic separation system in the feed water circulation path, suitable matrix structures, required condition of superconducting magnet, operation condition and procedure have been studied based on simulation and experiments. In case of AVT type thermal power plants, one of the suitable locations to install the separation system seems to be the drain of high pressure heater

where a part of feed water flows. In there, the concentration of scale is relatively high and the quantity of flow is around 400 to 500 m³/h in 200 °C and 20 atm. As a result of our experiments and simulations, it was confirmed the aligned structure of ferromagnetic mesh that the downstream wires arranged parallel to the upstream wires seems good to capture larger amounts of particles. To use the whole matrix to capture the particles uniformly and to extend the utilizable time of the system without cleaning of the matrix, lower applied magnetic fields is better as an operation condition. In this presentation, the scheme of this project and the recent progress of this study will be reported.

Acknowledgement

This work is partially supported by Advanced Low Carbon Technology Research and Development Program (ALCA) of JST Strategic Basic Research Programs.

Magnetic Separation of diverse Rare Earth Ions

Barbara Fritzsche ^{1*}, Daniel Fischer ¹, Zhe Lei ^{1,2}, Xuegeng Yang ², Kerstin Eckert ^{1,2}

¹Institute of Processing Engineering and Environmental Technology, Technische Universität Dresden, D-01069 Dresden, Germany; ² Institute of Fluid Dynamics, Helmholtz-Zentrum Dresden-Rossendorf (HZDR), Bautzner Landstrasse 400, D-01328 Dresden, Germany

*Corresponding author: Barbara.Fritzsche@tu-dresden.de

Rare earth (RE) elements are key to many green-energy technologies such as wind turbines and

hybrid electric vehicles. They are critical in the near future because their demand will outgrow the supply. Hence, the recycling of REs, is an important issue. Beside highthe temperature pyrometallurgy, hydrometallurgical route is the most wellapplied technique in rare earth extraction. The method is time-consuming and requires a large amount of non-recyclable chemicals. Hence, further innovations are necessary. One option is to exploit the magnetic properties of RE ions, based on their unfilled 4f orbits, to perform a magnetic separation step. The magnetic separation represents the

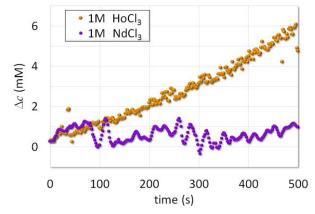


Fig. 1 Concentration gradient development for 2 different RE solutions 1 mm away from the free surface in 500 s of magnetic influence.

possibility to improve the separation efficiency of RE ions without applying high temperatures or large amounts of non-recyclable solvents. The magnetic separation of several RE ions in aqueous solutions was studied with Mach-Zehnder interferometer. The method employs the fact that the refractive index of the solution is a linear function of concentration. Under the action of inhomogeneous magnetic field, the fringes in the interferogram bend as the result of a change in the refractive index. The change in the refractive index is later converted into the change in the concentration. The magnetic field was applied above the cubic optical cuvette containing the RE solution by means of Halbach array, consisting 8

permanent magnets with dimensions of 10x10x40 mm³. The temporal evolution of the RE ions concentration in the optical cuvette was studied during the magnetization [1]. It was found that some RE ions (e.g. Gd, Dy) collect in the vicinity of the magnet [2], while some did not react with the applied magnetic field (e.g. Nd, Sm). The results are a good prospective for separation of rare earth ions by a magnetic field.

References

- [1] Pulko, B., Yang, X., Lei, Z., Odenbach, S., Eckert, K. Applied Physics Letter, 105: 232407. 2014
- [2] Lei, Z., Fritzsche, B., & Eckert, K. The Journal of Physical Chemistry C, 121(44): 24576-24587. 2017

Magnetic separation of Dy(III) from solution, stability issue and transport process

Zhe Lei ^{1,2*}, Barbara Fritzsche ², Xuegeng Yang ^{1,2}, Kerstin Eckert ^{1,2*}

¹ Institute of Fluid Dynamics, Helmholtz-Zentrum Dresden-Rossendorf (HZDR), D-01328 Dresden, Germany; ²Institute of Processing Engineering and Environmental Technology, Technische Universitaet Dresden, D-01069 Dresden, Germany

*Corresponding author: z.lei@hzdr.de; k.eckert@hzdr.de

The Kelvin force has a long history of being applied in separating particles with contrasting electromagnetic properties. In the past decades, a surprising effect of the Kelvin force on a local formation of enrichment of paramagnetic ions, despite the presence of a dominating thermal energy, has been repeatedly reported. This phenomenon inspires a magnetic separation technique of rare earth (RE) ions. Since the chemical similarity of the rare earth forces a large number of time-consuming extraction steps, efficiently exploited differences in the magnetic moments of the rare earth ions could speed up the process significantly. However, the application of such a magnetic separation step requires a sufficient understanding of the above-mentioned observations. Due to the huge difference in the order of magnitude between the kinetic energy and the magnetic energy, it actually seems unlikely that Kelvin force has a direct influence on the paramagnetic ions. In fact, an external source of a concentration gradient, e.g. evaporation, is needed. Evaporation gives rise to local enrichment at the interface by losing water molecules across the interface. Generally, the evaporation-driven concentration boundary layer is hydrodynamically unstable, because it is heavier than the underlying bulk fluid. It is the field gradient force, acting in the opposite direction to gravity, which suppresses the resulting Rayleigh-Taylor instability. We showed that the gravitational force acting on the boundary layer, expressed in a nondimensional manner by the Rayleigh number, is drastically diminished by the approximately five times larger Kelvin force. To further exploit the potential of magnetic separation, the limit of magnetic separation corresponding to an applied magnetic field as well as the accompanied transport process is pending for investigation.

- [1] Pulko, B., Yang, X., Lei, Z., Odenbach, S., Eckert, K. Applied Physics Letter, 105: 232407. 2014
- [2] Lei, Z., Fritzsche, B., & Eckert, K. The Journal of Physical Chemistry C, 121(44): 24576-24587. 2017
- [3] Lei, Z., Fritzsche, B., & Eckert, K. Physical Review E (submitted)
- [4] Yang, X., Tschulik, K., Uhlemann, M., Odenbach, S., & Eckert, K. The journal of physical chemistry letters, 3(23): 3559-3564. 2012

October 13, 2019, Session 2

Emergent transport phenomena in topological spin textures revealed by high magnetic field measurements

Yukako Fujishiro ^{1*}, Naoya Kanazawa ², Yoshinori Tokura ^{1, 2}

¹ Dept. Applied Physics, The Univ. of Tokyo, Bunkyo-ku, Tokyo 113-8656, Japan; ² RIKEN Center for Emergent Matter Science, Wako, Saitama 351-0198, Japan

*Corresponding author: fujishiro@cmr.t.u-tokyo.ac.jp

The interplay between topological spin textures and conduction electrons gives rise to emergent magnetic field which can be exploited for novel functionalities. One distinct example is a spin hedgehog lattice (Figure 1) which shows various emergent transport phenomena (e.g. topological Hall effect ^[1], magneto-resistivity^[2]), whose magnitude are quite large compared to the conventional skyrmion systems. In the search for even more gigantic emergent responses from topological spin textures, further understandings of the unusual transport properties in the spin hedgehog lattice is of great importance.

In this talk, we would like to report the high-magnetic-field study on the spin hedgehog lattice. In particular, we have discovered (i) large magneto-Seebeck effect in MnGe^[3], and also realized (ii) topological transitions between skyrmion- and hedgehog- lattice states in MnSi_{1-x}Ge_x (Figure 2)^[4]. We would like to discuss the unusual magnetic fluctuations discovered at high-magnetic-field regime, as well as the possible formation mechanisms of the spin hedgehog lattice which is beyond the conventional paradigm based on the Dzyaloshinskii-Moriya interaction.

This work is done in collaboration with The Institute of Solid State Physics (ISSP), Institute for

Materials Research (IMR), and Neutron Science and Technology Center, Comprehensive Research Organization for Science and Society (CROSS).

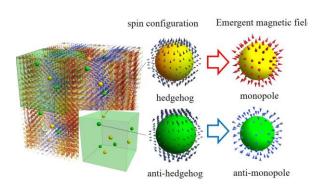


Fig. 1 Spin hedgehog lattice realized in MnGe.

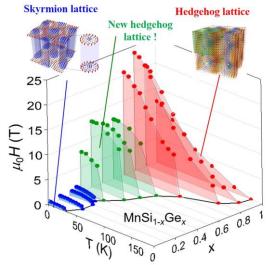


Fig. 2 Magnetic phase diagrams in MnSi_{1-x}Ge_x.

References

[1] N. Kanazawa et al., Phys. Rev. Lett 106, 156603 (2011).

- [2] N. Kanazawa et al., Nat. Commun. 7, 11622 (2016).
- [3] Y. Fujishiro*, N. Kanazawa* et al., Nat. Commun. 9, 408 (2018).
- [4] Y. Fujishiro et al., Nat. Commun. 10, 1059 (2019).

Effects of Berry curvature studied through thermal Hall conductivity measurements in 35 Tesla: electrons in a canted ferromagnet and Bogolyubov quasiparticles in a cuprate superconductor

M. Hirschberger¹, T. Loew², J. Xiong³, T. Liang1, T. Gao³, Y. Kaneko¹, J. B. Kemper⁴, G. Boebinger⁴, B. Keimer², N. P. Ong3, and Y. Tokura^{1, 5}

¹ RIKEN Center for Emergent Matter Science (CEMS), Wako 351-0198, Japan; ² Max Planck Institute for Solid State Research, 70569 Stuttgart, Germany; ³ Department of Physics, Princeton University, Princeton, NJ 08544; ⁴ Department of Physics, Florida State University, Tallahassee, FL 32310 and National High Magnetic Field Laboratory, Florida State University, Tallahassee, FL 32306;
 ⁵ Department of Applied Physics and Tokyo College, University of Tokyo, Bunkyo-ku 113-8656, Japan

Resistive high-field magnets are ideally suited for measurement of thermal transport coefficients in bulk samples, which necessitate relatively long (>1 second) relaxation times. We exemplify the power of high-field thermal transport studies, in particular of the thermal Hall effect κxy , in two cases:

- (1) In Nd2Mo2O7, a metallic ferromagnet with slightly canted spins, the thermal Hall signal allows us to study how inelastic scattering affects the anomalous Hall current. We also investigate how carrier doping tunes the relative weight of two contributions to the anomalous Hall current, namely the Karplus-Luttinger term proportional to the net magnetization, and the 'geometrical' Hall effect from scalar spin chirality. The latter dominates in low fields.
- (2) Thermal conductivity and thermal Hall effect measurements, being direct probes of the Bogolyubov quasiparticles near the nodal region of the d-wave gap, shed light on the fascinating field-induced phase transition to charge order in underdoped copper oxide superconductors (YBCO6.55).

ME composite PMNT/Metglas and magnetic sensor

<u>Haosu Luo</u>*, Wenning Di, Li Lu, Bingging Xu, Fei Hu, Xiefu Wang, Zhiyun Chen Shanghai Institute of Ceramics, Chinese Academy of Sciences, Shanghai 201800, China *Corresponding author: hsluo@mail.sic.ac.cn

The ME laminate composites were investigated with the sandwich structure of PMN-PT single crystal and Metglas. ME charge coupling coefficient α_Q , permittivity C, dielectric loss $\tan\delta$ are key parameters for ME chips used for magnetic sensing at low frequency. These parameters were tailored to enhance ME coupling effect and to reduce intrinsic electric noise for low frequency sensing application upon FOMs of ME composite. The multi-push-pull mode ME and multi- L-T mode composite were

designed and fabricated. A charge amplifier with ultra-low intrinsic noise has been used to get the ME coupling signal of ME laminate composite at low frequency. The ultrahigh sensitivity of magnetic anomaly signal was achieved in accordance with the modeling prediction. The noise equivalent magnetic induction of sensor has been achieved as 2pT/Hz^{1/2}@1Hz, 0.1pT/Hz^{1/2}@10Hz, and 9 fT/Hz^{1/2}@EMR.

Solvent-assisted magnetic manipulation of molecular orientation, film structure and charge transport of semiconducting polymers

Fapei Zhang^{1*}, Guoxing Pan^{1, 2}, Xuhua Xiao¹, Songlin Su²

¹ Anhui Province Key Laboratory of Condensed Matter Physics at Extreme Condition, High Magnetic Field Laboratory (HMFL), Chinese Academy of Science, Hefei 230031, P. R. China; ² Anhui University, Institutes of Physical Science and Information Technology, Hefei 230026, P.R. China *Corresponding author: fzhang@hmfl.ac.cn

Controlling molecular orientation and film ordering of organic semiconductors is crucial to achieve high performance devices such as organic field-effect transistors (OFETs) and organic photovoltaics (OPV) due to high anisotropy of the π -conjugated molecular structure^[1]. High magnetic field (HMF) provides a clean and versatile approach to induce molecular alignment for structural manipulation of organic materials. In the previous work, we have achieved large-area highly ordered and oriented films of the semiconducting polymers via solution casting process under HMF^[2]. However, finer control on the HMF-induced film growth is still needed to develop to achieve the desired structure. In particular, poor homogeneity of film thickness and morphology, which often occurs during solution-cast under HMF, deteriorates the performance and performance reproducibility of organic electronic devices.

To tackle these issues, we propose a novel magnetic alignment strategy: solvent vapor annealing (SVA) of the as-(spin) cast polymer films under HMF (up to 9T). Two kinds of the high-performance donor-acceptor (D-A) copolymers P (NDI2OD-T2) and DPPDTT were employed. By this strategy, we have achieved large-area texture structure of semiconducting polymers with a high homogeneity of film morphology and thickness. Polarized UV-vis absorption, AFM and GIXRD characterizations reveal that the chain backbones of the P (NDI2OD-T2) and DPPDTT in the films are highly aligned along the applied magnetic field (in Fig. 1(b)). More interestingly, it is found that the degree of chain alignment and film crystallinity are significantly enhanced compared to the films via solution-cast under HMF. Based on systematic microstructure analysis of the polymer films grown from various SVA conditions (cast solvents, annealing time and field strength), we proposed the magnetic alignment mechanism in SVA which emphasizes that tiny aggregates of the D-A copolymers, re-formed in the solvent-swollen films, initiate magnetic alignment and are followed by a solvent-induced self-assembly in viscous film matrix. In addition, the SVA process can be combined well with the time-modulated magnetic field technique reported previously^[2] to effectively control the orientation of π -conjugated planes of the backbones. Thus the degree of face-on molecular packing of P (NDI2OD-T2) is enhanced remarkably.

Polymer FETs were fabricated to assess the impact of magnetic alignment on charge transport properties. The devices based on the magnetically -aligned P (NDI2OD-T2) films exhibit a significant enhancement of electron mobility by a factor of 19 compared to the unaligned devices, as well as a

exceptionally large mobility anisotropy of 160 (ratio of $\mu_{\text{M}}/\mu_{\perp}$, $\mu_{\text{M}}/\mu_{\perp}$) denotes the mobility where channel current is parallel (perpendicular) to the field direction, respectively) (in Fig,1(c)). The aligned DPPDTT devices also show a remarkably enhanced mobility and mobility anisotropy of 6.0. The strategy proposed here presents a nice pathway to optimize film microstructures and thus improve the performance of OFETs and OPV.

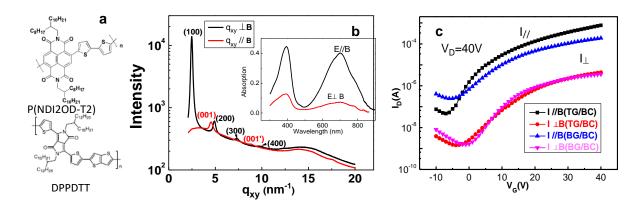


Fig. 1 (a) Chemical structure of P (NDI2OD-T2) and DPPDTT; (b) In-plane GIXRD patterns of the P (NDI2OD-T2) film from SVA under the HMF of 8 T. The inset shows the polarized UV-vis absorption spectra; (c) Transfer curves of top-gate/bottom-contact (**TG/BC**) and bottom-gate/Bottom-contact (**BG/BC**) FET devices (channel length: $2.5\mu m$, channel width: 2 mm) of the magnetically aligned P(NDI2OD-T2) film from SVA-HMF process. Channel current is parallel ($I_{1/2}$) and perpendicular ($I_{1/2}$) to the direction of the magnetic field applied during SVA.

References

[1] A. M. Hiszpanski, Y. L. Loo, Energy Environ. Sci. 7 (2014), 592-608.

[2] G. Pan, F. Chen, L. Hu, K. Zhang, J. Dai and F. Zhang, Adv. Funct. Mater. 25 (2015), 5126-5133.

Comparison of Crystal Growth Approaches and Novel Properties of Pure and Mixed Rare Earth Orthoferrites

¹ Institute of Solid State and Semiconductor Physics, Belarusian Academy of Science, 19 P. Brovka st.,22072 Minsk, Belarus; ² Shanghai Institute of Ceramics, Chinese Academy of Science,1295 Dingxi Road, 200050 Shanghai, People's Republic of China *Corresponding author: bars@physics.by

Taking in mind numerous future practical applications of antiferromagnets crystal growth technology, and especially scientific approach to the complex area of rare earth orthoferrites (REOF) and other optically transparent weak ferromagnets (WFM), will be of greater importance as crystal sizes and demands for structural perfections, homogeneity and defect control will increase. Demands for explosively rising density of information storage and sharply increasing speed of manipulation has triggered an extensive challenge of ways to control the magnetization of a functional medium by means of other than rapid external magnetization and/or temperature changes, caused by the ultrafast laser

radiation, assessing time scale of picoseconds or less. In that cases thermal origin of spin excitations considerably limits technical applications due to the repetitive frequency is limited by the cooling time. Last decade it has been shown experimentally in REOF that circularly polarized femtosecond laser pulses can be used to non-thermally excite and coherently control the pain dynamics in these WFM by the way of the inverse Faraday effect [1].

It is known that REOF solid solutions of a type Re_{1-x}Re²_xFeO₃ allow to tailor their properties by varying the type and relative content of rare earth ions [2]. Besides small magnetization moment these materials exhibit a giant Faraday rotation. Thus, Sm_{1-x}Re²_xFeO₃ solid solutions are the promising material for realizing a room temperature functionality, including ultrafast laser-induced magnetization control, ferroelectricity, etc. For example, using a single-shot magneto-optical imaging technique it has been shown that the excitation of Sm_{0.5}Pr_{0.5}FeO₃ with a circularly polarized 60 fs laser pulse (LP) can effectively trigger an ultrafast spin reorientation and create a homogeneous magnetic domain with the orientation of the magnetization defined by the helicity of the LP [3]. This observation reveals the possibility to coherently control a magnetic phase transition (PT) and create magnetic domains without applying any magnetic field. As it has been stated the control is mediated by long-living coherent spin precession which is excited long before the PT takes place. A striking feature of this mechanism is that the route of the phase transition can be controlled through three parameters independently: the helicity of the LP polarization, the initial temperature of the sample, or the LP fluence.

Crystal growth studies of REOFs have been provided by many groups through different experimental approaches. Although many efforts have been made, it has not been easy to get perfect single crystals. Either oxygen non-stoichiometry, or non-homogeneity caused by segregation as well as cracks and dislocations were usually found in crystals grown by floating zone (FZ) technique. Otherwise, a foreign ion contamination both form carriers/crucibles, and from solvents was a common case in the crystals grown from high temperature fluxed melts.

Last century the flux growth has been the most popular method of producing small REOF crystals suitable for magnetic, thermal, elastic and magneto-optical measurements. Although large and close to perfect crystals could be grown by this technique using controlled crystallization on seeds from relatively stable solvents based on the appropriate mixture of BaO, BaF_2 and B_2O_3 [4].

In the early 1970s, Fairholme et al. were the first to publish encouraging results on the growth of REOF crystals by the FZ technique [5]. The advantages of this technique were reported to be reduced growth time and less contamination revealing since neither a crucible, nor solvents are required. Since an extra high oxygen pressure was involved by Balbashov's group from Moscow this container-free approach has become a preferred growth method for various unique classes of magnetic oxides, especially for those showing extreme melt reactivity and high melting temperature [6]. The temperature of the molten zone, pooling and rotating rates, atmosphere environment and pressure in the growth chamber all play an important role in the crystal growth process. Last two decades a wide set of significant results in REOF growth by the FZ approach and their properties investigation have been published by research groups from China [7-9]. In our talk we will compare some of these results with the significant data provided by other groups mostly for the REOF systems, which are a very prospecting for future applications.

References

[1] Kimel, A.V., A. Kirilyuk, P. A. Usachev, R. V. Pisarev, A. M. Balbashov, and Th. Rasing, Nature 435 (2005) 655–657.

- [2] R. C. Sherwood, L. G. Van Uitert, and R. Wolfe, Physical Letters A, 25(1967) 297–298.
- [3] J.A. de Jong, I. Razdolski, A.M. Kalashnikova, R.V. Pisarev, A.M. Balbashov, A. Kirilyuk, Th. Rasing, and A.V. Kimel, Phys. Rev. Lett. 108 (2012) 157601.
- [4] S.N. Barilo, A.P. Ges, S.A. Guretskii, D.I. Zhigunov, A.A. Ignatenko, A.M. Luginets and E.F. Shapovalova, J. Cryst. Growth 108 (1991) 309–318.
- [5] R.J. Fairholme, J.P. Gill, and A. Marsh, Mat. Res. Bull. 6 (1971) 1131-1140.
- [6] A.M. Balbashov, and S.K. Egorov, J. Cryst. Growth 52 (1981) 498–504.
- [7] Xinwei Li, Motoaki Bamba, Ning Yuan, Qi Zhang, Yage Zhao, Maolin Xiang, Kai Xu, Zuanming Jin, Wei Ren, Guohong Ma, Shixun Cao, Dmitry Turchinovich, Junichiro Kono, Science 361 (2018) 794-797.
- [8] Ya-Jiao Ke, Xiang-Qun Zhang, Yue Ma & Zhao-Hua Cheng, Anisotropic magnetic entropy change in RFeO₃ single crystals (R = Tb, Tm, or Y), Nature comm, Scientific Reports | 6:19775 | DOI: 10.1038/srep19775.
- [9] Yabin Wang, Shixun Cao, Mingjie Shao, Shujuan Yuan, Baojuan Kang, Jincang Zhang, Anhua Wu, Jun Xu, J. Cryst. Growth, 318 (2011) 927-931.

Numerical simulation of mass transfer and flow near conically shaped electrodes under the influence of a magnetic field

M. Huang ^{1*}, G. Marinaro ^{1,2}, X. Yang ^{1,2}, K. Eckert ^{1,2}, G. Mutschke ¹

*Corresponding author: m.huang@hzdr.de

Magnetic-field assisted electrochemical deposition is a highly efficient method for synthesizing micro- and nano-structured deposits, which have gained much attention due to their numerous applications in areas including microscopy, super-hydrophobic and electrocatalytic materials [1,2]. It is well known that the beneficial influence of magnetic fields on transport and mixing of the electrolyte can be attributed to the action of the Lorentz force and the magnetic gradient force [3]. Fig. 1 schematically shows the flows induced by the Lorentz force f_L , the magnetic gradient force f_m , and the buoyancy force f_g near a conical cathode. The Lorentz force $f_L = j \times B$ is given by the vector product of the current density j and the magnetic flux density j and is creating an azimuthal primary flow around the cone [3]. The centrifugal force generated from this primary flow gives rise to a secondary flow which brings fresh bulk electrolyte downwards to the tip of the cone. The magnetic gradient force exists in inhomogeneous magnetic field and is defined as $f_m = \chi_{sol}/\mu_0(B \cdot \nabla)B$ with $\chi_{sol} = \sum_i \chi_i^{mol} c_i + \chi_{H_2O}$ denoting the total magnetic susceptibility of the electrolyte. Here μ_0 is the vacuum permeability, χ_{H_2O} is the susceptibility of water, c_i and χ_i^{mol} are the concentration and the molar susceptibility of species i, respectively. Depending on the temporal evolution of the concentration distribution in the electrochemical cell, the direction and the amplitude of the magnetic gradient force

may vary during the deposition process. Apart from the magnetic forces, the electrochemical reaction taking place at the cathode causes lower electrolyte density in this area, which gives rise to the buoyancy

¹ Institute of Fluid Dynamics, Helmholtz-Zentrum Dresden-Rossendorf, 01314 Dresden, Germany;

² Institute of Process Engineering and Environmental Technology, Technical University of Dresden, 01062 Dresden, Germany

force $f_g = g(\rho - \rho_0)$, where $g = [0, -9.81, 0] \text{ m/s}^2$ is the gravitational acceleration, and ρ_0 is the bulk density of the electrolyte. When the cathode is placed at the bottom of the electrochemical cell, the buoyancy force near the cathode tends to bring the electrolyte upwards, which in interaction with the magnetic forces will generate a complex three-dimensional flow.

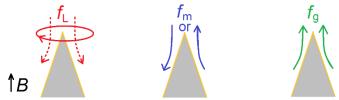


Fig. 1 Flow (schematically) generated by the Lorentz force $f_{\rm L}$ (primary and secondary flow drawn by solid and dashed lines, respectively), the magnetic gradient force $f_{\rm m}$, and the buoyancy force $f_{\rm g}$ near the conical cathode.

This flow can be expected to influence the mass transfer on the cathode. It is therefore possible to control the electrodeposition process by properly adjusting the magnetic fields imposed on the electrochemical cell [2, 3]. In the present work, the contribution of the magnetic forces during electrodeposition process on conically shaped copper and iron electrodes was studied by measurements and by numerical simulations. A permanent magnet was placed below the electrochemical cell, which generates a quasi-homogeneous vertical magnetic field near the Cu cone and high magnetic field gradients near the Fe cone due to the magnetization of the latter. This configuration ensures a high magnetic gradient force near the Fe cone, while for the Cu cone only the Lorentz force and the buoyancy force act. For the Cu cone, as shown in [4], there is good quantitative agreement of the concentration distribution between the simulation and the experimental results obtained by Mach-Zehnder interferometry. Also qualitative agreement with respect to the convection pattern was found. The Lorentz force can bring the bulk solution towards the electrode and thus enhance the mass transfer of the ions towards the cone tip, which is counteracted by the upward buoyancy flow originating from the bottom of the cone (Fig. 2(a)). For the magnetized Fe cone, the magnetic gradient force near the tip of the cone gives rise to a downward flow in this region, which further suppresses the buoyancy flow and enhances the local mass transfer, especially in the upper part of the Fe cone (Fig. 2(a)). A comparison of the deposit thickness along the conical surface without magnetic field, with a homogeneous field (Cu) and with an inhomogeneous field (Fe) is shown in Figure 2(b). It could be concluded that the conical growth is supported by the magnetic forces, especially in case of the Fe cone, which indicates the high potential of using magnetic forces as a beneficial tool in electrodeposition processes on ferromagnetic cones.

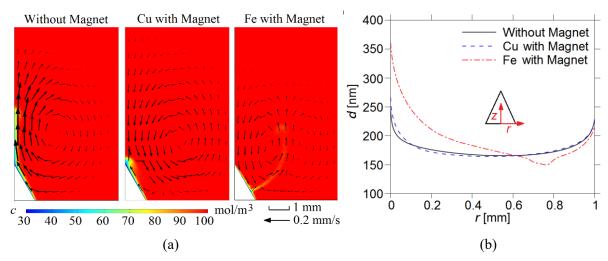


Fig. 2 (a) Concentration distribution superimposed with the meridional velocity vectors near a conical cathode without magnetic field, with a homogeneous field (Cu), and with an inhomogeneous field (Fe) after 10 s deposition. Only half of the cone is shown due to symmetry. (b) Deposit thickness along the conical cathode after 30 s deposition. The conical growth is supported by the magnetic forces especially in case of the Fe cone, as visible in a thick deposit near the Fe cone tip.

References

- [1] N. Wang, T. Hang, D. Chu and M. Li, Nano-Micro Letters 7 (2015) 347-352.
- [2] M. Uhlemann, K. Tschulik, A. Gebert, G. Mutschke, J. Fröhlich, A. Bund, X. Yang and K. Eckert, The European Physical Journal Special Topics 220 (2013) 287-302.
- [3] G. Mutschke, K. Tschulik, T. Weier, M. Uhlemann, A. Bund and J. Fröhlich, Electrochimica Acta 55 (2010) 9060-9066.
- [4] M. Huang, G. Marinaro, X. Yang, B. Fritzsche, Z. Lei, M. Uhlemann, K. Eckert and G. Mutschke, Journal of Electroanalytical Chemistry 842 (2019) 203-213.

Control of Crystallization by Magnetic Field

Isao Yamamoto*

Department of Physics, Yokohama National University, 79-5 Tokiwadai, Hodogaya-ku, Yokohama 2408501, Japan

*Corresponding author: yamamoto-isao-ds@ynu.ac.jp

Techniques for making large crystal with high quality has been investigated because good crystals give the intrinsic physical and chemical properties of the material and suggests its application. Various magnetic fields as a tool are applied to make a good crystal [1-3]. Liquid-liquid interfacial precipitation (LLIP) method is one of the techniques of crystallization from solution. First, two kinds of solvent are stacked to form their interface. One is a good solvent saturating with the desired material, and the other is a poor solvent for the material. In general, a solvent with low density is stacked on the other solvent with high density in order to prevent the convection owing to gravity. A supersaturated layer is generated near the two-dimensional interface due to interdiffusion of the two liquid. Seed crystals are born and grown in the supersaturated layer. The sedimentation speed is slower for small crystals and is accelerated with increasing size of crystal according to Stokes' law. When the grown crystal leaves from the interface and sunk to the bottom then the growth reaction is completed. The magnetic field and its gradient are considered to influence the crystallization processes of LLIP method. The generation of seed crystal and the growth rate are controlled by the magnetic field because the degree of the super-saturation depended on the diffusion of solution is controlled by the Lorentz force. The growth direction is controllable magnetically because the posture of crystal is controllable against the two-dimensional interface if the crystal has anisotropic magnetic susceptibility. In addition, the crystal size is controllable because the staying period at around the super-saturated layer, which corresponds the reaction period, is controllable according to apply of magnetic force parallel or antiparallel to gravity. Various materials were crystallized by using LLIP method under the influence of magnetic fields.

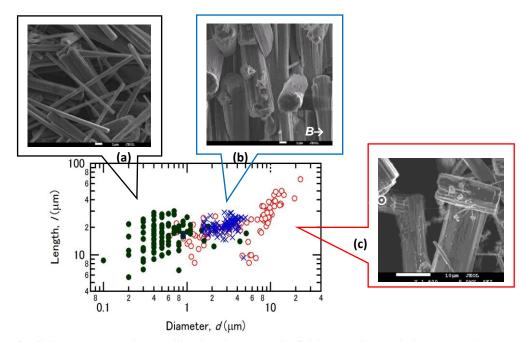


Fig. 1 Scatter plot for fullerene nano-rod crystallized under magnetic fields [4]. The symbols \bullet , \times , and \circ corresponded to the rod crystalized in (a) zero magnetic fields, (b) horizontal homogeneous field of 9.6 T, and (c) vertical field of B = 7.2 T with gradient of dB/dz = 58 T/m. The directions of magnetic flux were shown by allows. The scale bars indicated 1 m for (a) and (b), and 10 m for (c), respectively.

The magnetic field effects of the size, morphology, magnetic orientation, and quality of crystal were evaluated for C₆₀-fullerene nano-rod (FNR), NaCl salt, ice, glycine, taurine, lysozyme, thaumatin, etc[5]. For example, the long axis of FNR was oriented perpendicular to the magnetic flux as shown in Fig. 1(b). The volume of FNR was enlarged by 10 times in the homogeneous horizontal magnetic field of 13 T. Under the influence of the gradient vertical magnetic field, the volume was increased 100 times in the reduced gravity environment as shown by open circles in Fig. 1. The size effects were also recognized for other crystals. Moreover, crystal hobbit and morphology were changed as a magnetic field effect.

The magnetic field effect on size is applicable to crystallization of protein for drag discovery, because crystallization for many unknown proteins is hard to make a good large crystal. If huge crystal is precipitated then the protein is analyzed easily by XRD structure analysis. A hen egg white lysozyme was crystalized by the LLIP method under magnetic fields of up to 13 T. As a result, ten times huge protein crystals were observed under horizontal magnetic field with the gradient as shown in Fig. 2. Their XRD structure analysis showed that the crystal kept high quality with the maximum resolution of 1.22 Å and R-merge of 4.6% as shown in Fig. 2(a). The high mosaicity was also kept because the crystal aligned perfectly to magnetic flux as shown in Fig. 2(b). Crystallization is controllable by the aide of mechanical forces by magnetic fields.

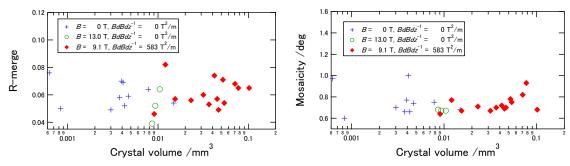


Fig. 2. Crystal volume dependency of (a) R-merge and (b) Mosaicity for Lysozyme under horizontal magnetic field[5,6]. The Lysozyme was crystalized by LLIP method using paramagnetic NiCl2 as a precipitant agent.

Acknowledgements: This work was partially supported by JSPS KAKENHI Grant No. 16K04946 and JASRI/Spring-8 Grant No. 2016B2899. Experiments were performed at Inst. Analysis Center of Yokohama National University and NIMS. The SAXS was measured at KEK-PF and BL38B1 in SPring-8, Japan.

- [1] S. Chandrasekhar, Philos. Mag. 43 (1952) pp. 501-532.
- [2] H. P. Utech and M. C. Flanagans, J. Appl. Phys. 37 (1966) pp. 2021-2024.
- [3] H. A. Chedzy and D. T. Hurle, Nature 210 (1966) pp. 933-934.
- [4] T. Onotou and I. Yamamoto, Proc. Materials Analysis and Processing in Magnetic Fields (2016).
- [5] I. Yamamoto et al., Proc. 42th MSJ Annual Meeting, 11pA-1 (2018).
- [6] T. Okabe and I. Yamamoto, 66th JSAP Spring Meeting (2019) pp. 08107 (in Japanese).

Tailoring the microstructure and properties of CoCrFeNi-based highentropy alloys using high magnetic field

Jun Wang ^{1*}, Jiaxiang Wang¹, Chendong Zhao¹, Yixuan He¹, Jinshan Li ¹, Eric Beaugnon ²

¹ State Key Laboratory of Solidification Processing, Northwestern Polytechnical University, Xi'an, 710072, China; ² Univ. Grenoble Alpes, INSA Toulouse, Univ. Toulouse Paul Sabatier, EMFL, CNRS, LNCMI, 38000 Grenoble, France

*Corresponding author: nwpuwj@nwpu.edu.cn

High-entropy alloys (HEAs) have recently attracted extensive attention for its unique alloy design concept that is multi-component alloys with equiatomic or near-equiatomic compositions [1]. Despite having the presence of a large number of components, HEAs generally show simple solid-solution structures rather than complicated intermetallic compounds, possess attractive properties according recent comprehensive research such as great integrated tensile properties, high hardness, superior wear-resistance, good corrosion-resistance and thermal stability.

High magnetic field is a powerful tool to tune the microstructure and improve the properties of materials. The application of high magnetic field (HMF) during materials processing process is considered an effective method to improve the mechanical properties, and it has been paid more attention in recent years.

In this study, high magnetic field, are introduced during the solidification and heat treatment process of several CoCrFeNi-based high-entropy alloys. Our results show that high magnetic field can affect the phase transformation process of high-entropy alloys and thus changing the microstructure and improving both the magnetic and mechanical properties. The mechanism of magnetic field on tailoring the microstructure and properties of high-entropy alloys are discussed in this study.

References

[1] E.P. George, D. Raabe, R.O. Ritchie, High-entropy alloys, Nature Reviews Materials, (2019) 1.

In-situ observation of solidification process of organic materials in magnetic fields and magnetic force fields

Kohki Takahashi ^{1*}, Iwao Mogi ¹, Satoshi Awaji ¹

Institute for Materials Research, Tohoku University, Sendai 980-8577, Japan

*Corresponding author: kohki@imr.tohoku.ac.jp

Producing higher quality and/or higher performance materials is required in various fields. Materials processing under external fields is one of the solutions for such a problem. Recently, many kinds of studies in magnetic fields have been conducted to synthesize high quality materials, since a magnetic field can be used easily thanks to the widespread use of cryogen-free superconducting magnets. In high magnetic field more than 10 T, for instance, magnetic field effects can be expected even for paramagnetic or diamagnetic materials. Materials in a magnetic field gradient receive a magnetic force, and a diamagnetic material can be levitated in the air when the upward repulsive magnetic force balances with the downward gravitational force. This phenomenon is so-called a magnetic levitation, which is considered to be a quasi-micro gravity condition. The magnetic levitation of diamagnetic materials enables a container less melting or a crystallization, which attracts attention as a novel materials processing technique employing a high magnetic field. Unexpected phenomena are sometimes observed during materials processing in magnetic fields, especially under the magnetic levitation condition, differing from the process in zero magnetic fields. So, it is important to observe the sample behavior in the process. We have developed special furnaces for heating and observing a sample in magnetic fields so far; the CO₂ laser furnace, the YAG laser furnace and the electric furnace. Recently, we have developed a new furnace using transparent glass heater. This furnace allows in-situ observation of the levitating, and melting and solidification behavior from three directions in heating and cooling process up to 300°C. As performance tests of the furnace, we have performed in-situ observation of melting and solidification process of several organic materials such as tartaric acid and urea in magnetic fields up to 19 T. In cooling process of urea, solidification from the supercooled state was observed. After cooling to room temperature, needle-like crystals were also observed above the solidified urea only in a gradient

magnetic field as shown in Fig. 1. A reasonable mechanism about formation these needle-like crystals has still not been clear. In the will presentation. we show observation results in various conditions of heating and cooling temperature pattern, magnetic field and magnetic force filed strength.

This work was supported by JSPS KAKENHI Grant Numbers 16K04942, 19K05290.

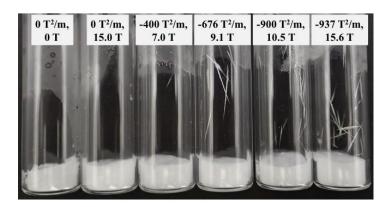


Fig. 1 Photograph of urea samples solidified in various magnetic field and magnetic force field conditions.

Magnetically Oriented Microcrystal Array and Suspension of Microcrystalline Lysozyme for Crystal Structure Analysis

F. Kimura^{1,2*}, K. Takeda³, A. Shirahama¹, Y. Hanazono³, T. Kimura^{1,4}, M. Wada¹, S. Horii², M. Yoshimura⁵, K. Hasegawa⁶, K. Takahashi⁷, Y. Ikemoto⁶, T. Tomizaki⁸

¹ Graduate School of Agriculture, Kyoto University, Kitashirakawa, Sakyo, Kyoto 606-8502, Japan

² Kyoto University of Advanced Science, Yamanouchi-Gotandacho, Ukyo-ku, Kyoto 615-8577, Japan

³ Graduate School of Science, Kyoto University, Kitashirakawa, Sakyo, Kyoto 606-8502, Japan

⁴ Fukui University of Technology, 3-6-1 Gakuen, Fukui 910-8505, Japan

⁵ National Synchrotron Radiation Research Center, Hsinchu 30076, Taiwan

⁶ Japan Synchrotron Radiation Research Institute, Sayo-cho, Hyogo 679-5198 Japan

⁷ Institute for Materials Research, Tohoku University, Katahira, Sendai 980-8577, Japan

⁸ Paul Scherrer Institute, Forschungssstrasse 111, 5232 Villegen PSI, Switzerland

*Corresponding author:kimura.fumiko@kuas.ac.jp

Microcrystals can be oriented under a modulating magnetic field to form a pseudo single crystal (MOMA, Magnetically Oriented Microcrystal Array), which can be used for X-ray single crystal analysis. MOMAs are prepared by dispersing microcrystallites in a medium such as a UV curable monomer or sol, followed by consolidating the medium after biaxial alignment is achieved. Using MOMAs, we have suceeded in determing the crystal structure from inorganic, organic, and protein microcrystals, where UV curable monomer was used for consolidating medium. However, many UV curable monomers are hydrophobic and hence incompatible with hydrophilic protein microcrystals. Acquous sols may be alternative. However, they are often immixible with precipitation medium for protein microcrystals. In this study, we try to find other way of consolidating the medium. We try to freeze the precipitation medium containing oriented protein microcrystals by immersing it in liquid nitrogen. We first prepared three-dimensional oriented microcrystalline suspension (MOMS) and

subjected it, immediately after the orientation is completed, to liquid nitrogen. The X-ray diffraction (XRD) measurements were carried out for a frozen MOMS, ex-situ MOMS (XRD was measured immediately after the suspension was removed from the modulated magnetic field) and in-situ MOMS (XRD was performed while the suspension was kept exposed to the modulated magnetic field). The intensity of the magnetic field ranged from 1.2 T (Fig. 1) to 19 T. We show that the indexing was successfully made using a frozen MOMA having a high degree of orientation.

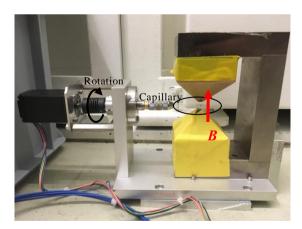


Fig. 1 Photograph of alignment unit (magnet and motor), KUχten.

Nanostructured SnSe integrated with Se quantum dots with ultrahigh power factor and thermoelectric performance from high magnetic field assisted hydrothermal synthesis

Rui Xu,¹ Jun Fang,² <u>Guodong Tang^{1*}</u>

¹MIIT Key Laboratory of Advanced Metallic and Intermetallic Materials Technology, School of Materials Science and Engineering, Nanjing University of Science and Technology, Nanjing 210094, China; ²Anhui Province Key Laboratory of Condensed Matter Physics at Extreme Conditions, High Magnetic Field Laboratory of the Chinese Academy of Science, Hefei 230031, Anhui, China.

* Corresponding author: tangguodong@njust.edu.cn

Thermoelectric materials that can directly convert thermal energy into electrical energy have great potential in solving the present energy crisis. SnSe has emerged as one of the most intriguing new thermoelectric materials since the discovery of the excellent thermoelectric properties of its single crystals. Here, we develop a new solution synthesized method (in situ magnetic field-assisted hydrothermal synthesis) for achieving new nanostructured SnSe integrated with Se quantum dots. The critical nucleation energy reduces and the nucleation rate increases during the hydrothermal synthesis process as a high magnetic field is applied, which leads to the presence of the homogeneous distribution of Se quantum dots and smaller nano grains. Enhanced density of states and the energy filtering effect contribute towards a significant enhancement in the Seebeck coefficient and power factor (PF) due to the Se quantum dots and smaller nano grains. The enhanced density of states was directly identified by ultraviolet photoelectron spectroscopic measurements. With the aid of a high magnetic field in solution chemistry, these materials maintain low thermal conductivity due to the Se quantum dots, smaller nano grains and nano precipitates. Benefiting from the enhanced power factor and reduced thermal conductivity, a high figure of merit (ZT) of ~ 2.0 at 873 K was achieved in a Se quantum dot/Sn_{0.99}Pb_{0.01}Se nanocomposite. This work paves the way for the design of prospective thermoelectric materials by applying an external high magnetic field.

Reference

[1] Rui Xu, Lulu Huang, Jian Zhang, Di Li, Jizi Liu, Jiang Liu, Jun Fang, and Guodong Tang, Journal of Materials Chemistry A 7 (2019) 15757.

Effects of super high static magnetic field on the microstructures of binary alloys during the bulk solidification process

Yunbo Zhong^{1*}, Tianxiang Zheng¹, Zhongming Ren¹, Francois Debray², Eric Beaugnon²

¹State Key Laboratory of Advanced Special Steels, Shanghai University, Yanchang Road No. 149,

Shanghai 200072, China; ²LNCMI, CNRS/UJF/INSA/UPS, 38042 Grenoble, France

*Corresponding author: yunboz@staff.shu.edu.cn)

1. Al-Cu alloys

Solidification of Al-Cu alloys has been investigated using a 29 Tesla super high static magnetic

field (SHSMF). The results show that, by imposing a 29 Tesla SHSMF, the size of primary phases and spacing of eutectic structure have been refined through the increase of undercooling which results from the suppression of diffusion coefficient (Fig. 1). The lattice constants is reduced and high dislocation density forms in the primary phase, which induces a solute trapping effects. The compression yield strength has been improved by about 42% from 268 Mpa to 462 Mpa for Al-26wt.%Cu and 42.5% from 248 Mpa to 431 Mpa for Al-40wt.%Cu. The maximum elastic strain increases from about 2% to 4.3% for Al-26wt.%Cu and from 2% to 4% for Al-40wt.%Cu. It is expected that SHSMF is beneficial to process materials with high mechanical properties.

2. Zn-Bi immiscible alloy

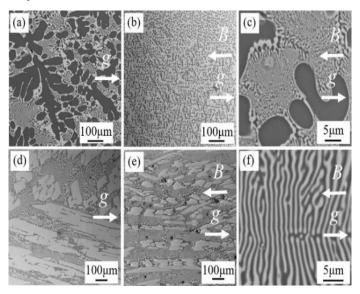


Fig. 1 BSE images of Al-Cu alloys. (a) 0 T, Al-26wt.% Cu; (b) 29 T, Al-26wt.% Cu. (c) 29 T, eutectic structure, Al-26wt.% Cu. The dark color represents α -Al, the mixed region is eutectic structure. (d) 0 T, Al-40wt.% Cu; (e) 29 T, Al-40wt.% Cu. (f) 29 T, eutectic structure, Al-40wt.% Cu.

In situ solidification experiments on Zn–6wt.% Bi immiscible alloys were conducted to investigate the droplet evolution under SHSMFs (Fig. 2). The results showed that a microstructure with extremely fine Bi-rich particles distributed in the matrix can be obtained under an SHSMF of 29 T. The average diameter of the Bi-rich phase decreased with increasing magnetic flux density. Stokes sedimentation disappeared when the SHSMF was larger than 18 T. Starting at an HSMF of 18 T, Bi-rich droplets grew via pure diffusion in the liquid matrix.

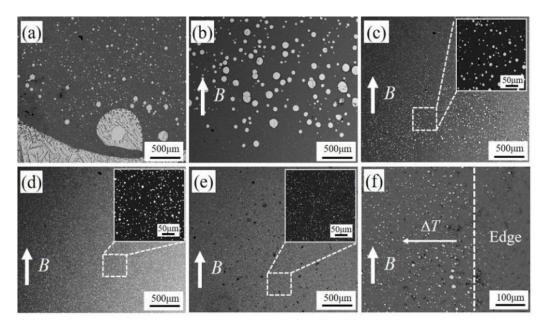


Fig. 2 BSE images of Al-Cu alloys. (a) 0 T, Al-26wt.% Cu; (b) 29 T, Al-26wt.% Cu. (c) 29 T, eutectic structure, Al-26wt.% Cu. The dark color represents α -Al, the mixed region is eutectic structure. (d) 0 T, Al-40wt.% Cu; (e) 29 T, Al-40wt.% Cu. (f) 29 T, eutectic structure, Al-40wt.% Cu.

Acknowledgements

The authors gratefully acknowledge the financial support of the National Natural Science Foundation of China (U1732276, No. 51704193), National Key Research and Development Program of China (2016YFB0301401), the Users with Excellence Program of Hefei Science Center CAS (2019HSC-UE010), Science and Technology Commission of Shanghai Municipality (No. 15520711000), Changjiang Scholars Program of China.

On the eutectoid decomposition of $Co_3B \rightarrow Co_2B + \alpha$ -Co in a Co-B eutectic alloy

Yixuan He^{1, 2, *}, Jinshan Li¹, Jun Wang¹, Eric Beaugnon²

¹ State Key Laboratory of Solidification Processing, Northwestern Polytechnical University, Xi'an Shaanxi 710072, China; ² Univ. Grenoble Alpes, INSA Toulouse, Univ. Toulouse Paul Sabatier, EMFL, CNRS, LNCMI, 38000 Grenoble, France

*Corresponding author: yixuanhe@mail.nwpu.edu.cn

The related eutectoid decomposition of $\text{Co}_3\text{B}\to\text{Co}_2\text{B}+\alpha\text{-Co}$ in the Co-B binary system were studied by in-situ measuring the magnetization. Results indicate that the eutectoid decomposition reaction is greatly affected by the undercooling temperature. When the undercooling is small (e.g., ΔT =92 K), the Co_3B phase is hardly decomposed and can be retained to room temperature. However, when the undercooling is large (e.g., ΔT =153 K), a clear and abrupt raising of magnetization is observed, which suggests that the eutectoid decomposition reaction takes place. Different from the reference, this reaction has a high reactivity (within 30 s) and can be react completely. The results is evidenced by the

characterization of the microstructures by EBSD and TEM.

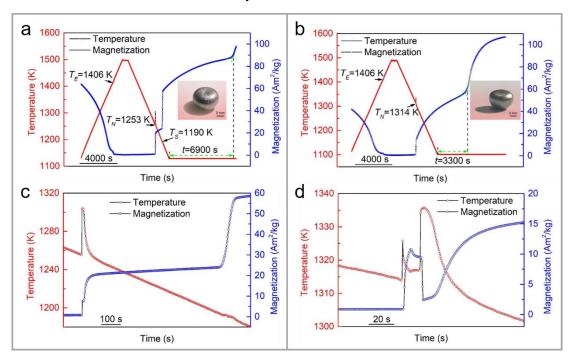


Fig. 1. The cooling and magnetization curve of $Co_{81.5}B_{18.5}$ alloy. The field intensity and gradient are 1.0383 T and 15.49 T/m, respectively. The inserts are the corresponding macrograph of the samples after solidification. The enlarged figures corresponding to the range around the solidification process in Figs. a and b are shown in Figs. c and d. Co_3B is ferromagnetic with the Curie temperature of 747 K. Co_2B is also ferromagnetic with the Curie temperature of 429K.

October 13, 2019, Session 3

Effects of space hypomagnetical fields on skeletal system and related mechanisms

<u>P Shang</u>^{1, 3*}, YR Xue^{1, 2, 3}, JC Yang^{1, 3, 4}, SJ Zhou^{1, 2, 3}

¹ Research & Development Institute of Northwestern Polytechnical University in Shenzhen, Shenzhen, China; ²School of Life Sciences, Northwestern Polytechnical University, Xi'an, China; ³ Key Laboratory for Space Bioscience and Biotechnology, Northwestern Polytechnical University, Xi'an, China; ⁴ Department of Spinal Surgery, People's Hospital of Longhua Shenzhen, Shenzhen, China *Corresponding author: shangpeng@nwpu.edu.cn

With the launch of the lunar exploration program, astronauts will inevitably be exposed to the space spatial hypomagnetic field (sHyMF) environment for long periods of time during long-distance space missions[1]. In addition to microgravity, the sHyMF also is an extreme environment in space, sHyMF exists on the surface of the moon or in the deep space of the solar system, and its magnetic intensity is less than 5 µT. Recently, we demonstrated that HyMF promoted additional bone loss in hindlimb unloading-induced bone loss, and the underlying mechanism probably involved in the increase of body iron storage[2,3]. Many studies have indicated that bone loss induced by mechanical unloading can be largely restored after skeletal reloading in GMF condition [4,5,6]. However, it is unknown whether this bone deficit can return to a healthy state under HyMF condition. Therefore, the purpose of this study is to examine the effects of HyMF on the recovery of microgravity-induced bone loss and illustrates the changes of body iron storage in this process. Our results demonstrated that there was lower bone mineral density (BMD) and bone mineral content (BMC) in the HyMF reloading group compared to the GMF reloading group. Reloaded mice in the HyMF condition had a worse microstructure of femur than in the GMF condition. Femoral mechanical properties were higher in the HyMF group compared with the GMF group. Simultaneously, more iron content was found under HyMF reloading than GMF reloading. In conclusion, these results showed that HyMF inhibits the recovery of microgravity-induced bone loss, probably by suppressing elevated iron levels return to physiological level.

- [1] Vico L, Hargens A. Skeletal changes during and after spaceflight. Nature Reviews Rheumatology, 2018, 14(4): 229.
- [2] Jia B, Xie L, Zheng Q, Yang P F, Zhang W J, Ding C, Qian A R, Shang P. A hypomagnetic field aggravates bone loss induced by hindlimb unloading in rat femurs. PloS one, 2014, 9(8): e105604.
- [3] Yang J, Meng X, Dong D, Xue Y, Chen X, Wang S, Shen Y, Zhang G, Shang P. Iron overload involved in the enhancement of unloading-induced bone loss by hypomagnetic field. Bone, 2018,
- [4] Lang T F, Leblanc A D, Evans H J, Ying L. Adaptation of the proximal femur to skeletal reloading after long-duration spaceflight. Journal of Bone & Mineral Research, 2010, 21(8): 1224-1230.
- [5] Vico L, Van R B, Vilayphiou N, Linossier M T, Locrelle H, Normand M, Zouch M, Gerbaix M, Bonnet N,

Novikov V. Cortical and trabecular bone microstructure did not recover at weight-bearing skeletal sites and progressively deteriorated at non-weight-bearing sites during the year following International Space Station missions. Journal of Bone & Mineral Research the Official Journal of the American Society for Bone & Mineral Research, 2017, 32(10): 2010.

[6] Ozcivici E, Judex S. Trabecular bone recovers from mechanical unloading primarily by restoring its mechanical function rather than its morphology. Bone, 2014, 67(5): 122-129.

Biological effects of magnetic fields and magnetoreception in insects

Weidong Pan ^{1*}, Yingchao Zhang ¹, Guijun Wan ², Fajun Chen ²

¹ Beijing Key Laboratory of Bioelectromagnetics, Institute of Electrical Engineering, Chinese Academy of Sciences, Beijing 100190, China; ² Department of Entomology, College of Plant Protection, Nanjing Agricultural University, Nanjing 210095, China

*Corresponding author: panwd@mail.iee.ac.cn

In last few decades there have been many reports of biological effects induced by magnetic fields on the development and metabolism of insects such as *Tenebrio molitor, Anopheles gambiae, Drosophila melanogaster, Musca domestica, Apis mellifera, Laodelphax striatellus and Nilaparvata lugens*. The most popular hypothesis for these effects is that magnetic fields affect rotation of membrane phospholipid molecules by virtue of their collective diamagnetic anisotropic properties allowing for summation of individual molecular anisotropies. Thus, magnetic fields mainly affect organisms by influencing membrane channel properties, e.g. sodium channels, calcium channels. In some cases, magnetic fields accelerated the postembryonic development of insects and increased larval weight in comparison with the Earth's magnetic field. The question of possible biological effects of magnetic fields remains controversial, markedly because no valid mechanism of interaction could be proposed so far for relevant exposure intensities.

On the other hand, the phenomenon of magnetoreception has been convincingly demonstrated in a number of diverse animal species including insects. Many types of insects undertake impressive seasonal mass migrations travelling up to thousands of kilometers to their ultimate destination. Series of experiments on insect magnetoreception was performed with species as honeybee, Drosophila and monarch butterflies. Models for how organisms sense the magnetic field have been suggested as the light-independent magnetite-based magnetoreception and the light-dependent radical pair mechanism. Recent work on *Caenorhabditis elegans*, flavin adenine dinucleotide and the magnetosensing complex has supplied further evidence for the two models, suggesting that they are not mutually exclusive and both could exist in organisms. Although the navigational mechanism and genetic control for migratory flight of insects are not well understood, a magnetic compass appears to be a plausible explanation. It is also possible that biological effects of magnetic fields on insects are medicated by magnetoreception since the precise biophysical origin of magnetosensitivity remains to be further elucidated.

- [1] Z.M Prolić, J.M.Lazarević, M.M.Mrdaković-Mitić, et al., Acta Ent.Serb.6(2001), 139-142.
- [2] E.Polidori, S.Zeppa, L.Potenza, et al., Bioelectromagnetics 33 (2012) 65-74.

- [3] A.D.Rosen, Cell Biochem. Biophys. 39 (2003) 163-173.
- [4] K. J. Lohmann, Nature 464(7292) (2010) 1140-1142.
- [5] T.Ritz, S.Adem and K.Schulten, Biophys. J.78(2000) 707-718.
- [6] S.Y. Qin, H.Yin, C.L.Yang, et al. Nature Materials 15(2) (2015) 217-226.
- [7] G.J.Wan, R.Yuan, W.J.Wang, et al. Anim. Behav. 121 (2016) 107-116.
- [8] W.D.Pan, G.J. Wan, J.J.Xu, et al. Sci.Rep.6(2016) 18771.

Biological effects of high static magnetic fields on *Caenorhabditis elegans* and their offspring

An Xu *, Mudi Wang, Lei Cheng, Zheng Yang, Baolin Yang, Ahmed Waqas
Key laboratory of high magnetic field and Ion beam physical biology, Hefei Institutes of Physical
Science, Chinese Academy of Sciences, Hefei, Anhui 230031, P.R.China
*Corresponding author: anxu@ipp.ac.cn

Understanding the effects of high static magnetic fields (SMFs) on living organisms is significant in health risk assessment, but underlying mechanisms are largely unexplored. The nematode Caenorhabditis elegans (C. elegans) as a well-established model system has many unique characteristics and distinct advantages in the discovery of fundamental biological responses in development, neurobiology and aging. We found that exposure of C. elegans eggs to 8.5 T SMF resulted in a timedependent lifespan decrease, whereas only slight changes were observed in young adult and L1 to L4 stages upon exposure to SMF lower than 5 T. Although SMF exposure did not alter brood size, development rate and stages were significantly modified by 8.5T SMF. Germ cell apoptosis dramatically increased upon exposure to 8.5 T SMF in adult worms, as confirmed by ced-3 and ced-4 mutants, and could be prevented by concurrent treatment with a free radical scavenger, dimethyl sulfoxide. Compared to wild-type worms, shorter lifespan and greater numbers of apoptotic cells were observed in abnormal methyl viologen sensitivity-1 (mev-1(kn1)) nematodes with increased sensitivity to oxidative damage. Furthermore, exposure to 8.5 T SMF increased expression of superoxide dismutase-3 (sod-3), which is thought to protect against oxidative stress. The offspring of L4 stage showed greater decrease in lifespan by exposure to 8.5 T SMF than egg's offspring, which was regulated through insulin-like signaling pathway. Our results provide novel information for better understanding the biological responses to high SMFs in living organism at different life stages and their underlying mechanism(s).

Multiple pathways involve in the bio-response to the hypomagnetic field

Ying Liu ^{1,2*}, Wei-chuan Mo ², Jing-Peng Fu ², Haitao Zhang ², Zijian Zhang ², Rong-qiao He ² School of Life Sciences, Beijing University of Chinese Medicine, Beijing 102488, China; ² State Key Laboratory of Brain and Cognitive Science, Institute of Biophysics, CAS, Beijing 100101, China *Corresponding author: yingliu@bucm.edu.cn (Ying Liu)

Multiple organisms have developed special ability of biomagnetosensation to the geomagnetic field (GMF) during the elution in GMF. However, the mechanisms for sensing the GMF is a key question remained to be elucidated in life science. Hypomagnetic field (HMF, $< 5 \mu T$, or 1/10 intensity of the GMF), which is a GMF-shielding condition and also a key factor in deep space, is necessary to study the role of GMF. Therefore, we constructed a set of HMF system for animal experiments and analysis at cellular/molecular levels, and found the HMF-exposed adult mice exhibited a prolonged alteration of the circadian drinking rhythm, an increase in thermal hyperalgesia and a decrease in general activity. Further analysis with cultured primary skeletal muscular cells confirms declined glucose metabolism rate, cell viability and mitochondria membrane potential in the HMF-exposed cells. These results indicate that HMF inhibits the mitochondrial activity and glucose metabolic process in skeletal muscular cells, which would probably reduce the exercise capacity in the mice. Furthermore, we found that HMF exposure accelerates the proliferation of adult neural progenitor/stem cells both in vivo and in vitro, which indicates a novel mechanism of the effects on brain function. The in vitro assay with isolated mitochondria and cell-free actin assembly system show that mitochondria and F-actin can response directly to HMF exposure, therefore could be good candidates to mediate the effects observed in the HMF. Moreover, we also found shielding of the GMF reduces hydrogen peroxide production in human neuroblastoma cell and inhibits the activity of CuZn superoxide dismutase. These results indicate multiple pathways involve in the bio-responses to the HMF. Further investigation would be necessary to explore the common and specific pathway(s) mediating the effects.

Funded by: the National Nature Science Foundation of China (No. 31870840), The External Cooperation Program of BIC, Chinese Academy of Sciences (No. GJHZ201302), and the Project of Chinese Academy of Sciences for the Development of Major Scientific Research Equipment (No. YZ201148).

Photosensitive magnetoreception of marine bacteria

Long-Fei WU 1,2*

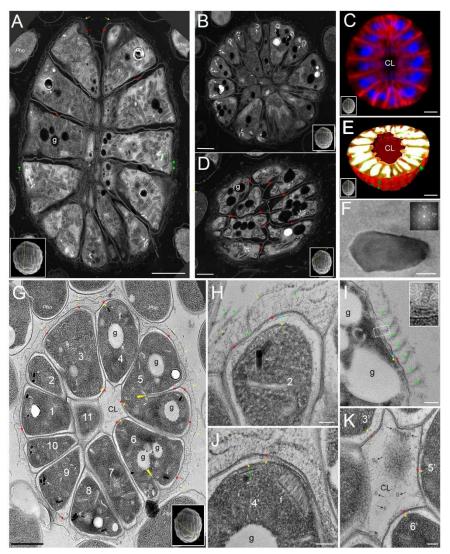
¹Aix Marseille University, CNRS, LCB, Marseille, 13402, France; ² International Associated Laboratory of Evolution and Development of Magnetotactic Multicellular Organisms (LIA-MagMC), CNRS-CAS

* wu@imm.cnrs.fr; long-fei.wu@univ-amu.fr

During the evolution various organisms from bacteria to vertebrates have developed magnetoreception capacity to exploit geomagnetic field as an orientation cue and maps while migrating or homing [1]. Among those, **magnetotactic bacteria** (MTB) have been extensively studied. MTB consist of a heterogeneous group of Gram-negative bacteria that are capable of synthesizing single domain magnetite (Fe₃O₄) or greigite (Fe₃S₄) crystals in intracellular organelles termed magnetosomes [2]. The magnetosomes confer on bacteria a magnetic moment dipole and allow the cells to align to and swim along geomagnetic field lines. This behavior, referred to as magnetotaxis, is essential for the bacteria swimming to and maintaining at the oxic-anoxic interface in chemically stratified water columns or sediments, where it is optimal for their growth [3]. To contribute to a comprehensive

understanding of bacterial magnetotaxis mechanism we studied the synthesis, structure and function of the intracellular compass (magnetosomes) and the propellers (flagella) of model magnetotactic bacteria. We found the most exquisite flagellar apparatus of marine magneto-cocci [4], and revealed a cytoskeleton-underpinned, chemotaxis-like mechanism that governs the magnetotaxis of magnetospirilla cells [5-7]. Besides these unicellular MTB, we are particularly interested in the multicellular magnetotactic prokaryotes (MMPs) or magnetoglobules that have opted both magnetoreception capacity and multicellularity during the evolution. Using high-pressure freezing/freeze substitution fixation technique we found that juxtaposed membranes adhere ~ 60 cells axisymettrically into several interlaced rows to achieve a one-layer hollow architecture with a peripherycore polarity. The cells are held by a well-patterned rimming lattice at the surface and surround a core lumen in the center of the ellipsoidal magnetoglobules. Magnetite crystals arrange in multiple chains at the periphery of MMP cells. Remarkably, thousands of flagellar at the periphery surface of cells underpin the coordinated swimming of magnetoglobules in response to mechanical, chemical, magnetic and optical stimuli, including a magnetotactic photokinesis behavior [8]. Close to the periphery side of the inner membranes, we observed a fence-like structure that looks like photosynthetic membrane lamellae and could be an appropriate candidate for accommodating photoreceptors involved in MMPs photosensing. Detailed structure and magnetotaxis behavior as well as the mechanisms involved will be discussed.

- 1. Johnsen, S. and K.J. Lohmann, *The physics and neurobiology of magnetoreception*. Nat. Rev. Neurosci., 2005. **6**(9): p. 703-712.
- 2. Bazylinski, D.A. and R.B. Frankel, *Magnetosome formation in prokaryotes*. Nat. Rev. Microbiol., 2004. **2**(3): p. 217-230.
- 3. Zhang, S.D., et al., Swimming behaviour and magnetotaxis function of the marine bacterium strain MO-1. Environ Microbiol Rep, 2014. **6**(1): p. 14-20.
- 4. Ruan, J., et al., Architecture of a flagellar apparatus in the fast-swimming magnetotactic bacterium MO-1. Proc. Natl. Acad. Sci. USA, 2012. **109**(50): p. 20643-20648.
- 5. Philippe, N. and L.-F. Wu, An MCP-like protein interacts with the MamK cytoskeleton and is involved in magnetotaxis in Magnetospirillum magneticum AMB-1. J. Mol. Biol., 2010. 400(3): p. 309-322.
- 6. Pradel, N., et al., *Biogenesis of actin-like bacterial cytoskeletal filaments destined for positioning prokaryotic magnetic organelles*. Proc. Natl. Acad. Sci. USA, 2006. **103**(46): p. 17485-17489.
- 7. Zhu, X., et al., Angle sensing in magnetotaxis of Magnetospirillum magneticum AMB-1. Integr Biol (Camb), 2014. **6**(7): p. 706-13.
- 8. Qian, X.X., et al., *Juxtaposed membranes underpin cellular adhesion and display unilateral cell division of multicellular magnetotactic prokaryotes*. Environ Microbiol, 2019, DOI: 10.1111/1462-2920.14710.



Axisymmetrical assembly of cells into a one-layer hollow architecture with periphery-core polarity of ellipsoidal magnetoglobules [8]

Arabidopsis Flowering Is Affected by Near-Null Magnetic Field

Chunxiao Xu*, Tao Song

Beijing Key Laboratory of Bioelectromagnetism, Institute of Electrical Engineering, Chinese Academy of Sciences, Beijing, China; Zhongguancun, Beijing, 100190, P. R. China. *Corresponding author: Chunxiao Xu, e-mail: xuchunxiao@mail.iee.ac.cn

Some migratory birds can use the geomagnetic field for their navigation. The blue light receptor, cryptochrome, was suggested to act as a magnetoreceptor based on the proposition that photochemical reactions were involved in sensing the geomagnetic field. Cryptochrome was firstly found in Arabidopsis, which was involved in photoperiodic flowering. To test the role of geomagnetic field in Arabidopsis growth, we grew Arabidopsis in a near-null magnetic field. We found that flowering time

of Arabidopsis grown in the near-null magnetic field was delayed, which was blue light intensity and cycle dependent. The near-null magnetic field weakened the blue light-dependent phosphorylation of cryptochrome, suggesting that function of cryptochrome was affected by near-null magnetic field. Transcriptions of flowering-related genes, *LFY* and *SOC1*, were downregulated by near-null magnetic field. These results suggest that near-null magnetic field suppresses Arabidopsis flowering by functional modification of cryptochrome. Moreover, we found that levels of GA₄, GA₉, GA₃₄, and GA₅₁ in Arabidopsis in near-null magnetic field were significantly decreased compared with the local geomagnetic field controls. Expressions of *GA20-oxidase* genes and *GA3-oxidase* genes were downregulated by near-null magnetic field. We also found that indole-3-acetic acid (IAA) level in roots of Arabidopsis in near-null magnetic field was significantly increased compared with the local geomagnetic field control, while IAA level in rosettes of Arabidopsis in near-null magnetic field was significantly lower than the control. These results suggest that the delay of flowering of Arabidopsis in near-null magnetic field is regulated by plant hormones, GA and IAA.

Magnetobiology based on external magnetic radiation and internal magnetism detection on *Sitobion avenae*

Juan He ^{1*}, Weidong Pan ^{2,3}, Yiling Wang ¹

¹ College of Life Science, Shanxi Normal University, Linfen, 041000, PR China; ² Beijing Key Laboratory of Bioelectromagnetics, Institute of Electrical Engineering, Chinese Academy of Sciences, Beijing 100190, China; ² Beijing Key Laboratory of Bioelectromagnetics, Institute of Electrical Engineering, Chinese Academy

*Corresponding author: hejuan@sxnu.edu.cn

Various reactions of living systems toward magnetic fields are controversial and inconclusive. Discovered suitable systems and new research idea are necessary to study this phenomenon. *S avenae* (Homoptera: Aphididae) could be an excellent specimen investigating insect adaptation and evolution with biological characteristics of parthenogenesis and high fecundity. In this study, External and internal magnetic radiation types were analyzed using *S. avenae* to study magnetobiology. The population demography with internal radiation were estimated with the first instar nymphs exposed 0.176 and 0.065 T magnetic fields under different periods (0.5 and 1 h, respectively). The results showed significantly different age—stage distributions of mortality were in the combination of 0.176 T-0.5 h and 0.065 T-1 h magnetic field radiation treatments.

Survival rate and fecundity data were used to project the population growth of *S. avenae* [1] using the TIMING-MSChart program [2].

$$lx = \sum_{j=1}^{k} s_{xj,}$$

x is age in days and j is the stage; k is the number of stages. The reproductive value (v_{xj}) represents the contribution an individual of age x and stage j for the future population and was calculated as:

$$v_{xj} = \frac{e^{r(x+1)}}{s_{xj}} \sum_{i=x}^{\infty} e^{-r(i+1)} \sum_{y=j}^{\beta} f_{iy} s_{iy}$$

Meanwhile, the parameters with external magnetism of closed hysteresis loop within the positive and negative ranges of 60 000 Oe was corresponding to the flying angle on hypomagnetic and geomagnetism environment. These findings first revealed the magnetic biology effect from the external magnetic radiation and internal measure of magnetic substances using *S. avenae* influences the biology and hysteresis loop of aphid indicated that this species contains magnetic substances. The approaches of integrating external magnetic radiation and internal measure of magnetic substances would possibly provide a powerful way to understand the Magnetobiology and undertaken in similar studies in other insect species simultaneously contained the magnetic substances and magnetic radiation.

References

[1] H. Chi, J Econ. Entomol. 83(1990)1143–1150.

[2] H. Chi. Online Available: http://140.120.197.173/Ecology/ (2017)

October 13, 2019, Session 4

0.05°C Resolution thermometry by using T2 relaxation of magnetic nanoparticles in NMR

Yapeng Zhang ¹, Wenzhong Liu ^{1*}

¹ School of Artificial Intelligence and Automation, Huazhong University of Science and Technology, Wuhan 430074, China

*Corresponding author: <u>LWZ7410@hust.edu.cn</u>

We present in this paper an approach for temperature measurement and imaging using magnetic nanoparticles based on low-field NMR T2 relaxation, which allows a high resolution of up to $0.05~^{\circ}$ C. To explore the feasibility of temperature measurement based on the T_2 relaxation, the compatibility between the temperature changing model of magnetic nanoparticles and the parameters of magnetic resonance system is assessed. The simulation results show that 5 nm magnetic nanoparticles have an optimum sensitivity to temperature under a magnetic field of $0.4166~^{\circ}$ T, and the corresponding T_2 relaxation time has the same optimum sensitivity. This conclusion is verified by the combination of a commercial magnetic resonance instrument and a commercial 5 nm magnetic nanoparticle contrast agent. Using a $0.47~^{\circ}$ T nuclear magnetic resonance instrument and 5 nm magnetic nanoparticles, with a concentration of Fe of 25 ug/mL or $100~^{\circ}$ mL, the best temperature resolution was obtained, of about $0.05~^{\circ}$ C. The results of the T_2 -weighted imaging experiment verify the feasibility of magnetic resonance imaging of temperature.

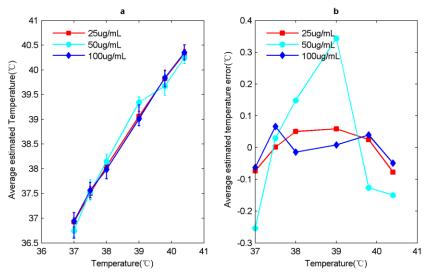


Figure 1. Temperature measurement results for different Fe concentrations and different temperatures using the 0.47 T NMR instrument. Means and standard deviations were obtained from the average of five temperature measurements (a) Average value of the estimated temperatures. (b) Average value of the estimated temperature errors.

[1] Le, H., Liu, W., Xie, Q., Pi, S. & Morais, P.C. A fast and remote magnetonanothermometry for a liquid environment. Measurement Science & Technology 27, 25901 (2016).

Engineered Magnetic Nanoparticle for Advanced Nanothermotherapy and Magnetic Resonance Imaging

Haiming FAN^{1*}

¹ Division of Life Science & Medicine, College of Chemistry & Materials Science, Northwest
University, Xi'an 710127, China
*Corresponding author: fanhm@nwu.edu.cn

Traditional superparamagnetic iron oxide (SPIO) formulations have been demonstrated the great potential for various biomedical applications such as protein/cell separation, biosensor, drug delivery, magnetic resonance imaging (MRI) and magnetic hyperthermia treatment. However, the application of these nanoparticles for cancer diagnostics and therapy has been largely hindered by poor stability, weak magnetic properties, insufficient MR detection sensitivity and low thermal conversion efficiency. The nanomagnetism-engineering strategies that include structure, composition, size and surface optimization have been developed in our recent works towards high-performance biomedical applications. In this talk, a series of advanced biomedical magnetic nanoplatform for high efficient MRI contrast agent and hyperthermia agent will be presented such as innovative ferrimagnetic vortex-domain iron oxide nanorings (FVIO) platform, surface modified SPIO platform, ultrasmall ferrites nanoparticles and magnetic Janus nanoparticles, which could overcome the drawbacks facing to conventional SPIO. For example, FVIO possesses a ferrimagnetic vortex domain structure, in which magnetization is circumferential to the ring without stray fields. This unique magnetic structure endows these FVIOs with negligible remanence and coercivity that can reduce greatly dipole-dipole interactions and enable a good colloidal stability, but much high saturation magnetization and susceptibility in comparison with SPIOs. Under the external field, FVIOs will subject to a transition from vortex state to onion state and move along the field direction rapidly. Benefits from their unique magnetic properties, FVIO formulations have exhibited both high MR r₂* relativity and high specific absorption rate (SAR). Combined with the enhanced permeability and retention effect arising from the relatively large particle size, the highly biocompatible FVIOs allows us to design high sensitively MRI contrast agent and highly efficient hyperthermia agent for early-diagnostics and efficacious treatment of various types of cancers. In summary, the development of these advanced magnetic nanoplatforms paves the way for future magnetic nanoparticle-based nanomedicine.

- [1] X. L. Liu, M. L. Peng, G. L. Li, H. M. Fan* et al. "Ultrasonication-Triggered Ubiquitous Assembly of Magnetic Janus Amphiphilic Nanoparticles in Cancer Theranostic Applications", Nano Lett. 19 (2019) 4118-4125.
- [2] H. Zhang, L. Li, H. M. Fan* et al. "Ultrasmall Ferrite Nanoparticles Synthesized via Dynamic Simultaneous Thermal Decomposition for High-Performance and Multifunctional T1 Magnetic Resonance Imaging Contrast Agent", ACS Nano 11 (2017), 3614-3631.
- [3] X. Liu, L. Zhao, H. M. Fan* et al. "Magnetic vortex nanorings: A new class of hyperthermia agent for highly efficient in vivo regression of tumors", Adv Mater. 27 (2015), 1939-1944.
- [4] H. M. Fan, M. Olivo, B. Shuter, "Quantum dot capped magnetite nanorings as high performance nanoprobe for multiphoton fluorescence and magnetic resonance imaging", J. Am. Chem. Soc. 132 (2010), 14803-14811.
- [5] H. M. Fan*, M. Olivo, "Magnetic nanorings and nanotubes for cancer detection and therapy", Nanomedicine and Cancer, Editor: Professor Victor R Preedy, Science Publisher, 2011.

Positive Magnetic Resonance Angiography by Ultrafine Ferritin-based Iron Oxide Nanoparticles

 $\frac{\text{Yao Cai}^{1,2,5,*}}{\text{Yuqing Wang}^3}, \\ \text{Huangtao Xu}^{1,2,4,5}, \\ \text{Changqian Cao}^{1,2,5}, \\ \text{Rixiang Zhu}^5, \\ \text{Xu Tang}^6, \\ \text{Tongwei Zhang}^{1,2}, \\ \text{Yongxin Pan}^{1,2,4,5,*}$

¹Biogeomagnetism Group, Key Laboratory of Earth and Planetary Physics, Institute of Geology and Geophysics, Chinese Academy of Sciences, Beijing 100029, China; ²France-China International Laboratory of Evolution and Development of Magnetotactic Multicellular Organisms, Chinese Academy of Sciences, Beijing 100029, China; ³National Center for Nanoscience and Technology, Beijing 100190, China; ⁴University of Chinese Academy of Sciences, Beijing 100049, China; ⁵PGL, Institute of Geology and Geophysics, Chinese Academy of Sciences; Beijing 100029, China; ⁶Transmission Electron Microscope Laboratory, Institutions of Earth Science, Chinese Academy of Sciences, Beijing 100029, China

*Corresponding author: caiyao@mail.iggcas.ac.cn; yxpan@mail.iggcas.ac.cn

Iron oxide nanoparticles with good biocompatibility can serve as safe magnetic resonance imaging contrast agents. Herein, we report that ultrafine ferritin-based iron oxide (hematite/maghemite) nanoparticles that were synthesized by controlled biomimetic mineralization using genetically recombinant human H chain ferritin, can be used as positive contrast agent in magnetic resonance angiography. The synthesized magnetoferritin with an averaged core size of 2.2 nm (hereafter named as M-HFn-2.2) shows r_1 value of 0.86 mM⁻¹s⁻¹ and r_2/r_1 ratio of 25.1 at 7 T magnetic field. Blood pool imaging on mice using the M-HFn-2.2 nanoparticles, which was injected through a tail vein by single

injection at a dose of 0.54 mM Fe/kg mouse body weight, enabled detecting detailed vascular nets at 3 minutes post injection. The signal intensity continuously enhanced up to 2 hours post injection, much longer than the commercial magnevist (Gd-DTPA) contrast. Moreover, biodistribution examination indicates that organs of liver, spleen and kidney safely cleared the injected nanoparticles within one day after the injection, demonstrating no risk of iron overload. Therefore, this study sheds light on developing high-performance gadolinium free positive magnetic resonance contrast agents for biomedical applications.

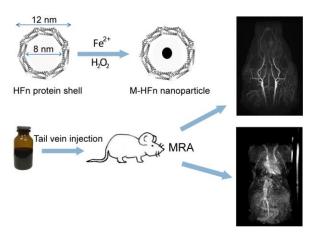


Fig.1 Schematic illustration of MHFn nanoparticles

Magnetic Nanoparticles for Self-regulating Temperature Hyperthermia

Renpeng Yang, Xiaogang Yu, Xudong Zuo, Chengwei Wu, Wei Zhang*

Department of Engineering Mechanics, State Key Laboratory of Structure Analysis for Industrial

Equipment, Dalian University of Technology, Dalian 116024, China

*Corresponding author: W. Zhang, e-mail address: wei.zhang@dlut.edu.cn

Magnetic induction hyperthermia is considered as an accurate, efficient and green method for treating malignant tumors. Basically, magnetic media are introduced to the tumor region by implantation or intervention and will generate heat upon the application of local external alternating magnetic field. Since normal cells possess higher heat resistance and resilience than tumor cells, the tumor cells can be killed without affecting normal tissue if the temperature can be maintained accurately within 42-45°C. As monitoring hyperthermia temperature in vivo with minimal invasion is still a challenge, magnetic nanoparticles with low Curie temperature (42-45°C) are highly desired. The Curie temperature is the temperature at which ferromagnetic materials lose their intrinsic permanent magnetic properties and consequently lose their ability of aligning to external fields and thus facilitating the conversion of external electromagnetic energy into highly localized heat. The Curie temperature therefore gives an upper limit to the operational temperature for the magnetic media. The ability to tune the Curie temperature to a value just above the treatment temperature would be an expedient route to control the hyperthermia temperature and realize self-regulation in practical use of magnetic media as both heater and fuse-limiter.

Here, we report a novel Cr^{3+} substituted Co-Zn ferrite ($Zn_{0.54}Co_{0.46}Cr_{0.6}Fe_{1.4}O_4$), whose Curie temperature is 45.7°C. Under clinically acceptable magnetic field conditions, the nanoparticle suspensions demonstrate reasonable self-regulating temperature behavior and have a specific absorption rate (SAR) of 6.53 W g⁻¹, which is over 21 folds higher than the SAR standard for magnetic nanoparticles used in hyperthermia (0.3 W g⁻¹). The evaluation of the in vitro cytotoxicity of the nanoparticles indicates biocompatibility, which points to a novel set of magnetic nanoparticles for use in self-regulating hyperthermia [1-4].

- [1] W. Zhang, X. G. Yu, H. Li, D. L. Dong, X. D. Zuo, C. W. Wu, Journal of Magnetism and Magnetic Materials 489 (2019) 165382.
- [2] X. D. Zuo, C. W. Wu, W. Zhang, W. Gao, RSC Advances, 8 (2018) 11997-12003.
- [3] W. Zhang, X. D. Zuo, Y. Niu, C. W. Wu. Nanoscale, 9 (2017) 13929-13937, front cover.
- [4] W. Zhang, X. D. Zuo, D. M. Zhang, C. W. Wu, R. Silva, Nanotechnology, 27 (2016) 245707.

Magneto-Optical Detection of Agglomeration and Deagglomeration of Magnetic Nanoparticles in Aqueous Solutions

Hitoshi Watarai

Institute for NanoScience Design, Osaka University, Toyonaka, Osaka, Japan *Corresponding author: watarai@chem.sci.osaka-u.ac.jp

Magnetic nanoparticles (MNPs), typically such as nanoparticles of magnetite, have been widely used in immunological analyses and biological separations combined with surface functionalization of MNPs. These techniques utilize the property of the nano-sized magnet of MNPs dispersed as colloids in solution, which can agglomerate after the reaction with analyte and can be trapped by a permanent magnet from the outside. The agglomeration of MNPs, which is usually observed by the turbidity, can be used very often as the measure of the event of specific interactions between MNPs and analytes. However, the measurement of the initiation of agglomeration of MNPs by the turbidity is sometimes difficult, therefore, an alternative and reliable detection method is required. MNPs show various kinds of magneto-optical phenomena in solutions. The rotational motion of MNPs in solutions can be reduced when MNPs combine with larger molecules or particles. Therefore, it will be measured by a magnetic birefringence and/or a magnetic linear dichroism. The birefringence of solution can be measured as the difference in the refractive index between the horizontally and vertically polarized lights by using a nonabsorbing light. In the present study, we have applied Sagnac effect to measure the magnetic birefringence of MNPs. Sagnac effect is a unique optical interferometry, which was first reported 1913 [1]. Sagnac effect has been applied to measure the magnetic orientation of MNPs [2, 3]. The orientation of light absorbing MNPs in UV-Vis region can also be observed by the polarization spectrometry. In the present study, the magnetic orientational linear dichroism (MLD) of MNPs is applied to detect the critical nucleation and agglomeration of MNPs in solutions. MLD is the difference between the absorbances for a horizontally and a vertically polarized lights, which is induced by a magnetic field applied from a transversal (horizontal) direction to the light beam through a sample cell.

1. Magnetic Sagnac effect for the analysis of agglomeration and deagglomeration of magnetic nanoparticles.

Magnetic Sagnac apparatus was built on an aluminum optical breadboard by using the components of a He-Ne laser, a polarizing beam splitter (PBS), three mirrors to make a Sagnac optical loop, a Wollaston prism and a balanced detector. Then, two beams generated by a PBS were circulated in the loop to the reversed directions with each other. Magnetic field up to 59.2 mT was applied to the cell (10 mm optical pass length) by using a permanent magnet which was set on a motorized stage. To balance the initial intensities of two beams after the Wollaston prism, a z-cut single crystal quartz plate (10 mm x 10 mm x 0.5 mm) set on a rotation stage was inserted in the loop and tilted with a proper angle before applying a magnetic field. The phase shift between the two beams was increased depending on the increase of magnetic field and the increase of the concentration of MNPs (EMG707, Ferrotec, Japan). The magnetic field dependence was analysed by Langevin equation, and the two parameters of the apparent magnetic moment and the saturated phase shift of MNPs were obtained. The observed parameters for COOH-modified MNPs in water reflected the change of dispersion state under the addition of a cationic surfactant, cetyltrimethylammonium bromide (CTAB). When the agglomeration of MNPs with CTAB occurred, the magnetic Sagnac effect was significantly decreased. The agglomeration was thought to be due to the charge neutralization by CTA⁺. But, when excess CTAB was

added to the dispersion, the magnetic Sagnac effect was observed again and the two parameters were given in almost same values as before the agglomeration. This result clearly showed that the deagglomeration of MNPs occurred by the adsorption of excess amount of the cationic CTA⁺ on the surface of the MNPs [3].

2. Magnetic linear dichroism for the detection of critical agglomeration of magnetic nanoparticles in solution.

MLD spectra of MNPs dispersions were measured in the range of 300-700 nm by a spectropolarimeter (J-820E, Jasco), using a pair of permanent magnets on both sides of the quartz cell with 1 or 10 mm optical path length. A magnetic field was changed in the range of 0 - 186.5 mT or 0 – 35.6 mT.

An aqueous dispersion of 0.00625 % magnetite MNPs (10 nm magnetite, W-40, Taiho Kogyo, Japan) in a the cell showed clear MLD spectra in the UV-Vis wavelength region, when a magnetic field was applied, while no change was observed in the absorption spectra. On the other hand, the MNPs in a UV curable resin film prepared under no magnetic field didn't show any MLD spectra. However, the curable resin sample prepared under a magnetic field exhibited clear LD spectra, depending on the rotation angle of the sample film. Then, it was confirmed that the directions of the axis of easy magnetization and the optical transition moment of MNPs are parallel and the observed MLD spectra in a solution were due to the rotational orientation of MNPs by a magnetic force.

A COOH modified MNPs (0.0165%) dispersed in water showed significant MLD spectra, but the addition of a cationic surfactant reduced the MLD intensity accompanied by the large red shift of the maximum MLD wavelength. This result confirmed the observation of the magnetic Sagnac effect that the negatively charged surface of COO- MNPs was neutralized by the positively charged surfactant ion and the agglomeration of MNPs progressed. In the lower concentration of MNPs (0.00165%), the addition of the cationic surfactant or metal ions showed the characteristic increase of MLD just before the significant decrease of MLD due to the agglomeration in the higher concentration of additives. The increase of MLD in the low concentration of the additives suggested the formation of smaller agglomerates under the magnetic field. From the magnetic field dependence of the MLD values, the initial association number of MNPs was estimated by using Langevin equation analysis.

- [1] G. Sagnac, C. R. Acad. Sci., Paris, 157 (1913) 708-710.
- [2] P. Zu et al., Opt. Lett., 37 (2012) 398-400.
- [3] H. Watarai, Z. Chen, and S. Chen, Anal. Sci. 32 (2016) 715-717.
- [4] H. Watarai, and Z. Chen, Bull. Chem. Soc. Jpn. 92 (2019) 949–951.

Magnetic Susceptibility to Measure Magnetic Nanoparticle Concentration from NMR Spectroscopy

Silin Guo, Pu Zhang, Wenzhong Liu

School of Artificial Intelligence and Automation, Huazhong University of Science and Technology, Wuhan, China

INTRODUCTION: Magnetic nanoparticles (MNPs) have been used as the MRI contrast agent several years. However, due to magnetic nanoparticles do not produce magnetic resonance signals, there is a lack of research on their magnetization in nuclear magnetic resonance (NMR). In this study, a method based on NMR spectroscopy is presented to assess the concentration of magnetic nanoparticles.

METHODS: Magnetization of magnetic nanoparticles is described by Langevin function. Under the magnetostatic field H_0 , the total magnetization of MNPs in the space is

$$M = NM_s \frac{\pi d^3}{6} \left(coth \left(\frac{M_s \frac{\pi d^3}{6} \mu_0 H_0}{kT} \right) \right)$$

$$-\frac{kT}{M_s \frac{\pi d^3}{6} \mu_0 H_0}$$

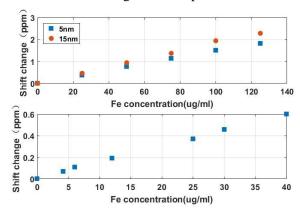


Figure 1. (a)Shift change of 5nm (square mark) and 15nm (round mark) samples at different concentrations from 25 to 125 ug/ml. (b) Shift change of 5nm (square mark) at the concentration range of 4.2 to 40 ug/ml.

Where, N is the concentration of the MNPs, M_s is the saturation magnetization of the MNPs, d is the diameter of MNPs, H is the amplitude of applied field, μ_0 is the vacuum permeability, k is Boltzmann constant, T is the absolute temperature.

The magnetization makes the magnetic field inhomogeneous. Nuclei sense the sum of the static magnetic field and of the field originated by the magnetic nanoparticles. As the particles generate spherical induced magnetic field, the magnetic flux density B_0 can be defined as $\mu_0 \left(H_0 + \frac{4\pi}{3} M \right)$. As the chemical shift is defined as a relative shift to the Larmor frequency of a reference molecule in parts per million (ppm): $\delta = \frac{\nu_{samp} - \nu_{ref}}{\nu_{ref}}$, the shift change made by magnetic nanoparticles $\Delta \delta = \frac{4\pi}{3} M = \frac{4\pi}{3} \chi$.

The shift change of different samples at different concentrations are shown as Figure 1.

RESULTS: In the experiment, deuteroxide (Aldrich-450510, Sigma-Aldrich) was used as reagents to prepare test samples. The Fe concentration of the original samples was 5mg/ml and the diameter of MNPs were 5nm (SHP-05-25, Ocean NanoTech) and 15nm (SHP-15-50, Ocean NanoTech). In the standard 5mm nuclear magnetic tube, the amount of sample used was about 400ul. We used the 43MHz NMR spectrometer (Spinsolve 43, Emphor Fzco) to measure the shift. The experiment results show that the shift changes have a good linear relationship with the sample concentration, which is in line with theoretical expectation.

CONCLUSION: This paper aims to discuss a method to study the magnetization of MNPs in NMR. Based on NMR paramagnetic shift, the signal of the concentration lower than 25ug/ml can be gotten when the field is 1T. The experiment results proved that it is feasible to measure the magnetic susceptibility by NMR paramagnetic shift and shows the possibility to improve the imaging resolution of MPI system, if using the NMR technique for signal detection. Based on the temperature sensitivity of MNPs, there is also a possibility to measurement the MNPs' temperature information from the shift change.

- [1] Pell, Andrew J., G. Pintacuda, and C. P. Grey. "Paramagnetic NMR in solution and the solid state." Progress in Nuclear Magnetic Resonance Spectroscopy (2018).
- [2] Hankiewicz, J. H., et al. "Ferromagnetic particles as magnetic resonance imaging temperature sensors." Nature Communications 7(2016):12415.
- [3] Babićstojić, Branka, et al. "Ultrasmall iron oxide nanoparticles: Magnetic and NMR relaxometric properties." Current Applied Physics 18.2(2017).

Determination of Anisotropic Magnetic Susceptibility of High Temperature Superconducting Particles

<u>Fumiko Kimura</u> ^{1, 2*}, Shigeru Horii ^{1,2}, Hayato Kashiwagi ¹, Daisuke Notsu ¹, Toshiya Doi ¹, Masahisa Wada ^{3,4}, Tsunehisa Kimura ^{3,5}

*Corresponding author: kimura.fumiko@kuas.ac.jp

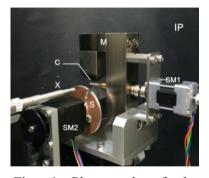
Introduction

REBa $_2$ Cu $_3$ O $_y$ and REBa $_2$ Cu $_4$ O $_8$ are superconducting ceramics having high critical temperatures. Biaxial orientation is required for the practical use of theses superconducting materials. Since these crystals are orthorhombic, three-dimensional orientation under modulated rotating magnetic field is possible. It is desirable to know the anisotropy of the magnetic susceptibility to determine the fabrication condition for the biaxial magnetic field orientation of the microcrystal. It is possible to determine the anisotropic magnetic susceptibility by a SQUID measurement of biaxially oriented sample. [1] In this study, we determine the anisotropic magnetic susceptibility of ErBa $_2$ Cu $_4$ O $_8$ (Er124) by orientation fluctuation via the half widths of the X-ray diffraction spots.

Experimental

Preparation of Er124 single crystal [2] Re-calcining (800 to 925 ° C for about 12 hours) several times of Er: Ba: Cu at molar ratio of 1: 2: 4 at atmospheric pressure was conducted by solid phase reaction method to obtain (Er123 + CuO). The obtained (Er123 + CuO) and KOH were mixed at a weight ratio of 5: 6 in an alumina crucible, and Er124 single crystals were grown in the crucible by a flux method under an atmospheric pressure. The obtained Er124 single crystals were ground using an agate mortar, and further ground using a ball mill to obtain a fine sample powder.

Magnetic Orientation and X-ray Diffraction Experiment Microcrystals were suspended in a viscosity calibration standard solution JS160,000 (manufactured by Nippon Grease Co., Ltd., viscosity 140 Pa s). The sample was poured into a capillary and the capillary was set between a pair of permanent magnets generating 1 T, and modulated rotating of sample was conducted. The rotation speeds of the capillary was changed every 90 °. The lower rotation speed ω_s was fixed at 6 rpm, and the higher speed ω_f was changed from 7.5 to 30 rpm. A disk-shaped shutter (two grooves having a width of 10 ° at 0 ° and 180 °) was placed between the



1 Photograph of the Fig. magneto-rotation unit mounted in-house on an X-ray diffractometer. (C): a glass capillary, (X): an X-ray collimator, (SM1 and SM2): stepping motors, (S): a shutter with a diameter of 44 mm, (M): a pair of neodymium magnets generating ca. 1 T, and (IP): an imaging plate at the back.^[3]

magneto-rotation unit and the X-ray collimator, and was rotated in synchronization with the rotation of

¹ Graduate School of Energy Science, Kyoto University, Yoshida-Honmachi, Kyoto 606-8501, Japan

² Nagamori Institute of Actuators, Kyoto University of Advanced Science, Kyoto 615-8577, Japan

³ Division of Forestry and Biomaterials, Kyoto University, Kitashirakawa, Kyoto 606-8502, Japan.

⁴ College of Life Sciences, Kyung Hee University, Yongin-si 446-701, Republic of Korea.

⁵ Fukui University of Technology, 3-6-1 Gakuen, Fukui 910-8505, Japan

the sample. After orientation was completed, in-situ X-ray diffraction experiments were performed.

<u>Data processing</u> Diffraction intensity as a function of the azimuthal angle β was obtained using 2DP software (manufactured by RIGAKU Co., Ltd.) from the original diffraction patterns. The peaks of

the azimuth angle plots were fitted using the Igor Pro software (WaveMetrics) to calculate the half width of the peak.

Results and Discussion

Owing to the slit of the shutter, diffraction images equivalent to those from a single crystal were obtained. Some examples are shown in Fig. 2. Er124 is orthorhombic, and the χ_1, χ_2 and χ_3 axes correspond to the b, a and c axes of the crystal lattice, where the values of χ_1, χ_2 and χ_3 are defined as $\chi_1 > \chi_2 > \chi_3$. When the modulated rotating magnetic field is applied, the χ_3 axis is aligned parallel to the rotating axis (the capillary long axis), while χ_1 , and χ_2 axes are rotating at the rotational speed of the capillary. As shown in Fig. 2, {020} and {200} diffraction points are observed every 90 ° because the angle between the χ_1 and χ_2 axes are orthogonal.

The magnetic energy E is expressed by equation (1).

$$E = C_{\theta}\theta^{2} + C_{\phi}\phi^{2} + C_{\eta}\psi^{2}$$
 ----- (1)

Here, θ , ϕ and ψ are Euler angles around the χ_2 , χ_3 and χ_1 axes (see Fig. 3). C_θ , C_ϕ , and C_ψ are a function of magnetic field strength, magnetic susceptibility anisotropy, volume of crystal, and ω_f/ω_s . The fluctuation around the energy minimum is expressed by the following equation using the Boltzmann distribution.

$$\langle \psi^2 \rangle = 8k_B \pi (1+r) T \mu_0 / (B^2 (2+\pi-2r+\pi r) V(\chi_2 - \chi_3))$$
 ----- (2)

$$\langle \theta^2 \rangle = 8 k_B \pi (1+r) T \mu_0 / (B^2 (-2+\pi+2r+\pi r) V(\chi_1 - \chi_3)) ----- (3)$$

$$\langle \phi^2 \rangle = 4k_B \pi (1+r) T \mu_0 / (B^2 (2+\pi)(-1+r) V (\chi_1 - \chi_2))$$
 ----- (4)

Here, $k_{\rm B}$ is Boltzmann constant, $r = \omega_{\rm f}/\omega_{\rm s}$, T is absolute temperature, μ_0 is permeability of vacuum, B is magnetic field strength, and V is the values of particles. Here, the fluctuations of (200), and (020), in the diffr

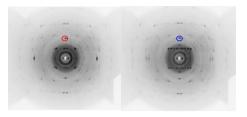


Fig. 2 in-situ X-ray diffraction images taken at two different angles (0 and 90°, respectively) obtained with the ration of $\omega_{\rm f}/\omega_{\rm s}$ =9 /6 rpm. Spots in red and blue circles correspond to {020} and {200}, respectively.

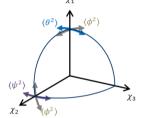


Figure 3 Mean square fluctuations $\langle \psi^2 \rangle$ of the χ_2 axis about the χ_1 axis, $\langle \theta^2 \rangle$ of the χ_2 axis, and $\langle \phi^2 \rangle$ of the χ_2 and axes about the χ_3 axis. [3]

volume of particles. Here, the fluctuations of $\{200\}$ and $\{020\}$ in the diffraction pattern of Fig. 2 correspond to $\langle \psi^2 \rangle$ and $\langle \theta^2 \rangle$. The half width is determined from an azimuthal plot of each diffraction point, each half width was plotted against r, and fitting was performed using equations (2) and (3) to obtain the anisotropy of the magnetic susceptibility $\chi_2 - \chi_3$ and $\chi_1 - \chi_3$. The values determined were 2.2 \times 10⁻⁴ and 2.9 \times 10⁻⁴, respectively. These values are very close to the anisotropic susceptibility of Er247 [1] whose structure is similar to the compound under investigation. On the other hand, the value of $\chi_1 - \chi_2$ was not evaluated because of the poor resolution arising from the slit width of 10°.

Acknowledgment

This work was partly supported by the A-STEP, JST and JSPS KAKENHI Grant Number JP17H03235.

References

- [1] S. Horii et al., J. Appl. Phys. 115 (2014) 113908.
- [2] M. Yamaki et al., Jpn. J. Appl. Phys. 51 (2012) 010107.
- [3] C. Tsuboi et al., J. Appl. Cryst. (2016). 49, 2100–2105.

The effects of constant magnetic field on the properties of polymers, biopolymers and their composites

Ewa Miękoś 1*, Marek Zieliński 1

¹ University of Lodz, Faculty of Chemistry, Department of Inorganic and Analytical Chemistry * e-mail address: ewa.miekos@uni.lodz.pl

In the era of the problem associated with enormous pollution of the natural environment with plastics, the search for new materials based on natural ingredients with better physicochemical parameters is a must and at the same time a global trend.

The aim of the study was to develop a model for controlling the properties of polymers and biopolymers using a constant magnetic field (s.p.m.) with an induction value of $B=0.5\,\mathrm{T}$. The field was used for the duration of polymerization processes of the tested samples. Research also included collecting information on the effects of s.p.m. on the materials received. It is about changes in structure, magnetic properties and mechanical strength. The components of the prepared samples were, among others, natural polymers such as chitosan or cellulose, which would facilitate their degradation in the natural environment.

The research concept assumed two variants. They were aimed at determining the changes in the structure, physicochemical properties of the materials obtained created in a constant magnetic field environment with a magnetic induction value of B = 0.5 T (variant 1) and created without the field (B = 0) (variant 2).

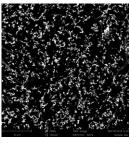
Two groups of samples were prepared. The first based on epoxy resin (Ep 5), while the second based on silicone two-component rubber (Gumosil B). Admixtures in various percentages were added to both. These were: cellulose powder, chitosan, magnetite (Fe₃O₄), titanium dioxide (TiO₂) and silica gel (SiO₂).

By scanning electron microscopy (SEM), the surfaces and cross-sections of individual materials were examined.

ANALYSIS OF MICROSCOPIC TESTING SEM

Scanning Electron Microscope (SEM) - Phenom XL with integrated EDS detector.

Ep5 + Fe₃O₄ (magnetite) 10%)





 $\mathbf{B} = \mathbf{0}$

 $\mathbf{B} = \mathbf{0.5T}$

The mechanical properties of the obtained materials were also tested. The use of a constant magnetic field and the addition of some admixtures caused favorable changes in the parameters of some polymers and biopolymers such as: bending strength, tensile strength, impact resistance and elasticity (Young's modulus).

Influence of electromagnetic stirring frequency on the grain refinement of Cu-15Ni-8Sn alloy during horizontal continuous casting

Zhe Shen ¹, Jiale Zhu ¹, Lang Ren ¹, Tianxiang Zheng ¹, Yunbo Zhong ^{1*}

¹ State Key Laboratory of Advanced Special Steel & School of Materials Science and Engineering,

Shanghai University, Shanghai 200072, China

*Corresponding author: yunboz@staff.shu.edu.cn (Yunbo Zhong)

Cu-Ni-Sn alloys, which are expected to replace the Cu-Be alloys, have been widely used for electrical switchgear, springs and connectors owing to their high corrosion resistance, high thermal conductivity and excellent electric conductivity after aging heat treatment. Continuous casting is an excellent method to produce aluminum alloy and copper alloys with high manufacturing efficiency. However, the traditional continuous casting method also brings some difficult technical problems, such as highly columnar macrostructure, serious segregation, and shrinkage porosity. These problems will result in the weak hot workable performance during the forging or rolling process, thereby yielding poor mechanical property. Grain refinement is a quite effective way to improve the deformability property and tensile strength. The electromagnetic stirring (EMS) has been used to modify the columnar to equiaxed transition (CET) [1, 2] and then refine the grain size [3, 4]. In this paper, the EMS was applied to obtain a fine, uniform equiaxed grain structure with high tensile strength during the horizontal continuous casting of Cu-15Ni-8Sn alloy. The effects of the electromagnetic stirring frequency (EMSF) on the grain refinement have been investigated. The results show that the application of the EMS is beneficial to the grain refinement, which can be attributed to the homogenization of temperature at the solidifying front and the remelting of dendritic arms.

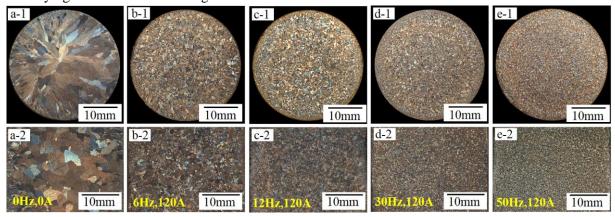


Fig. 1 The macrostructures of cross section and longitudinal section with and without the EMS: (a-1) and (a-2) 0 Hz, 0 A; (b-1) and (b-2) 6 Hz, 120 A; (c-1) and (c-2) 12 Hz, 120 A; (d-1) and (d-2) 30 Hz, 120 A; (e-1) and (e-2) 50 Hz, 120 A.

References

- [1] G. Reinhart, N. Mangelinck-Noël, H. Nguyen-Thi, T. Schenk, J. Gastaldi, B. Billia, P. Pino, J. Härtwig, and J. Baruchel, Mater. Sci. Eng. A 413 (2005) 384-388.
- [2] S. Eckert, B. Willers, P.A. Nikrityuk, K. Eckert, U. Michel, and G. Zouhar, Mater. Sci. Eng. A 413 (2005) 211-216.
- [3] W. Jin, F. Bai, T. Li, and G. Yin, Mater. Lett. 62 (2008) 1585-1588.
- [4] V. Metan, K. Eigenfeld, D. Räbiger, M. Leonhardt, and S. Eckert, J. Alloy. Compd. 487 (2009) 163-172.

Effect of high static magnetic field on the microstructural evolution and mechanical enhancement of Al-20wt.%Si ribbon during the annealing process

Tianxiang Zheng, Zhe Shen, Bangfei Zhou, Wenhao Lin, Xu Chen, Yunbo Zhong*
State Key Laboratory of Advanced Special Steel & Shanghai Key Laboratory of Advanced
Ferrometallurgy & School of Materials Science and Engineering, Shanghai University, Shanghai
200444, China;

* Corresponding author. E-mail address: yunboz@staff.shu.edu.cn (Y.B. Zhong).

Al-20wt.%Si hypereutectic alloys were designed to study the effects of high static magnetic field (HSMF) and annealing treatment on the microstructure evolution, atoms diffusion and on the resultant mechanical properties from micro scale to atomic scale. The results indicate that the size of primary silicon particles (PSPs) increased with increasing the temperature, while, it decreased with increasing the magnetic flux density (MFD). The solid solubility of Al matrixes were 0.84wt.% and 0.53wt.% for the ribbons annealed at 0 T and 8 T. HSMF decreased the precipitation rate of Al from PSPs and retained the solute trapping effect in PSPs during the annealing process. After annealing the ribbon, Al matrix retained the lattice distortions under the effect of HSMF. The application of a HSMF led to the coexistence of fine grain strengthening, dislocations strengthening and solid solution strengthening as a

result of the hardness and elastic modulus increased with increasing the MFD. In comparison with the ribbon annealed at 8 T, the hardness and elastic modulus have been improved 139.47% and 1053.2%, respectively, for the ribbon annealed at 0 T. This paper presents a new way to design heat treatment and even solidification processes for metallic materials through controlling the diffusion process assisted by using a HSMF.

The morphologies of PSPs in the ribbons annealed under various MFDs are shown in Fig. 1. It is seen that PSP gradually develops into a nearly sphere shape with increasing the temperature from 400 °C to 550 °C. For the ribbons no mater annealed with or without a HSMF, the size of PSPs increases when the temperature increased from 400 °C to 550 °C and decreased when the MFD increased from 0 T to 8 T.

Acknowledgements

The authors gratefully acknowledge the financial support of the National Natural Science Foundation of China (U1732276, No. 51704193), National Key Research and Development Program of China (2016YFB0301401), the Users with Excellence Program of Hefei Science Center CAS (2019HSC-UE010), Science and Technology Commission of Shanghai Municipality (No. 15520711000), Changjiang Scholars Program of China.

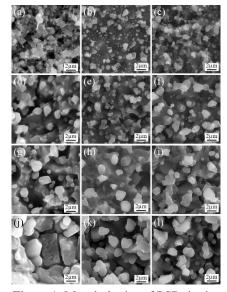


Figure 1. Morphologies of PSPs in the deeply etched ribbons annealed under various MFDs and temperatures. (a) 0 T, 400 °C; (b) 4 T, 400 °C; (c) 8 T, 400 °C; (d) 0 T, 450 °C; (e) 4 T, 450 °C; (f) 8 T, 450 °C; (g) 0 T, 500 °C; (h) 4 T, 500 °C; (i) 8 T, 500 °C; (j) 0 T, 550 °C; (k) 4 T, 550 °C; (j) 8 T, 550 °C.

Morphological Evolution of Solid-Liquid Interface during the Directional Solidification of Zn-2wt.%Bi Monotectic Alloy under a Vertical Static Magnetic Field

B.F. Zhou¹, T.X. Zheng¹, Y.B. Zhong^{1*}, Z.M. Ren ¹

¹ State Key Laboratory of Advanced Special Steel, Shanghai University Shanghai, PR China

The morphology of solid-liquid interface has a great influence on the directionally solidified microstructure of the alloys. A stable solid-liquid interface morphology is conducive to the formation of good microstructures [1]. However, at a larger pulling speed, the front of solid-liquid interface is easily unstable due to the dependence of solute concentration and phase transition temperature. The effects of solute convection, forced flow and other factors on interfacial instability have also been extensively studied [2-4]. The vertical static magnetic field (VSMF) can effectively suppress the thermo-solute convection in the fluid and couple the thermoelectric effects to form a thermoelectric magnetic convection [5-6]. The VSMF has been applied in directional solidification processes to improve the solidification state at the front of solid-liquid interface [7].

In this work, the solid-liquid interface morphology of Zn-2wt.% Bi monotectic alloy under different magnetic flux densities and different pulling speeds was studied. In the absence of VSMF, with the increase of pulling speed (1 μ m/s to 3 μ m/s), the morphology of solid-liquid interface changed from flat to cellular. With further increasing of pulling speed (3 μ m/s to 10 μ m/s), the depth of cellular cavity decreased gradually. Directional solidification results in the formation of Bi-rich second phase in the shape of fibers or droplet array. The diameter of Bi-rich droplets at the front of the solid-liquid interface increased with the increase of pulling speed and convection. This is mainly due to the combined action of Marangoni motion and intense convective motion caused by the increase of pulling speed. With the increase of magnetic flux density (0.1 T to 5 T), the depth of cellular cavity decreased and the diameter of Bi-rich droplets at the front of solid-liquid interface decreased when the pulling speed was 3 μ m/s. The application of VSMF stabilized the movement of Bi-rich droplets at the front of the solid-liquid interface and promoted the transition of the interface to a flat shape. The application of a VSMF changed the solid-liquid interface to be straight. The inhomogeneous distribution of sBi-rich droplets caused by convection was improved obviously, and the morphology of directionally solidified microstructure was more regular.

The authors gratefully acknowledge the financial support of the National Key Research and Develop- ment Program of China (Grant Nos. 2016YFB0301401 and 2016YFB0300401), the National Natural Science Foundation of China (Grant Nos. U1860202, U1732276, 50134010, and 51704193), and the Science and Technology Commission of Shanghai Municipal- ity (Grant Nos. 13JC14025000 and 15520711000).

- [1] H. Nguyen Thia, B. Drevetb, Journal of Crystal Growth 253(2003) 539-548.
- [2] R. J. Schaefer, S. R. Coriell, Metallurgical and Materials Transactions A 15.12(1985) 2109-2115.
- [3] S. R. Coriell, R. F. Boisvert, R. G. Rehm and R. F. Sererka, Journal of Crystal Growth 46.4(1981) 479-482.
- [4] A. Ludwig, W. Kurz, Acta Materialia, 44.9(1996):3643-3654.
- [5] X. Li, A, Gagnoud, Z.M. Ren, Y. Fautrelle and R. Moreau, Acta Materialia 57.7(2009):2180-2197.
- [6] P. Lehmann, R. Moreau, D. Camel and R. Bolcato, Acta Materialia 46.11(1998): 4067-4079.
- [7] J. Wang, Y. Fautrelle, Z. M. Ren, H. Nguyen-Thi, G. Salloum Abou Jaoude, G. Reinhart, N. Mangelinck-Noël, X. Li, and I. Kaldre, Applied Physics Letters 104.12(2014) 121916.

Aixal magnetic field induced the columnar-to-equiaxed transition during the directionally solidified Cu-15Ni-8Sn alloy

Ganpei Tang ¹, Zhongze Lin ¹, Zhe Shen ¹, Jiale Zhu ¹, Tianxiang Zheng ¹, Yunbo Zhong ^{1*}

State Key Laboratory of Advanced Special Steel & School of Materials Science and Engineering,

Shanghai University, Shanghai 200072, China

*Corresponding author: yunboz@staff.shu.edu.cn (Yunbo Zhong)

Due to the large solidification interval of Cu-15Ni-8Sn alloy, the precipitated Sn element is easily segregated between the Cu-Ni dendritic channels. In order to eliminate the segregation of Cu-15Ni-8Sn alloy, it is necessary to induce the columnar-to-equiaxed transition (CET) of the Cu-Ni dendrite. In this paper, the CET of Cu-15Ni-8Sn alloy has been successfully induced by an axial magnetic field-assisted directional solidification. This is attributed to the fact that the thermal electromagnetic force acting on the tip and root of the dendrite during the directional solidification under an axial magnetic field forms a torque effect that will break the dendrites and induce the CET.

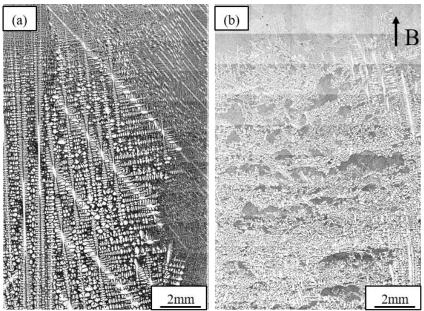


Fig. 1 Solid-liquid interface quenched by Cu-15Ni-8Sn alloy at a temperature gradient of 2.5 K/mm and a growth rate of 10μ m/s at different magnetic field intensities: (a) 0T; (b) 0.5T.

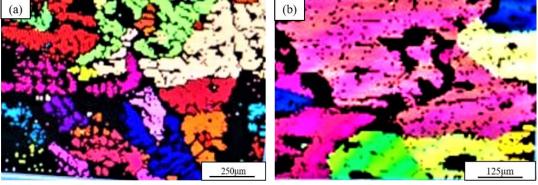


Fig. 2 EBSD map of the directionally solidified Cu-15Ni-8Sn alloy under an 0.5T axial magnetic field: (a) in the mushy zone; (b) in the directional solidification zone.

Preparation of Co-doped ZnO diluted magnetic semiconductor via hydrothermal method under a static magnetic field

Licheng Dong¹, Yunbo Zhong^{1*}, Tianxiang Zheng¹, Zhe Shen¹, Bangfei Zhou¹

State Key Laboratory of Advanced Special Steels, Shanghai University

Shanghai 200072, China

*Corresponding author: yunboz@staff.shu.edu.cn

In the past few years, diluted magnetic semiconductors (DMSs) have attracted much attention owing to their unique magnetic properties and potential applications in many fields. ZnO based DMSs systems have been an attractive semiconductor after the theoretical prediction by Dietl [1]. The magnetic field-assisted approach has been applied in the synthesis of Co-doped ZnO diluted magnetic semiconductor via hydrothermal method. The effect of magnetic field on the structure, morphology and magnetic properties of the samples are characterized. Figure1(a) displays SEM images of the samples, which clearly indicates that the Zn_{0.95}Co_{0.05}O samples are nanorods in shape. The HRTEM image implies that Zn_{0.95}Co_{0.05}O nanorods grow along the (001) plane. X-ray diffraction and X-ray photoelectron analysis reveals that Co ions have been doped in the hexagonal wurtzite ZnO and there are not any other detectable phases. In addition, Figure1(b) shows the magnetization (*M-H*) loops of Zn_{0.95}Co_{0.05}O nanorods measured at room temperature (300K). Magnetization measurements implies that all of the Zn_{0.95}Co_{0.05}O samples are room-temperature ferromagnetic and the magnetic field can significantly improve the magnetism of the products.

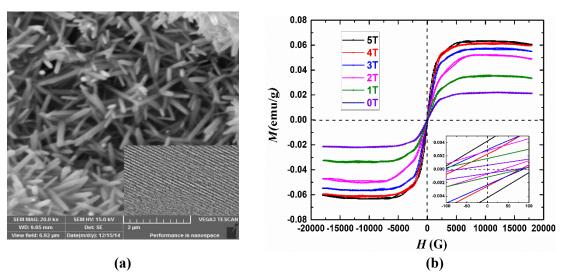


Figure 1. (a) SEM image and (b) M-H curves of the samples prepared in various magnetic field intensities

Acknowledgements

The authors gratefully acknowledge the financial support of the National Natural Science Foundation of China (U1732276, No. 51704193), National Key Research and Development Program of China (2016YFB0301401), the Users with Excellence Program of Hefei Science Center CAS (2019HSC-UE010), Science and Technology Commission of Shanghai Municipality (No. 15520711000), Changjiang Scholars Program of China.

[1]T. Dietl, H. Ohno, F. Matsukura, J. Cibert, D. Ferrand, Science 287 (2000) 1019-1022.

Growth of single crystals of the weak ferromagnet Fe₃BO₆

N.Liubachko ^{1*} and S.Barilo ¹

¹ SSPA "Scientific-practical materials research centre of NAS of Belarus", Minsk, Belarus * e-mail address: n_lubochko@mail.ru

Two ternary compounds are known to occur within tire binary section Fe_2O_3 —B2O3 of the ternary system iron—boron—oxygen [1]. The green calcite-type $FeBO_3$ has been intensively studied in the past with respect to magnetooptical applications since it combines partial transparency in the visible with a spontaneous magnetization at room temperature (7N = 348 K) [2]. $FeBO_3$ is a so-called easy-plane weak ferromagnet with canted spins lying in the hexagonal (0001) plane. Bulk single crystals of $FeBO_3$ in sizes up to $8 \times 6 \times 4 \text{ mnr}^3$ have been grown from the vapor phase [3]. These large crystals have made possible the magnetic and optical characterization of the material.

Similar data on the other Fe(III) borate, Fe₃B0₆, are sparse. The compound has an orthorhombic crystal structure which has recently been refined [1]. It is isotypic to that of the mineral norbergite,

Mg₃SiO₄(0H)₂ [3], Fe₃BO₆ is a canted weak easy-axis ferromagnet. Below 415 K, the spins are oriented parallel to the [001] direction with canting along [100]. Between 415 K and the Neel temperature of 508 K the spin orientation is parallel to [100] with canting along [001] [2].

The aim of the present investigation is to study the relations in the system and to use the results as a guide to determine the optimum conditions to grow single crystals of iron borate.

The Fe_3BO_6 single crystals were grown from the flux consisting of 8,3 mass% Fe_2O_3 + 48,3 mass% B_2O_3 + 7,6 mass% PbO + 35,8 mass% PbF₂. The saturation temperature was

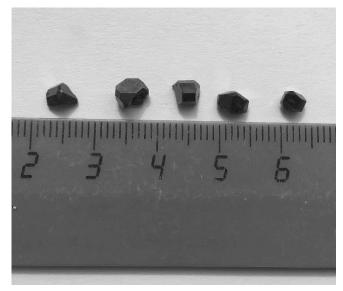


Fig 1. The typical yield of Fe₃B0₆ crystals

determined with the help of probe crystals to be Tsat ≈ 890 °C. The fluxes with the mass of 500 g were prepared by melting of the Fe₂O₃, B₂O₃, PbO and PbF₂ oxides at the temperature of 1000 °C, using a platinum crucible. The flux was kept during 4 h at this temperature for homogenization. After wards the flux temperature was decreased down to T = Tsat + 10 °C, the platinum ring carrier was settled down into the flux, and carrier's rotation of 30 revolutions per minute was switched on. After 60 min the flux temperature was decreased down to T = Tsat – 10 °C. Then the temperature was decreased with velocity of (1–3) °C/24 h. The total duration of crystal growth was about 14 days. The crystals with linear dimensions up to 4–6 mm were grown. The typical yield of Fe₃BO₆ crystals is seen in Fig.1.

A simplified XRD pattern in Fig. 2 infers a preferred growth in single Fe3BO6 crystals. The most intense XRD peak observed in the (221) reflections at 0.2631 nm d_{hkl} -value thus ascribes to a preferred (221) growth of Fe3BO6 crystallites. Two reflections (230) and (600) from the lateral surfaces of a crystal lattice share the second and third most intense peaks at 0.2477 nm and 0.1675 nm of dhkl-values respectively. In a bulk polycrystalline Fe3BO6, three most intense peaks occur in other reflections (121),

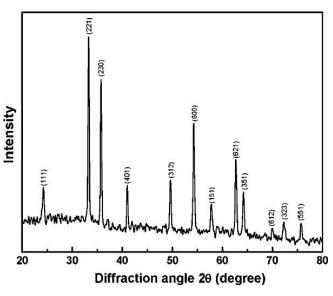


Fig 2. XRD pattern in Fe3BO6 crystals

(311), and (232) at 0.2953, 0.2558, and 0.1660 nm respectively.

The following conclusions can be drawn from experiments on the growth of Fe₃BO₆ crystalls:

- [a] Using the flux composition and temperature regime crystals up to 4-6 mm in diameter were obtained.
- [b] Starting from the preliminary results the growth conditions of Fe3BO6 single crystals were optimized: the content of Fe $_2$ O $_3$ and B $_2$ O $_3$ in the flux was lowered and a new temperature regime including appreciably decreased soak temperature and starting temperature of the slow cooling was applied. Using these

conditions the reproducible growth of large Fe_3BO_6 crystals (occasionally up to 7 mm across) of a high perfection was achieved.

References

[1] R. Diehl and G. Brandt, Acta Cryst. B 31 (1975) p.1662.

[2] J.P. Attfield, A.M.T. Bell, L.M.R. Martinez, J.M. Greneche, R. Retoux, M. Leblanc, R.J. Cernik, J.F. Clarke and D.A. Perkins, J. Mater. Chem. 9 (1999) p.205.

[3] J.G. White, A. Miller and R.E. Nielsen, Acta Crystallogr. 19 (1965) p.1060.

Magnetic Fluid Based on Liquid Metal

Sen Chen 1,3, Hong-zhang Wang2, Jing Liu 1,2,3*

¹ Technical Institute of Physics and Chemistry, Zhongguancun East Rd.29, Haidian District, Beijing, China; ² University of Chinese Academy of Sciences, Yuquan Rd.19(A), Shijingshan District, Beijing, China; ³Tsinghua University, Shuangqing Rd.30, Haidian District, Beijing, China,

* Corresponding author: jliu@mail.ipc.ac.cn

Gallium-based liquid metals combined with metal and fluid properties are attracting increasing attention from academia and industry due to their excellent thermal conductivity, electrical conductivity, fluidity and non-toxicity. In recent years, it has gradually been widely used in the fields of thermal management, flexible electronics, additive manufacturing, biomedicine, soft machines, and microfluidics [1-3]. Among these many excellent characteristics, the huge surface tension of liquid metal is one of the points that cannot be ignored. In general, liquid metal has a surface tension of 700 mN, which is the currently known liquid with the highest surface tension. Because of its large surface tension, liquid metal exhibits rich interfacial phenomena such as self-driven motion, surface convection, periodic oscillation, amoeba motion, serpentine motion, etc. [4-7]. Further research has found that liquid metal has a rich deformation behavior under the stimulation of many external factors. Current research has

shown that liquid metals can respond to electricity, magnetism, sound, light, and heat [8-10].

The discovery of many behaviors of liquid metal has made us aware of the possibility of liquid metal soft machines or robots. In order to realize the liquid metal soft machines, flexible curing of liquid metal with excellent fluidity is one of the important functions. However, achieving solid-liquid transitions of liquid metals has always been an urgent challenge. Experiment found that the magnetic liquid metal will solidify under the action of magnetism, which suggests that we can use the external magnetic field to control the rapid solid-liquid change of the liquid metal to achieve shaping. Experiments have shown that the magnetic field can dramatically affect the Young's modulus of liquid metal. Further, we have proposed several methods for preparing magnetic liquid



Fig. 1 Magnetic fluid based on liquid metal with the ability of solid-liquid transformation.

metals to improve the stability of magnetic liquid metals during long-term operation. In addition, the magnetic fluid itself is worth studying because of its magical properties. And we believe that this research will enrich the knowledge of magnetic fluids.

References

- [1] Q. Wang, Y. Yu, J. Yang, Advanced Materials. 27, 7109–7116, 2016.
- [2] X. Yang, S. Tan, Z. He, Applied Thermal Engine. 119, 34–41, 2017.
- [3] Y. Yu, F. Liu, R. Zhang, et al, Advanced Materials Technology. 2, 1700173, 2017.
- [4] B. Yuan, L. Wang, X. Yang, et al, Advanced Science. 3, 1600212, 2016.
- [5] J. Zhang, Y. Yao, L. Sheng, et al, Advanced Materials. 27, 2648-2655, 2015.
- [6] L. Hu, L, Wang, Y, Ding, et al, Advanced Materials. 28, 9210-9217, 2016.
- [7] S. Chen, X. Yang, Y. Cui, et al, ACS Applied Materials & Interface. 10, 22889-22895, 2018.
- [8] L. Sheng, Z. He, Y. Yao, et al, Small. 11, 5253-5261, 2015.
- [9] S. Tan, H. Gui, B. Yuan, et al, *Applied Physics Letters*. 107, 071904, 2015.
- [10] SA. Chechetka, Y. Yu, X. Zhen, et al, Nature Communications. 8, 15432, 2017.

MnFe₂O₄/Coffee Waste biocarbon composites dominated by size dependent magnetic component for microwave absorption materials

Ali Hassan^{1, 2}, Wei Ding^{2, 3}, Yuecheng Bian^{1, 2}, Adnan Aslam^{1, 2}, Zhigao Sheng^{1*}

¹Anhui Province Key Laboratory of Condensed Matter Physics at Extreme Conditions, High Magnetic Field Laboratory, Chinese Academy of Sciences, Hefei 230031, China

²University of Science and Technology of China, Hefei 230026, China

³Key Laboratory of Materials Physics, Institute of Solid State Physics, Chinese Academy of Sciences, Hefei 230031, China

In order to prepare MnFe₂O₄/coffee waste (MFO/CW) biocarbon composites having size dependent magnetic component, MnFe₂O₄ were ball milled for 0, 8 16 and 24 h and biocarbon was prepared by coffee waste. Depending upon the ball milling time of the magnetic component, four samples of MFO/CW composites were prepared and called them as 0 h-MFO/CW, 8 h-MFO/CW, 16 h-MFO/CW and 24 h-MFO/CW for 0, 8, 16 and 24 h milling time, respectively. Microwave absorption properties of these composites have been done; which show significant enhancement of microwave

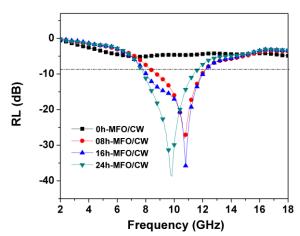


Figure 1: RL curves of the MFO/CW at different ball milling times.

absorption performance in ball milled samples. Even after 8 h ball milling time minimum reflection loss (RL) is improved by more than three and half times as compare to without ball milled sample. Minimum RL of -8.1, -30, -35.8 and -38.6 dB has been attained at 0, 8, 16 and 24 h ball milling time, respectively. Our results specifically indicate that microwave absorption properties of the composites can be controlled by changing the grain size of the magnetic material according to our desire or need.

*For correspondence: TEL, +86-551-65592095

E-mail, zhigaosheng@hmfl.ac.cn

Low density and efficacious EM wave absorption material based on biocarbon obtained from Wheat straw

Muhammad Adnan Aslam ^{1,2}, Ali Hassan^{1,2}, Ding Wei ³, Yuecheng Bian^{1,2}, Caixing^{1,2}, Qiangchun liu⁴, Zhigao Sheng ^{1*}

¹Anhui Province Key Laboratory of Condensed Matter Physics at Extreme Conditions, High Magnetic Field Laboratory, Chinese Academy of Sciences, Hefei 230031, China; ²University of Science and Technology of China, Hefei 230026, China; ³Key Laboratory of Materials Physics, Institute of Solid State Physics, Chinese Academy of Sciences, Hefei 230031, China; ⁴School of Physics and Electronics Information, Huaibei Normal University, Huabei 235000, China

 *E -mail: zhigaosheng@hmfl.ac.cn

Low-density carbon-based dielectrics have drawn extensive attention for electromagnetic absorption and shielding. Herein, microporous carbon has been obtained from facile carbonization and subsequent KOH activation of wheat straw waste and its microwave absorption properties have been studied. The as prepared carbon reflects altered morphology by KOH activation with numerous micropores. The activated sample synthesized at 600 °C possesses much higher absorption. Different loading ratios (8-20%) of active material were used to make the samples. Sample with 20% carbon ratio presents reflection loss of -40 dB at 15 GHz with an operational bandwidth of 2 GHz (from 14 to 16

GHz) corresponding to 2 mm sample thickness. Three-dimensional porous bed formed after activation promotes multiple reflections, in addition, interfacial polarization and dipolar relaxation contributes to excellent microwave attenuation. In contrast, non-activated bio carbon possesses very low absorption corresponding to its low dielectric loss. Consequently, chemically activated porous carbon is a potential candidate to be used as low-density protection shield from microwaves.

Acceleration of Liquid-Solid Redox Reaction with a Magneto-Catalyzed Method

<u>Caixing Liu</u> ^{1,2}, Yang Yang ¹, Yuecheng Bian ^{1,2}, Zongwei Ma ¹, Chun Zhou ¹, Qianwang Chen ^{1,2}, Yuping Sun ^{1,3}, and Zhigao Sheng ^{1*}

¹ Anhui Province Key Laboratory of Condensed Matter Physics at Extreme Conditions, High Magnetic Field Laboratory, Chinese Academy of Science, Hefei 230031, China; ² University of Science and Technology of China, Hefei 230026, China; ³ Key Laboratory of Materials Physics, Institute of Solid State Physics, Chinese Academy of Sciences, Hefei 230031, China

*Corresponding author: zhigaosheng@hmfl.ac.cn

In a conventional catalyzed reaction, the catalysts can accelerate the reaction rate dramatically, while they are generally difficult to be separated from the reaction products. To overcome this, finding a noncontact catalytic method holds a great promise for chemical industry. In this chemical catalog, electrostatic catalysis has been developed at first ^[1]. In addition, another remote and noncontact solution is the magnetic field. So far, several magnetic field effects on the chemical reactions have been discovered ^[2]. However, the exploring of magneto-catalyzed method and their dominant factors has not been carried out much to date.

In this manuscript, by taking a liquid-solid redox reaction Zn/CuSO₄ as a model system, we present a remote and non-touched magneto-catalyzed method that can accelerate chemical reaction efficiently. The effects from intensity (B) and product of intensity and gradient $(B\nabla B)$ of applied magnetic field are distinguished and the dominant role played by the B has been confirmed. With B = 8.4 T, 22 times enhancement of reaction rate and 7700 J/mol reduction of activation energy were achieved. With evidenced by

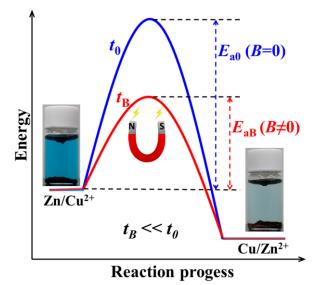


Fig. 1 Reduction of activation energy by magnetic field.

microscopic observations and compared experimental results, the field induced magnetohydrodynamics effects on the formation of Zn-Cu galvanic cells, the area of Cu/Cu²⁺ interfaces, as well as the reaction

rate have been discovered. These observations provide a new route for the remoted catalysis of chemical reaction by the magnetic field.

References

- [1] Albert C. Aragonès, Naomi L. haworth, Nadim Darwish, et al. Nature 2016, 531 (7592), 88-91.
- [2] Hisayoshi Matsushima, Andreas Bund, Waldfried Plieth, Electrochim Acta 2007, 53 (1), 161-166.

Magneto-Optical Systems Built in High Magnetic Field Laboratory

Zongwei Ma ¹, Chun Zhou ¹, Zhigao Sheng ^{1*}

¹ Anhui Key Laboratory of Condensed Matter Physics at Extreme Conditions, High Magnetic Field Laboratory, Chinese Academy of Sciences, Hefei 230031, China *Corresponding author:zhigaosheng@hmfl.ac.cn

Optical methods are widely used to perform time-, space-, and energy-resolved characterization of material properties (e.g. electronic structure, magnetic order, etc.) with high sensitivity [1-4]. At High Magnetic Field Laboratory, we have built a number of high- and low-field optical measurement systems, including:

1) THz-TDS systems under high and low fields

This system is capable of characterizing the low energy excitation, such as spin waves of materials in the 0.1-3 THz band in the (0-0.3 T, 90-800 K) or (0-7 T, 4-300 K) field and temperature range.

2) MOKE/Faraday systems under high and low fields

The MOKE/Faraday measurement systems for 0-35 T water-cooled magnet and 0-0.7 T coil magnet was built respectively, in which the latter can realize micro-MOKE measurements and magnetic domain imaging at a spatial resolution of ~1 micron.

3) SHG System

The polarization-resolved second-harmonic-generation (SHG) system based on an 800 nm femto-second laser can help to characterize the polarization state of the sample in the 10-400 K range, from which the spatial inversion symmetry and phase-transition behavior can be analyzed.

4) Ultra-fast pump-probe system

Transient absorption and time-resolved MOKE response of the sample under a femtosecond optical pump can be measured. The excitation and relaxation dynamics of electrons and spin waves can thus be investigated with a time resolution of ~200 fs.

5) Spectroscopy systems

Fiber-based spectroscopy systems are built on a 0-8 T superconducting magnet and the 0-35 T water-cooling magnet to obtain the absorption and luminescent spectra of materials under high magnetic fields in the 200-2800 nm range for electronic structure analysis.

The above systems provide multi-faceted characterization approaches for a variety of materials, for example, magnetic thin films, van der Waals crystals, multiferroic materials, etc. The results are important to help reveal the influence of magnetic fields on the electronic structure and magnetic order of these materials, as well as the ultrafast dynamics happening in them.

References

- [1] M. Fiebig, V. V. Pavlov and R. V. Pisarev, J. Opt. Soc. Am. B 22 (2005) 96-118.
- [2] A. Kirilyuk, A. V. Kimel, and Theo Rasing, Rev. Mod. Phys. 82 (2010) 2731-2784.
- [3] C. Gong, L. Li, Z. Li, et al. Nature, 546 (2017) 265-269.
- [4] C. Jin, E. C. Regan, A. Yan, et al. Nature, 567 (2019) 76-81.

Acceleration of Kirkendall Effect process in silicon nanospheres using magnetic fields

Yuecheng Bian, ^{1,2} Wei Ding, ³ Lin Hu, ¹ Zongwei Ma, ¹ Long Cheng, ¹ RanranZhang, ¹ XuebinZhu, ³ XianwuTang, ³ JianmingDai, ³ Jin Bai, ³ YupingSun, ¹ Zhigao Sheng. * ¹ Anhui Province Key Laboratory of Condensed Matter Physics at Extreme Conditions, High Magnetic Field Laboratory, Chinese Academy of Science, Hefei 230031, china; ² University of Science and Technology of China, Hefei 230026, China; ³ Key Laboratory of Materials Physics, Institute of Solid State Physics, Chinese Academy of Sciences, Hefei 230031, China. *Corresponding author: E-mail: zhigaosheng@hmfl.ac.cn

We firstly show that the magnetic fields can act as an independent parameter to accelerate Kirkendall effect in a liquid reaction system. By taking silicon-based nanospheres as the model, it was demonstrated that the magnetic fields could efficiently shorten the time of the Kirkendall effect process at relative low reaction temperatures. The hollow structure of product obtained in 5 h under a magnetic field of 1 T is the same as that consumed 24 h without a magnetic field.

Reference

[1] Y. C. Bian, W. Ding, L. Hu, Z.W. Ma, L. Cheng, R. R. Zhang, X. Zhu, X. W. Tang, J.M. Dai, J. Bai, Y. P. Sun and Z. G. Sheng, CrystEngComm, 2018, 20, 710.

Enhanced backbone alignment and charge transport of a semiconducting diketopyrrolopyrrole copolymer by solvent vapor annealing under high magnetic field

Xuhua Xiao ^{1, 2}, Guoxing Pan¹, Songlin Su^{1, 2}, Xuebin Zhu³, Fapei Zhang^{1*}

¹ Anhui Province Key Laboratory of Condensed Matter Physics at Extreme Conditions, High Magnetic Field Laboratory (HMFL), Chinese Academy of Sciences, Hefei 230031, P. R. China; ² University of Science and Technology of China Hefei 230026, P. R. China; ³ Key Laboratory of Materials Physics Institute of Solid State Physics Chinese Academy of Science Hefei 230031, P. R. China *Corresponding author: fzhang@hmfl.ac.cn

Controlling the molecule orientation of organic semiconductors is crucial to improve the performance of electronics devices. The achievement of polymer chain alignment in macroscopic scale

promotes the formation of fast long-range intrachain conduction pathway, and also enhances the ordering of π - π stacking for efficient interchain hopping, via the chain extension in the crystallinites and at the chain ties [1,2]. Therefore the aligned film structure is important to improve charge transport.

Herein, we report a straightforward method to achieve large-area highly aligned film of a diketopyrrolopyrrole- bithiophene polymer (PDPP2TBT) by solvent vapor annealing (SVA) of the asspun films under high magnetic field. The structural characterizations disclose that the chain backbones of PDPP2TBT in the films are highly aligned to the applied magnetic field during SVA while the films exhibit high crystallinity. A mechanism is proposed to explain magnetic alignment, based on the reformation of chain aggregates in the wet film exposed to solvent vapor. Field-effect transistors (FETs) based on the magnetically aligned PDPP2TBT films exhibit an enhancement of hole mobility (maximum value of 1.56 cm²/Vs) by a factor of 6 compared to the unaligned devices, as well as mobility anisotropy of three. Temperature-dependent FET mobility measurement reveals a remarkable lowering of thermally activated energy for carrier hopping in the aligned film compared to unaligned one. The results indicate the formation of rapid intra-chain charge conduction pathway parallel to the chain alignment direction, which originates from the alignment-induced backbone extension and enhanced order of interchain packing.

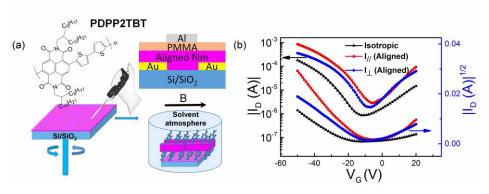


Fig.1 (a) Schematic diagram of the SVA process for the fabrication of the aligned polymer films; (b) Typical transfer curves for the TG/BC OFETs of an unaligned film as well as the aligned films with the channel current parallel ($I_{//}$) and perpendicular (I_{\perp}) to the magnetic field direction, respectively.

References

[1] B. G. Kim, E. J. Jeong, J. W. Chung, S. Seo, B. Koo and J. Kim, Nat Mater, 2013, 12, 659-664. [2] J. Xu, H. C. Wu, C. Zhu, A. Ehrlich, L. Shaw, M. Nikolka, S. Wang, F. Molina-Lopez, X. Gu, S. Luo, D. Zhou, Y. H. Kim, G. N. Wang, K. Gu, V. R. Feig, S. Chen, Y. Kim, T. Katsumata, Y. Q. Zheng, H. Yan, J. W. Chung, J. Lopez, B. Murmann and Z. Bao, Nat Mater, 2019, 18, 594-601.

Magnetic features of the magnetoreceptor MagR revealed via its tetramer

Peilin Yang¹, Tiantian Cai¹, Yuebin Zhang², Qiu-Yun Tan³, Kedong Wang³, Zhen Guo¹, Guohui Li², Bing-Wu Wang⁴, & Can Xie^{1,5}

¹State Key Laboratory of Membrane Biology, Laboratory of Molecular Biophysics, School of Life Sciences, Peking University, Beijing 100871, China; ²State Key Laboratory of Molecular Reaction Dynamics, Dalian Institute of Chemical Physics, Chinese Academy of Sciences, 457 Zhongshan Rd, Dalian 116023, China; ³State Key Laboratory of Nuclear Physics and Technology, Peking University, Beijing 100871, China; ⁴College of Chemistry and Molecular Engineering, Peking University, Beijing 100871, China; ⁵Beijing Computational Science Research Center, The Chinese Academy of Engineering Physics, Beijing 100084, China

The ability of animals to perceive guidance cues from Earth's magnetic field for orientation and navigation has been supported by a wealth of behavioral experiments, yet the nature of this sensory modality remains fascinatingly unresolved and wide open for discovery. MagR has been proposed as a putative magnetoreceptor based on its intrinsic magnetism and its complexation with a previously suggested key protein in magnetosensing, cryptochrome (Cry), to form a rod-like polymer structure. Here, we report the hierarchical assembly of MagR via a designed single-chain tetramer of MagR protein (SctMagR). The magnetic features of SctMagR was simulated and validated by designed experiments, providing insights into the unresolved origin of the intrinsic magnetic moment, which is of considerable interest in both biology and physics.

The Iron-Sulfur Cluster Binding of MagR: An Updated Model

Zhen Guo¹, Can Xie^{1, 2}

¹State Key Laboratory of Membrane Biology, Laboratory of Molecular Biophysics, School of Life Sciences, Peking University, Beijing 100871, China ²Beijing Computational Science Research Center, The Chinese Academy of Engineering Physics, Beijing 100084, China

MagR has been proposed as a putative animal magnetoreceptor based on its intrinsic magnetism and its ability to form complex with a previously suggested key protein in magnetosensing, cryptochrome (Cry). MagR is a protein that exhibits iron-sulfur cluster binding, however, the type of iron-sulfur cluster and its binding sites remains unknown. Here in this study, the iron-sulfur cluster of MagR was characterized as [3Fe-4S] or [4Fe-4S] with Electron Paramagnetic Resonance (EPR) measurements. Three classical iron-sulfur cluster binding sites (C60, C124, C126) and one unconventional binding site (E128) were further identified by mutagenesis, Ultraviolet—visible spectroscopy and EPR measurement. Thus, an updated structural model of MagR was built and optimized.

Effects of Power Frequency Magnetic Field on Cell Behaviour in MCF-7 Cells

Liyuan Liu¹, Guirong Ding^{*}

¹ Department of Radiation Protection Medicine, AirForce Medical University
Xi' an, Shaanxi, PRC, 710032
*Guirong Ding: dingzhao@fmmu.edu.cn

PURPOSE OF RESEARCH: Epidemiological studies suggest that exposure to power frequency magnetic fields may be a risk factor for breast cancer in humans [1]. To study the relationship between exposure to 60-Hz magnetic fields (MFs, 5 mT) and breast cancer, human breast cancer (MCF-7) cells was used as experimental subjects to investigate the effects of power frequency magnetic field on cell behavior with or without X - ray radiation in MCF-7 cells.

MATERIALS AND METHODS: The MCF-7 cells were divided as sham, MFs (5 mT), X-ray (4 Gy or 12 Gy) and combined group (4 Gy + 5 mT or 12 Gy + 5 mT). Cell growth was measured by a particle counter (Beckman Coulter). Cycle distribution and apoptosis of cells after exposure was measured by flow cytometry. P21, Bax, and Bcl-2 Expressions were measured by western-blotting.

RESULTS: The influence of the magnetic field on the proliferation of MCF-7 breast tumor cells was evaluated. Figure 1 shows that exposure to the 60-Hz MF has little or no effect on the growth of MCF-7 cells.

To determine the effects of exposure to MFs and/or X rays on cell cycle progression, cell cycle distribution was assessed by flow cytometry after exposure to MF ($60\,Hz$, $5\,mT$) for 4, 8, and 24 h, with or without pretreatment with 4 Gy X rays. As shown in Fig. 2, MF alone has no effect on cell cycle distribution in MCF-7 cells. At 4 h after X-irradiation, cells showed slight

accumulation in the G2/M phase and the percentage of G2/M cells was A 4h

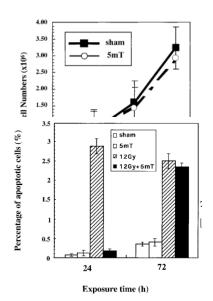
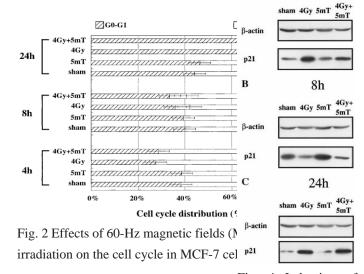


Fig. 3 Effects of 60-Hz magnetic fields (MFs) and/or X-ray irradiation on apoptosis in MCF-7 cells.



elevated from 18 to 25%. At 8 h postirradiation the increased level of G2/M cells became more obvious, while the S phase population declined from 47 to 6%. This may be because cells could not pass through the G2/M checkpoint.

Fig. 4 Induction of p21 after exposure to 60-Hz magnetic fields (MFs) and/or X-ray irradiation in MCF-7 cells.

With the recovery of the G2/M checkpoint, cells finally accumulated in the G1 phase at 24 h. Exposure to the magnetic field has no effect on the X-ray-induced G1 and G2 phase arrest within 24 h.

Exposure to 60-Hz MF alone did not induce apoptosis in MCF-7 cells. At 24 and 72 h after 12 Gy X-irradiation, only a few cells (about 2-3%) entered the apoptosis pathway. Interestingly, exposure to the MF for 24 h following irradiation significantly decreased X-ray-induced apoptosis from about 3 to 0.2%. However, this effect was not found at the 72 h time point (Fig. 3). To confirm the effect on cell growth of the exposure to MFs with or without X-irradiation, p21 expression was determined by Western

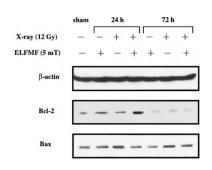


Fig. 5 Induction of Bax and Bcl-2 after exposure to 60-Hz magnetic fields (MFs) and/or X-ray irradiation in MCF-7 cells.

blotting. As shown in Fig. 4, the MF alone has no effect on p21 expression. After 4 Gy X-irradiation, p21 expression clearly increased at 4 h, and maintained a high level for at least 24 h. The MF had no effect on X-ray-induced p21 expression. To explore the mechanism by which the MF decreased X-ray-induced apoptosis in MCF-7 cells, the expression of the apoptosis regulatory proteins, Bax and Bcl-2, was determined. Exposure to the MF decreased the X-ray-induced Bax expression at 24 h, although its expression was very weak (about 1.5-fold of sham exposure) after a high dose of irradiation (12 Gy). At 72 h, no effect of MF on X-ray-induced Bax expression was found. In the case of Bcl-2, X-irradiation had no effect on its expression. However, X-irradiation (12 Gy) followed by MF exposure induced a significant increase in Bcl-2 expression (about 3-fold of

sham exposure) at 24 h (Fig. 5). This effect was not found at the 72-h time point.

CONCLUSION: The exposure to 60-Hz MFs has no effects on the growth of MCF-7 cells, but it might transiently suppress X-ray-induced apoptosis through increasing the Bcl-2/Bax ratio.

Reference

[1] Li W, Ray RM, and Thomas DB, Am J Epidemiol. 2013; 178(7):1038-1045.

Effects of hypomagnetic field on neurotransmitter, hormone and blood parameters in laboratory rodents

Lanxiang Tian^{1, 2*}, Yingying Zhang^{1, 2}, Bingfang Zhang^{1, 2}, Yongxin Pan^{1, 2}

¹ Biogeomagnetism Group, Key Laboratory of Earth and Planetary Physics, Institute of Geology and Geophysics, Chinese Academy of Sciences, Beijing, 100029; ² France-China International Laboratory of Evolution and Development of Magnetotactic Multicellular Organisms, Beijing 100029

*Corresponding author: tianlx@mail.iggcas.ac.cn

The role of geomagnetic field in growth and development of living organisms on Earth has paid more and more attentions in recent years. The weakening of geomagnetic field strength would cause a variety of biological responses. In this study, we aimed to investigate the effects of continuous exposure to hypomagnetic field on neurotransmitter, hormone content and blood routine parameters in 8-week-old C57BL/6 mice. The contents of neurotransmitters and hormones including gamma-aminobutyric

acid (GABA), serotonin (5-HT), dopamine (DA), acetylcholine (Ach), noradrenaline (NA), thyroxine (T4) and growth hormone (GH) in the brain tissue or serum samples were measured using LC-MS and ELISA methods. Meanwhile, we also measured the levels of four kinds of important hormones (androgen, estrogen, T4, GH) in 3-week-old SD rat. We found that the contents of 5-HT and NA in the brain tissues of mice exposed to hypomagnetic field decreased significantly after 1-week exposure (P < 0.05), and the contents of 5-HT in serum decreased significantly after 3-week exposure (P < 0.01). The contents of T4 decreased significantly at the 3rd, 6th, 12th week (P < 0.05). However, there was no continuous decrease for several weeks in these parameters. Blood routine examination showed that the number of white blood cells (WBC) of mice increased significantly at the 1st week [1]. While the hormone levels in the blood of the rats had shown significant continuous decrease since 2-week. After 1-week recovery in geomagnetic field condition, the hormone levels of rats began to recover, and basically returned to the level of normal geomagnetic field after the second week of recovery in geomagnetic field condition. The number of WBC of rats in HMF group had significantly increased (P<0.05) since the 3-week exposure [2]. These results showed that the response to the exposure to hypomagnetic field for mice and rats were not completely consistent, for example the levels of T4 and GH had continuous decrease for several weeks in rats, not in mice. It may be due to the species difference. The study indicates that T4 and WBC may be physiological parameters sensitive to the hypomagnetic field exposure in laboratory rodents, which should be paid special attention to in future studies.

References

- [1] Zhang Y Y, Tian L X. Effects of hypomagnetic field on neurotransmitter, hormone and blood parameters in male mice (in Chinese). Chinese Journal of Zoology, 2019, 54(4), 538-548.
- [2] Tian L X, Pan Y X. The geomagnetic field effects on animals: A review (in Chinese). Chin Sci Bull, 2018, 63, doi: 10.1360/N972018-00650.

The Effects of High-frequency Repetitive Transcranial Magnetic Stimulation on Cognition and Neuronal Excitability in Neonatal Mice

Chong Ding ¹, Haijun Zhu ¹, Guizhi Xu ^{1*}

Hebei University of Technology, Tianjin, China

* Guizhi Xu: gzxu@hebut.edu.cn

Repetitive transcranial magnetic stimulation (rTMS) is a noninvasive brain stimulation technique that has been paid attention to with increasing interests as a therapeutic neural rehabilitative tool. Studies confirmed that high-frequency rTMS could improve the cognitive performance in behavioral test as well as the excitability of the neuron in animals [1] [2]. However, it is not clear how rTMS affects the cognition and neuronal excitability, and little is known about the underlying cellular and molecular mechanisms of rTMS.

In this study, neonatal female Kunming mice (one-week old) were randomly divided into four groups: control group (with no rTMS, n=6), rTMS *in-vitro* group (with brain-slice stimulation, immediate effect group, n=6), rTMS 1 d group (with rTMS for 1 d, short-term effect group, n=6) and rTMS 15 d group (with rTMS for 15 consecutive days, cumulative effect group, n=6). In the whole

experimental design, for the rTMS 15 d group, from the first day of the experimental design to the 15th day, one session of rTMS was applied daily for 15 consecutive days. From the 16th day to the 21th day, behavioral tests were performed. On the 22nd day, the patch-clamp experiment was performed. For the rTMS 1 d group, one session of rTMS was applied only on the 15th day, the schedule of behavioral tests and patch-clamp experiment was the same as the rTMS 15 d group. For the control group, mice were treated with no rTMS, the schedule of behavioral tests and patch-clamp experiment was the same as the rTMS 15 d group. For the rTMS *in-vitro* group, rTMS and behavioral tests were not applied to the living mice. Bain slices were prepared only on the 22nd day, one session of rTMS was applied to a brain-slice and then recorded the electrophysiological properties immediately on this brain-slice.

Data analysis of behavioral tests showed that the cognition of neonatal mice had been significantly enhanced in the rTMS 15 d group compared with the control group, but this phenomenon did not show in rTMS 1 d group. Data analysis of patch-clamp experiment indicated that compared with the control group, electrophysiological properties of the rTMS *in-vitro* group and the rTMS 15 d group showed similar trends, that was, significant improvement. Furthermore, the improvement was more significant in the rTMS 15 d group. Similarly, this phenomenon did not show in rTMS 1 d group.

Accordingly, we speculate that high-frequency rTMS is able to enhance the cognitive ability of female neonatal Kunming mice, and rTMS has an immediate and cumulative effect on the neuronal excitability in hippocampal DG neurons. And changes in electrical properties and improvement in the excitability of DG neurons may be one of the mechanisms of the effects of rTMS on these changes. On the other hand, these results could be useful in optimizing rTMS protocols for further research and clinical application.

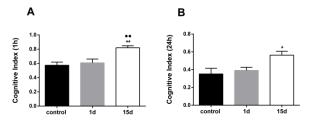


Fig. 1 Cognitive Index (1 h and 24 h) of NOR test. * $P \le 0.05$, ** $P \le 0.01$ vs. control group; •• $P \le 0.05$ vs. rTMS 1 d group.

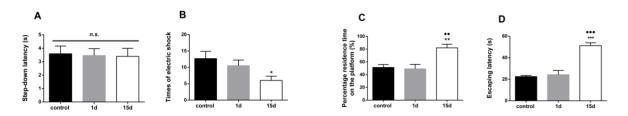


Fig. 2 Data analysis of step-down test. (A) Step-down latency. (B) Times of electric shock. (C) Percentage residence time on the platform. (D) Escaping latency. ** $P \le 0.05$, *** $P \le 0.001$ vs. control group; *• $P \le 0.01$, *•• $P \le 0.001$ vs. rTMS 1 d group; n.s. no significant difference.

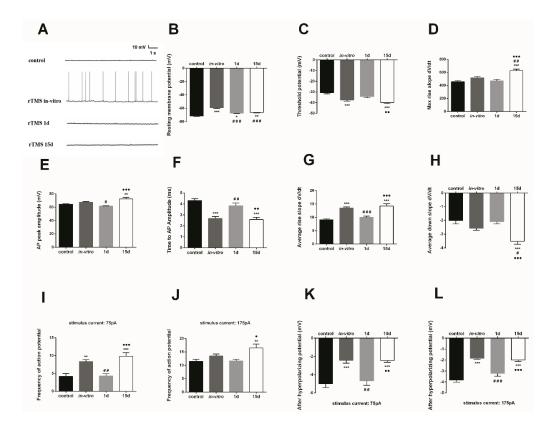


Fig. 3 Data analysis of patch-clamp. (A) Diagram of RMP. (B) RMP. (C) Threshold potential. (D) Max rise slope. (E) AP peak amplitude. (F) Time to AP amplitude. (G) Average rise slope. (H) Average down slope. (I, J) Frequency of AP. (K, L) AHP. $*P \le 0.05$, $**P \le 0.01$, $***P \le 0.001$ vs. control group; $*P \le 0.05$, $**P \le 0.01$, $***P \le 0.001$ vs. rTMS in-vitro group; $*P \le 0.05$, $**P \le 0.01$, $***P \le 0.001$ vs. rTMS 1 d group; n.s. no significant difference.

References

- [1] Banerjee J, Sorrell ME, Celnik PA, Pelled G. PloS one 12 (2017) e0170528.
- [2] Wang HL, Xian XH, Wang YY. Neurobiol Learn Mem 118 (2015)1-7.

The Effects of Repetitive Transcranial Magnetic Stimulation on the Cognition and Neuronal Excitability of Mice

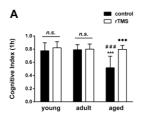
Haijun Zhu ¹, Chong Ding ¹, Guizhi Xu ^{1*}

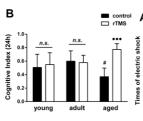
Hebei University of Technology, Tianjin, China

* Guizhi Xu: gzxu@hebut.edu.cn

Repetitive transcranial magnetic stimulation (rTMS) is a noninvasive technology of brain stimulation and neural activation used in cognitive neuroscience research [1]. rTMS has been widely used in the study of basic neurology and neurological diseases [2] [3]. However, little is known about the underlying cellular and molecular mechanisms of TMS, and the mechanism by which rTMS affects the deterioration of learning and memory caused by aging needs to be elucidated. In this study, 20 young

female Kunming mice (2-3-months-old) and 20 adult female Kunming mice (9-10-months-old) as well as 12 aged female Kunming mice (14-15-months-old) were purchased from Beijing Huafukang Bioscience. Animals of each age group were divided randomly into two groups, one group was treated with rTMS, and the other group was treated as a control group with no rTMS, n = 10 for young and adult rTMS groups, n = 10 for young and adult control groups, and n = 6 for aged rTMS and control groups. In the experimental design, the animals in the control groups were not treated with rTMS, and the animals in the rTMS groups received rTMS treatment for a specific amount of time each day (8:00-10:00 am, 1000 pulses, and total time was 80 s) for 15 consecutive days. Then, novel object recognition (NOR) and step-down tests were performed to examine cognition for all mice in both the rTMS and control groups. After the behavior tests, all the mice were sacrificed, and the brains were used for electrophysiological recordings. Data analysis showed that cognition of mice deteriorated and neuronal excitability of hippocampal dentate gyrus (DG) neurons degenerated significantly as the age increased. Cognitive damage and degeneration of some electrical properties were alleviated in the rTMS-treated groups, especially in the aged rTMS-treated group. We speculate that the deterioration of cognition in female Kunming mice caused by aging was shown to be related to degradation of some electrical properties of DG neurons, and changes in electrical properties and improvement in the excitability of DG neurons may be one of the mechanisms of the effects of rTMS on the improvement in cognition.





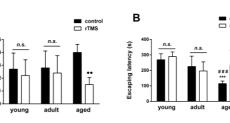


Fig 1 Cognitive Index (1 h and 24 h) of NOR test. *** $P \le 0.001$ vs. young control group, ${}^{\#}P \le 0.05$, ${}^{\#\#}P \le 0.001$ vs. adult control group, ${}^{\bullet\bullet\bullet}P \le 0.001$ vs. aged control group, ${}^{n.s}$. no significant difference.

Fig 2 Data analysis of step-down test. (A) TES. (B) EL. *** $P \le 0.001$ vs. young control group, ** $P \le 0.001$ vs.adult control group, *• $P \le 0.01$, *•• $P \le 0.001$ vs. aged control group, n.s. no significant difference.

High static magnetic field inhibit osteosarcoma growth by promoting intracellular iron accumulation and increasing ROS

Shenghang Wang^{1,2,3}, Zhihao Zhang^{1,2,3}, Dandan Dong^{1,2,3}, Peng Shang*^{2,3}

¹ School of Life Sciences, Northwestern Polytechnical University, Xi'an Shaanxi, 710072, China; ² Key Laboratory for Space Biosciences and Biotechnology, Northwestern Polytechnical University, Xi'an Shaanxi, 710072, China; ³ Research & Development Institute of Northwestern Polytechnical University in Shenzhen, Shenzhen, China

*Corresponding author: shangpeng@nwpu.edu.cn

Osteosarcoma is the most common malignant tumor of the bone. Multiply studies have shown that magnetic fields have inhibitory effect on a variety of tumors *in vitro* and *in vivo*. However, the influence

and mechanism of high static magnetic field (HiSMF) on osteosarcoma is still unclear. Previous study indicated that HiSMF could cause iron accumulation in osteosarcoma MG63 cells. Excessive intercellular iron can cause ROS arise by participating in Fenton Reaction, and showing cytotoxicity. Therefore, the objective of this study is to explore the effect of HiSMF on osteosarcoma in vitro and in vivo, and its relationship with iron metabolism. In this study, a HiSMF is generated by a non-refrigerant superconducting magnet (CRYOF12/150; Oxford Instruments, Oxon, UK) for in vitro experiment. The magnetic field strength of the HiSMF between 1-2 T was generated by homemade permanent magnets for 10 days in vivo study. The osteosarcoma cell lines U-2 OS and K7M2 were chosen as the in vitro experimental objects, the K7M2 cells lines and BALB/c mice were chosen for the in vivo study. Exposing to HiSMF, the cell proliferation ability, colony formation ability, cell viability, the expressions of iron metabolism related genes, intracellular iron content, LIP (labile iron pool) level and intercellular ROS were characterized by CCK-8 assays, clonogenic assays, Western Blot, atomic absorption spectroscopy and flow cytometry, respectively. The body weight and osteosarcoma tumor growth were measured every 2 day. The data showed that the proliferation and viability of osteosarcoma cells U-2 OS and K7M2 has been significant suppressed by HiSMF exposures. After 48 h HiSMF exposures, the intracellular iron content, LIP and ROS had significantly increased; the expression of NCOA4 and FTH1 had significantly increased. The effect of 1 h per day HiMSF exposure could inhibit osteosarcoma growth in mice. In conclusion, the HiSMF could increase intracellular ROS levels, which caused by increasing the expression of FTH1, NCOA4 and intracellular iron accumulation. HiSMF could suppress osteosarcoma proliferation and growth in vitro and in vivo by increasing intercellular ROS. It suggests that HiSMF has application potential as a physical auxiliary means for the osteosarcoma therapy.

Effects of high static magnetic fields on the recovery of microgravity-induced bone loss in mice

YR Xue^{1,2,3}, JC Yang^{1,3,4}, SJ Zhou^{1,2,3},P Shang^{1,3*}

¹ Research & Development Institute of Northwestern Polytechnical University in Shenzhen, Shenzhen, China; ² School of Life Sciences, Northwestern Polytechnical University, Xi'an, China; ³ Key Laboratory for Space Bioscience and Biotechnology, Northwestern Polytechnical University, Xi'an, China; ⁴ Department of Spinal Surgery, People's Hospital of Longhua Shenzhen, Shenzhen, China *Corresponding author: shangpeng@nwpu.edu.cn

With the advancement of science and technology, magnetic fields are widely used in transportation (high-speed rail, magnetic levitation), medical and health, defense and military, mobile communications and other fields. Meanwhile, the health hazards of GMF receives more and more attention. The most common is the magnetic resonance imaging (MRI) commonly used in hospitals. Previous studies have shown that exposure to static magnetic fields (SMFs) have the effects of promote osteoblast differentiation in vitro, increase bone formation, accelerating fracture healing, promote the wound healing and treating nonunion in vivo and in clinical studies[1,2]. Recently, our research found that static magnetic fields have a certain effect on recovery of microgravity-induced bone loss, and the body iron content has changed[3]. However, there is not quantitative results due to diversity of magnetic field

parameters leads to magnetic field dose-effect relationships at present. Therefore, the purpose of this study is to investigate the effects of different strengths of high static magnetic field (HiSMF) on the recovery of microgravity-induced bone loss, and to illustrate the change of body iron storage in this process. Our study adopt different strength of high static magnetic fields to research the effect of HiSMF on microstructure and mechanical properties of mice bone. The results indicated that 4-week HLU reduced the bone biomechanical properties or deteriorated bone microarchitecture, 2-4 T HiSMF promoted the recovery of bone loss induced-HLU, while exposure to 6-8 T and 10-12 T HiSMF reloading significantly inhibited the recovery of bone loss and bone mechanical properties. Moreover, we observed that iron content might be involved in the biological effect of HiSMF. In conclusion, HiSMF have a certain effect on recovery of microgravity-induced bone loss, probably by changed iron content of the bone.

References

[1] Andrew C, Bassett L, Pawluk R J, Pilla A A. Augmentation of Bone Repair by Inductively Coupled Electromagnetic Fields. Science, 1974, 184(4136): 575-577.

[2] Zhang J, Ding C, Ren L, Zhou Y, Shang P. The effects of static magnetic fields on bone. Prog Biophys Mol Biol, 2014, 114(3): 146-152.

[3] Yang J, Meng X, Dong D, Xue Y, Chen X, Wang S, Shen Y, Zhang G, Shang P. Iron overload involved in the enhancement of unloading-induced bone loss by hypomagnetic field. Bone, 2018, 114(235-245).

Investigating the physiological effects of $2-12\,\mathrm{T}$ high static magnetic field exposure on bone in mice

Jiancheng Yang ^{1, 2, 4}, Gejing Zhang ^{3, 4}, Dandan Dong ^{3, 4}, Hao Zhang ¹, Peng Shang ^{2, 3, 4*}

¹ Department of Spinal Surgery, People's Hospital of Longhua Shenzhen, Shenzhen, China; ² Research & Development Institute of Northwestern Polytechnical University in Shenzhen, Shenzhen, China; ³

School of Life Sciences, Northwestern Polytechnical University, Xi'an, China; ⁴ Key Laboratory for Space Bioscience and Biotechnology, Northwestern Polytechnical University, Xi'an, China *Corresponding author: shangpeng@nwpu.edu.cn

With the rapid development of industrial technology and biomedical science, human beings have more and more opportunities to be exposed to static magnetic fields (SMFs) with higher-intensity. The most common high static magnetic field (HiSMF) is the MRI scanner in hospitals. For the biological effects of HiSMF, there are only some short-term exposure reports, and they focus on the study of brain, heart and blood. There are few studies pay attention to the effects of HiSMF on the skeletal system. This study aimed to investigate the physiological effects of HiSMF on bone in mice.

In this study, 8-week-old male C57BL/6 mice were exposed to the geomagnetic field (GMF) and HiSMF of 2–4 T, 6–8 T, and 10–12 T generated by a non-refrigerant superconducting magnet (CRYOF12/150; Oxford Instruments, Oxon, UK) for 28 days. At the endpoint, the microstructure in the femurs and the lumbar vertebrae L3 were examined by micro–computed tomography, the mechanical properties in the tibias were determined by a three-point bend test, and bone turnover was analyzed by serum biochemistry, histochemistry staining, and western blot assay.

Compared with the GMF, HiSMF of 2-4 T significantly improved the microstructure of the femurs and mechanical properties of the tibias, and enhanced osteoblastogenesis, increased the number of osteocytes in trabecular bone, and inhibited osteoclastogenesis in the femurs. The level of serum TRAP-5b, a maker for bone resorption, was increased in mice under HiSMF of 2-4 T. HiSMF of 6-8 T had a mild damage effect on microstructure of the femurs but no obvious effect on mechanical properties of the tibias, and had a suppression effect on the number of osteoblasts on the surface of cancellous bone but no obvious effects on osteocytes and osteoclasts in the femurs. HiSMF of 10-12 T destroyed the microstructure of the femurs and mechanical properties of the tibias, and reduced the number of osteoblasts and elevated the surface of osteoclasts in the femurs.

In conclusion, this study revealed the physiological effects of long-term HiSMF exposure on bone in mice at first time. These findings contribute to understanding the biological effects of HiSMF on skeletal system, and providing a theoretical basis to develop the magnetic therapy equipment which is used for adjuvant therapy on osteoporosis in the future.

The effects of iron oxide nanoparticles combined with static magnetic field on osteoblasts and osteoclasts in vitro and on unloading-induced bone loss in vivo

Gejing Zhang ^{1, 4}, Jiancheng Yang ^{1, 3, 4}, Zheyuan Zhang ^{1, 4}, Peng Shang ^{1, 2, 4*}

¹ School of Life Sciences, Northwestern Polytechnical University, Xi'an, China; ² Research & Development Institute of Northwestern Polytechnical University in Shenzhen, Shenzhen, China;

³ Department of Spinal Surgery, People's Hospital of Longhua Shenzhen, Shenzhen, China;

⁴ Key Laboratory for Space Bioscience and Biotechnology, Northwestern Polytechnical University, Xi'an, China

*Corresponding author: shangpeng@nwpu.edu.cn

Bone remodeling happens throughout life to maintain the integrity of the skeleton. In the course of bone remodeling, the old and damaged bone are dissolved by osteoclasts (bone resorption cells) and new bone is yielded by osteoblasts (bone formation cells). At present, iron oxide nanoparticles (IONs) have been used for treating iron deficiency, as contrast agents for magnetic resonance imaging and as drug carriers. In recent years, IONs have been reported to affect the regeneration of bone tissue, especially promote osteogenic differentiation of mesenchymal stem cells (MSCs) and preosteoblasts [1]. Moreover, static magnetic fields (SMF) have been shown to resist osteoporosis and promote fracture healing by regulating the proliferation and differentiation of cells such as MSCs, osteoblasts and osteoclasts [2]. It should be noted that IONs are superparamagnetic and an external magnetic field is able to magnetize IONs which are internalized into cells, offering a powerful tool to control cell behaviors. Indeed, uptake of the Fe₃O₄/BSA particles significantly promoted the osteogenic differentiation of MSCs under a SMF [3]. However, there were few reports about the conjunction effect of IONs and SMFs on osteoblasts and osteoclasts, and on bone turnover in animal. Herein, we aimed to investigate the effects of IONs combined with SMF on osteoblasts and osteoclasts in vitro and on unloading-induced bone loss in vivo.

The FDA-approved IONs compound, ferumoxytol, was used in this study. For cell experiments,

SMF of 2 T, generated by a non-refrigerant superconducting magnet, was applied in the culture of Raw264.7 pre-osteoclasts and MC3T3-E1 osteoblasts in the presence or absence of ferumoxytol. The differentiation of osteoblasts and osteoclasts were evaluated. For animal experiment, we designed a small magnet with SMF of 1.5 T in a hole of 1 cm diameter. 8-week-old male BALB/C mice, with or without intravenous injection of ferumoxytol, were subjected to hindlimb unloading (HLU, a classic analog microgravity model is used to induce bone loss of rodent hindlimb) and the left hindlimb of mice were immobilized and inserted into the hole with 1.5 T SMF one hour a day for 28 days. At the endpoint, bone mineral content (BMC) and bone mineral density (BMD) in the left hind legs were examined by DEXA. The microstructure in the left femurs were determined by micro—computed tomography, the mechanical properties in the left tibias were detected by three-point bend test.

In osteoblasts, the results showed the application of external SMF could promote the osteogenic differentiation of MC3T3-E1 cells. And ferumoxytol with low concentration could also enhance the osteogenic differentiation in the absence or presence of external SMF. The combination of IONs and SMF had a synergistic enhancing effect on osteoblast differentiation. In osteoclasts, the results showed the osteoclastic differentiation and bone resorption capacity of Raw264.7 cells were inhibited separately by external SMF or ferumoxytol. The marriage of IONs and external HiSMF was found most effective in decelerating osteoclastic differentiation and bone resorption capacity. In mice, HLU of 28 days dramatically reduced BMC and BMD in the femurs and tibias and led to a severe damage on cancellous bone microstructure of the femurs and bone strength of the tibias. There was no an obvious difference in BMD and BMC between unloaded mice and IONs treated mice of unloading. However, SMF exposure significantly inhibited the decrease in BMC and BMD of the left hind legs induced by HLU in mice with or without IONs treatment. HLU-induced damages in cancellous bone microstructure of the left femurs and bone strength of the left tibias were significantly prevented by SMF exposure or ferumoxytol treatment separately. Moreover, IONs and SMF was found to exert a moderate synergistic protection effect on bone microstructure and mechanical properties.

In conclusion, the combination of IONs and SMF had a stronger promoting effect on the osteogenic differentiation of osteoblasts, a more powerful inhibitory effect on the differentiation and bone resorption capacity of osteoclasts, and a better resistance to HLU-induced bone loss. These results demonstrate the combined effects of SMF and IONs on bone system are the new translational researches field in skeletal related diseases, such as osteoporosis, bone fracture, and bone defect.

References

- [1] A. Tautzenberger, A. Kovtun, and A. Ignatius, International Journal of Nanomedicine 7 (2012) 4545-4557.
- [2] J. Zhang, C. Ding, and P. Shang, Prog Biophys Mol Biol 114 (2014) 146-152.
- [3] P. Jiang, Y. Zhang, C. Zhu, et al., Acta Biomaterialia 46 (2016) 141–150.

Static magnetic field regulates Arabidopsis root growth via auxin signaling

Yue Jin^{1#}, <u>Wei Guo</u>^{1#}, Xupeng Hu^{2#}, Mengmeng Liu¹, Xiang Xu¹, Fenhong Hu¹, Yiheng Lan³, Chenkai Lv³, Yanwen Fang⁴, Mengyu Liu⁴, Tieliu Shi³, Shisong Ma⁵, Zhicai Fang⁴, Jirong Huang^{1*}

¹Shanghai Key Laboratory of Plant Molecular Sciences, College of Life Sciences, Shanghai Normal

University, Shanghai 200234, China; ²Institute of Plant Physiology and Ecology, Chinese Academy of Sciences, Shanghai 200032, China; ³Shanghai Key Laboratory of Regulatory Biology, School of Life Sciences, East China Normal University, Shanghai, 200241, China; ⁴Heye Health Industrial Research Institute of Zhejiang Heye Health Technology, Anji Zhejiang 313300, China; ⁵School of Life Sciences, University of Science and Technology of China, Hefei 230026, China.

* Corresponding author: huangjr@shnu.edu.cn # These authors contributed equally to this work.

Static magnetic field (SMF) plays important roles in biological processes of many living organisms. In plants, however, biological significance of SMF and molecular mechanisms underlying SMF action remain largely unknown. To address these questions, we treated *Arabidopsis* young seedlings with different SMF intensities and directions. Magnetic direction from the north- to south-pole was adjusted in parallel (N0) with, opposite (N180) and perpendicular to the gravity vector. We discovered that root growth is significantly enhanced by 600 mT treatments except for N180, but not by any 300 mT treatments. N0 treatments lead to more active cell division of the meristem, and higher auxin content that is regulated by coordinated expression of PIN3 and AUX1 in root tips. Consistently, N0-promoted root growth disappears in *pin3* and *aux1* mutants. Transcriptomic and gene ontology analyses revealed that in roots 85% of the total genes significantly down-regulated by N0 compared to un-treatment are enriched in plastid biological processes, such as metabolism and chloroplast development. Lastly, no difference in root length is observed between N0-treated and untreated roots of the double cryptochrome mutant *cry1 cry2*. Taken together, our data suggest that SMF-regulated root growth is mediated by CRY and auxin signaling pathways in *Arabidopsis*.

Alternating Magnetic Fields Coupled with Magnetic Nanocubes Can Turn on the Force and the Heat for Synergistic Cancer Treatment

<u>Jiaojiao Wu 1, Yu Cheng 1* </u>

¹ The Institute for Biomedical Engineering and Nano Science, School of Medicine, Tongji University, Shanghai, P.R. China

 $*Corresponding\ author: yucheng@tongji.edu.cn$

Mechanical and thermal properties are crucial physical parameters to regulate the cancer cell fate. Magnetic nanoparticles (MNPs) with unique magnetic responses can be utilized as antennas of the magnetic field, which hold the great promise to spatiotemporally manipulate the mechanical and thermal properties of cells [1, 2]. Although either magneto-mechanical force (MF) or magnetic hyperthermia (MH) has shown the promise to damage cancer cells, little is known about how the cell responses to both mechanical and thermal signals. Here, we proposed a mechanical-thermal induction therapy (MTIT) strategy for cancer treatment via alternating magnetic fields coupled with 60 nm RGD modified zinc-doped iron oxide nanocubes (RGD-IONs) to exert mechanical forces under a 15 Hz rotating field to sensitize the cells and followed by the mild hyperthermia under a 375 kHz field. The increased lysosomal membrane permeability (LMP) was observed during MTIT, which further induced the dysfunction of mitochondria. Importantly, we found the MTIT had a synergistic effect to efficiently treat

Magneto-mechanical thermal induction therapy (MTIT) Magneto-mechanical forces (MF) Magnetic hyperthermia (MH) Sensitization Biochemical signals $\vec{\tau} = \vec{m} \times \vec{B}$ RMF: 375 kHz Cell death

Fig. 1 Scheme of MNPs performed magneto-mechanical thermal induction therapy (MTIT) under dual frequencies of magnetic fields.

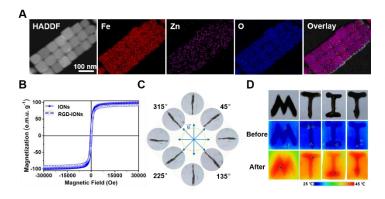


Fig. 2 Characterization of the RGD-IONs' physical properties. A) Elemental mapping analysis. B) M-H curves. C) Magneto-mechanical force response. D) Magnetic thermal properties.

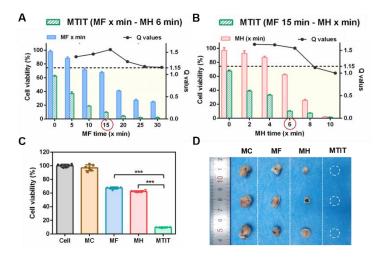


Fig 3. The synergistic effect of MTIT both *in vitro* and *in vivo*. A) MTIT with various MF time and MH 6 min. $Q \ge 1.15$ represents the synergistic effect occurred. B) MTIT with MF 15 min and varied MH time. C) and D) were anticancer effect on U87 cells and animal models respectively.

the cancer cells. The reactive oxygen species (ROS) acted as one of the key signals in the synergistic effect of mechanical and thermal stimulation, which could be elevated and programmable via the alternating frequency fields. *In vivo* evidences revealed the effectiveness of MTIT for treating the glioma and breast cancer. By remote control of the dual physical triggers via RGD-IONs to cells, MTIT is promising for targeted and precise cancer treatment, especially for deeper tumor.

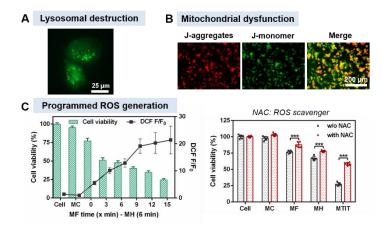


Fig. 4 The mechanisms of MTIT from subcellular structures to biochemical signals. A) Lysosomal membrane permeabilization increased. B) Mitochondrial membrane potential decreased. C) Programmed ROS generation controlled the cell viability.

References

[1] C. Wu, Y. Shen, and M. Chen, Advanced Materials 30 (2018) 1705673.

[2] S-h. Noh, S. H. Moon, and T-H. Shin, Nano Today 13 (2017) 61-76.

Thermostable iron oxide nanoparticle synthesis within recombinant ferritins from the Piezophilic Hyperthermophile Pyrococcus CH1

<u>Jiacheng Yu</u> ^{1,2}, Tongwei Zhang ^{1,2}, Huangtao Xu^{1,2}, Yao Cai ^{1,2}, Yongxin Pan ^{1,2}, and Changqian Cao ^{1,2}*

¹ Key Laboratory of Earth and Planetary Physics, Institute of Geology and Geophysics, Chinese Academy of Sciences, Beijing 100029, P. R. China; ² France-China Joint Laboratory for Evolution and Development of Magnetotactic Multicellular Organisms, Chinese Academy of Sciences, Beijing 100029, China;

*Corresponding author: changqiancao@mail.iggcas.ac.cn

Thermostable nanoparticles have great applications in oil/gas industry and catalysis. However, the process of synthesis of these thermostable nanoparticles are extremely tedious and money cost. Here, a novel thermostable ferritin named PcFn, originally from the hyperthermophilic archaeon Pyrococcus yayanosii CH1, was overexpressed in Escherichia coli and purified, which could successfully direct synthesis of thermostable magnetoferritins (M-PcFn) by a facile and one-pot method. TEM images show that the protein cage of M-PcFn is intact and the iron oxide cores of M-PcFn with an average core size of 4.7 nm, and magnetic parameters indicate M-PcFn is typical superparamagnetism. Both of the PcFn and M-PcFn can resist the temperature as high as 110 °C, which are nearly the same as previously reported Pyrococcus furiosus ferritin (PfFn)^{1, 2} and its magnetoferritin of M-PfFn, but significantly higher than human H-chain ferritin (HFn) and its magnetoferritin of M-HFn. After heating at 110 °C for 30 minutes, the PcFn and M-PcFn still kept their secondary structure and the PcFn retain 87.4% iron uptake activity. This remarkable thermal resistance of PcFn and M-PcFn provides potential application in elevated temperature fields.

Keywords: iron oxide nanoparticles, ferritin, Pyrococcus CH1, thermostability

Acknowledgements

This work was supported by grants from National Natural Science Foundation of China (No: 41574062, 41774076, respectively)

References

[1] Tatur, P. L. Hagedoorn, M. L. Overeijnder and W. R. Hagen, *Extremophiles*, 2006, 10, 139-148.
[2] J. Tatur, W. R. Hagen and P. M. Matias, *J Biol Inorg Chem*, 2007, 12, 615-630.

MNPs Promote the M2 Subtype towards M1-like Subtype Macrophages and Microglias

Yingze Li¹, Chang chen¹*, Yu Cheng²*

¹ Tongji University School of Medicine, Shanghai, China. <u>liyingze2017@163.com</u>; ¹*: Department of Thoracic Surgery, Shanghai Pulmonary Hospital, Tongji University School of Medicine, Shanghai, China. chenthoracic@163.com; ²* The Institute for Biomedical Engineering & Nano Science, Tongji University School of Medicine, Shanghai, China. <u>yucheng@tongji.edu.cn</u>

Macrophage is an important immune cell, which is involved in both non-specific defense and specific defense functions in vivo. Microglial cells are macrophages in the central nervous system. Both macrophages and microglial cells have high functional plasticity. M1 subtype cells promote inflammation and anti-tumor growth, while M2 can resist the aggregation of inflammatory cells. Magnetic nanoparticles can transform the function of macrophage, which can promote M2 macrophages to M1 [1]. Some people also use MNPs to regulate the transformation of M1 towards M2 by binding cells, so as to directly regulate the subtype of macrophages without passing the resting cells [2]. However, this research is still incomplete. The efficiency of polarity transformation is the key to biological effect, and the two-way transformation of M1 and M2 subtype is also not unified at present. To solve these problems, we proposed to use MNPs as a research platform to improve the efficiency of the cell subtype conversion by using external magnetic field of specific frequency, so as to achieve controllable two-way free transformation between M1 and M2 subtypes.

We selected a size of 20nm MNPs as the experimental platform (figure 2A). Polylysine (PLL), a hydrophilic polypeptide with low cytotoxicity, was coated on the surface of MNPs. With the successful modification of PLL, the material was charged with a potential of +30mV, which was more conducive to adhesion to the cell surface (figure 2B). At the same time, as the surface of the material changes from oily to hydrophilic PLL, the dispersion of MNPs in the aqueous phase increases, and the measured hydration particle size decreases (figure 2C, 2D).

Secondly, in order to obtain two mature cell subtypes, we selected RAW 264.7 and bv-2 cell lines. Resting cells were treated with 20 ng/ml IFN- γ and 10 pg/ml LPS for 24 hours to obtain M1 subtypes, 20 ng/ml IL-4 and 20 ng/ml IL-13 for 48 hours to obtain the M2 subtype cells. We discovered obvious changes in the shape of the two subtypes after induction factor differentiation, which preliminarily confirmed the success of induction (figure 3A). We further verified the successful induction of resting cells by using RT-PCR to detect the gene level (figure 3B, 3C). Cells induced by IFN- γ and LPS showed higher expression levels in markers such as CD80, IL-1 β and TNF- α . And cells induced by IL-4 and IL-

13 showed high expression of CD163, IL-4, IL-10 and Arg-1.

Next, we investigated the endocytosis efficiency and toxicity of the MNPs platform with macrophages and microglias. We set 0, 10, and 20 ug /ml MNPs to co-culture with the cells. We found the macrophage and microglia cell lines had high endocytosis efficiency on the MNPs platform coated with PLL polypeptides (figure 4A). After 24 hours co-culture, cell viability was measured by adding different concentrations of materials. We found that cell viability was almost unaffected by the presence of materials within the concentration of 40 ug /ml (figure 4B). Cells were collected from 0, 10, 20 and 40 ug /ml materials after 24 hours of co-culture with cells, and the successful endocytosis MNPs were quantified. It was not difficult to find that the content of MNPs successfully endocytosis increased with the increase of iron concentration (figure 4C, 4D).

We hypothesized that the presence of IFN-γ, LPS and other inducible differentiation factors would promote the transformation effect of cell subtype by using MNPs. In future experiments, we will determine the efficiency of MNPs on the transformation of two subtypes and hope to find the inducible factor that can synergistic promote the transformation. At the same time, we also expect that by using specific magnetic field, macrophages can freely and reversibly transform between M1 and M2 subtypes, providing new therapeutic methods for the treatment of immune system diseases and tumors.

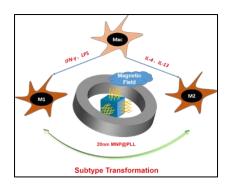


Figure 1. Schematic of cell subtype.

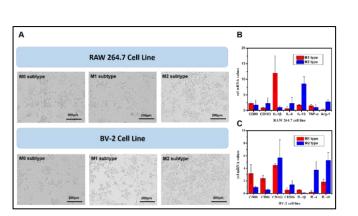


Figure 3. Morphological and gene level changes after induction of resting cells

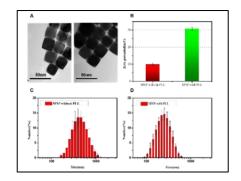


Figure 2. The characterization of MNPs transformation by MNPs and magnetic field.

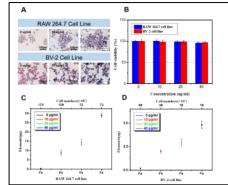


Figure 4. Effects of MNPs at different concentrations on cells

References

- [1] Laskar A, Eilertsen J, Li W and Yuan XM, Biochem Biophys Res Commun 11 (2013) 737-742.
- [2] Kang H, Wong SHD, Pan Q, Li G and Bian L, Nano Lett, 3 (2019) 1963-1975.

Micro-Therapeutic System Enhanced Nitric Oxide Release for Gas Therapy

Feng Tao, Yao Qin, Yu Cheng*

The Institute for Biomedical Engineering and Nano Science, School of Medicine, Tongji University, Shanghai 200092, P.R. China

*Corresponding author: yucheng@tongji.edu.cn

Nitric oxide (NO) plays a special role in cancer cells and tumor microenvironment, which could determine the rate of tumor progression, therapeutic effect and prognosis. The low flux of NO (100-500 nM) promotes tumorigenesis via the nitrosative signal, while high NO flux (>1 μ M) causes apoptosis and mitochondrial dysfunction for therapeutic dose through genotoxicity and protein modification. Thus, local high NO flux in the tumor microenvironment (TME) is critical for promoting tumor cell apoptosis, especially this process is triggered in the response of TME. In present work, we show a strategy of constructing M1 macrophages with input/fuel dual-functional nanocapsules as a micro-therapeutic system for gas therapy via enhanced NO release. This new micro-therapeutic system is promising in the application of bioinspired intelligent treatment.

Gas therapy is an emerging and promising therapeutic area, in which nitric oxide (NO) therapy has made considerable progress [1-3]. NO is a lipophilic, highly diffusible and short-lived molecule synthesized in vivo by the oxidation of L-arginine under the catalysis of nitric oxide synthase (NOS) [4]. In vivo, inducible nitric oxide synthase (iNOS), which is non-calcium-dependent and mainly synthesized by M1 macrophages, is mainly responsible for NO production for a long time. However, in the tumor microenvironment (TME), there is mainly the immunosuppressive oncogenic M2-like tumorassociated macrophages (TAMs), rather than the pro-inflammatory M1 macrophages with anti-tumor activity. Thus, re-educating the M2 macrophages to the tumoricidal M1 macrophages to provide elevated iNOS for NO production is necessary in gas therapy against tumor cells. Herein, we proposed a strategy of constructing M1 macrophages with input/fuel dual-functional nanocapsules as a micro-therapeutic system for gas therapy via enhanced NO release. As shown in Fig. 1, input/fuel dual-functional nanocapsules constructed from degradable polymer micelles loaded with NO prodrug L-arginine and magnetic nanoparticles, for NO release and re-educating tumor-promoting M2-like TAMs to the tumoricidal M1-like phenotype, respectively. In addition, magnetic nanoparticles could induce the heat to stimulate hydrogen peroxide (H₂O₂) production in cells under magnetic fields. And then M1 macrophages provide endogenous iNOS and H₂O₂ with L-arginine to enhance NO release against cancer cells in TME. Based on the bioinspired feedback mechanism, this established micro-therapeutic system is promising as a candidate for intelligent treatment systems.

Key-words: Micro-therapeutic System, Nitric Oxide, Magnetic Re-education, Gas Therapy

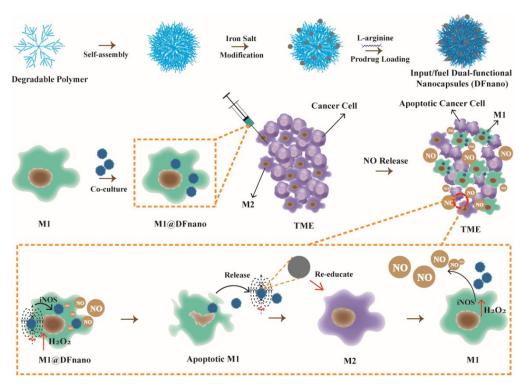


Fig. 1 Micro-therapeutic system enhanced nitric oxide release for gas therapy.

References

- [1] K. Zhang, H. X. Xu, X. Q. Jia, Y. Chen, M. Ma, L. P. Sun and H. R. Chen, ACS nano 10.12 (2016) 10816-10828.
- [2] Y. Kang, J. Kim, J. Park, Y. M. Lee, G. Saravanakumar, K. M. Park, W. Choi, K. Kim, E. Lee, C. Kim and W. J. Kim, Biomaterials (2019) 119297.
- [3] X. B. Jia, Y. H. Zhang, Y. Zou, Y. Wang, D. C. Niu, Q. J. He, Z. J. Huang, W. H. Zhu, H. Tian, J. L. Shi and Y. S. Li, Advanced Materials 30.30 (2018) 1704490.
- [4] J. Fan, N. Y. He, Q. J. He, Y. Liu, Y. Ma, X. Fu, Y. J. Liu, P. Huang and X. Y. Chen, Nanoscale 7 (2015) 20055-20062.

Focusing Fe₃O₄ particles using time-varying magnetic field

<u>Ya-Li Liu</u> ¹, Fiaz Ahmad ¹, Jing-Jie Chen ¹, Tuo-Di Zhang ¹, Ya-Jing Ye ¹, Wei-Hong Guo ¹, Peng Shang ^{1, 2}, Da-Chuan Yin ^{1,2*}

¹ Institute for Special Environmental Biophysics, Key Laboratory for Space Bioscience and Biotechnology, School of Life Sciences, Northwestern Polytechnical University, Xi'an 710072, PR China; ² Shenzhen Research Institute of Northwestern Polytechnical University, Shenzhen 518057, Guangzhou, PR China

*Corresponding author: yindc@nwpu.edu.cn

Magnetic drug targeting (MDT) is one of the methods of drug targeting. In MDT, Fe₃O₄ is usually used to carry drugs and deliver drugs to the target site by using external magnetic field, which can reduce

side effects and improve efficacy [1-3]. It can be seen that in MDT, a magnet system that can create suitable magnetic field is necessary.

In this paper, a rotating magnetic field device was constructed in which two magnets placed face to face can be rotated around an axis intermediate the two magnets. A container containing suspension Fe₃O₄ particles was fixed at the position of the rotating axis. When the magnet pair remains still, the Fe₃O₄ particles will cluster to two regions as shown in the first picture of Fig. 1. When the magnet pair rotates, instead of gathering in the wall of the container, the Fe₃O₄ particles will quickly cluster together in the middle of the container within 1 minute (Fig. 1).

Our experiments showed that materials attracted by magnetic fields (such as paramagnetic, superparamagnetic, ferromagnetic, and ferrimagnetic materials) are difficult to aggregate in a static magnetic field, but they can be focused through time-varying magnetic fields. This work can be useful for the application like the design and manufacture of focusing magnet systems for drug targeting, materials processing, and other processes requiring non-contact manipulation of magnetic materials.

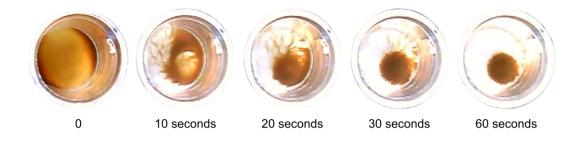


Fig. 1 Aggregation process of Fe₃O₄ particles at 50 rpm after about 12 minutes of static magnetic field.

References

[1] Y. L. Liu, J. J. Chen, F. Ahmad, et al., IEEE Transactions on Biomedical Engineering DOI 10.1109/TBME.2019.2940029, IEEE.

[2] Y. L. Liu, D. Chen, P. Shang, and D. C. Yin, Journal of Controlled Release 302(2019) 90-104.

[3] I. Venugopal, N. Habib, and A. Linninger, Nanomedicine 12 (2017) 865-877.

Effects on the heating efficiency of magnetoferritin nanoparticles in an alternating magnetic field

Huangtao Xu^{1, 2}, Yongxin Pan^{1, 2*}

¹Biogeomagnetism Group, Key Laboratory of Earth and Planetary Physics, Institute of Geology and Geophysics, Chinese Academy of Sciences, Beijing 100029, China; ² University of Chinese Academy of Sciences, Beijing 100049, China

*Corresponding author: <u>yxpan@mail.iggcas.ac.cn</u>

The superparamagentic magnetoferritin is a potential bio-nanomaterial for tumor magnetic hyperthermia because of their actively tumor targeted outer protein shell, uniform and tunable nanosized inner mineral core, mono-dispersity and good biocompatibility [1, 2]. Here, we investigated

influenced factors on the heating efficiency and the heating generation mechanism of magnetoferritin in aqueous in an alternating magnetic filed. Effects of core-size, Fe concentration, viscosity coefficient, and field frequency and amplitude were investigated. We successfully synthesized superparamagnetic iron oxide nanoparticles (MHFn) with magnetite and/or maghemite cores based on human heavy chain ferritin. Meanwhile, We found that the max temperature rise and specific loss power are 14.2 °C (at 6 minutes) and 68.6 W/g, respectively, obtained at 805.5 kHz and 19.5 kA/m with core size 4.8 nm MHFn at 5mg[Fe]/ml. Additionally, the temperature rise and specific loss power augmented with increased core size, iron concentration, alternating magnetic filed frequency and amplitude. Furthermore, the calculated effective relaxation time was basically equal to Néel relaxation time and the specific loss power was insensitive to viscosity of solution, we proposed that the heating mechanism of MHFn nanoparticles are dominated by Néel relaxation. This work has provide new insights into the heating efficiency of MHFn nanoparticles and future applications for tumor hyperthermia and thermoablation therapy, heat-triggered drug release, and so on.

References

[1] C. Cao, X. Wang, Y. Cai, L. Sun, L. Tian, H. Wu, X. He, H. Lei, W. Liu, G. Chen, R. Zhu, Y. Pan, Targeted In Vivo Imaging of Microscopic Tumors with Ferritin- based Nanoprobes Across Biological Barriers, Advanced Materials 26(16) (2014) 2566-2571.

[2] C. Massner, F. Sigmund, S. Pettinger, M. Seeger, C. Hartmann, N.P. Ivleva, R. Niessner, H. Fuchs, M.H. de Angelis, A. Stelzl, N.L. Koonakampully, H. Rolbieski, U. Wiedwald, M. Spasova, W. Wurst, V. Ntziachristos, M. Winklhofer, G.G. Westmeyer, Genetically Controlled Lysosomal Entrapment of Superparamagnetic Ferritin for Multimodal and Multiscale Imaging and Actuation with Low Tissue Attenuation, Advanced Functional Materials 28(19) (2018).

Magnetic Confinement of Diamagnetic Objects for Space Utilization

Zi-Qing Wu¹, Yong-Ming Liu^{1,2}, Da-Chuan Yin^{1*}

¹ Institute for Special Environmental Biophysics, Key Laboratory for Space Bioscience and Space Biotechnology, School of Life Sciences, Northwestern Polytechnical University, Xi'an 710072, Shaanxi, PR China; ² School of Biological Engineering, Sichuan University of Science and Engineering, Zigong 643000, Sichuan, PR China *Corresponding author: yindc@nwpu.edu.cn

Utilization of the space environment provides invaluable opportunities for researchers to fulfill challenging tasks that are impossible on Earth. Longtime sustainable containerless and simultaneously weightless condition is a desirable physical environment that can be easily obtained in outer space [1, 2]. However, in a space station, due to unpredictable disturbances, i.e., g-jitter [3, 4], objects that are floating in containerless and weightless conditions may not be able to stay motionless at a specific location, making it difficult to conduct any investigation of the objects.

In this study, we propose a method to confine objects without energy consumption using permanent magnets. Two types of confinement apparatuses made of permanent magnets were designed and manufactured. The apparatuses were used to demonstrate the capability of the magnetic field to confine

diamagnetic objects without mechanical contact. Figure 1 showed the schematic illustration of diamagnetic confinement under microgravity environment in space and normal gravity on the earth under a neutral buoyancy force environment.

We took confinement of a water droplet as an example and calculated the confinement performance of the two apparatuses. The results showed that the idea of using permanent magnets to confine diamagnetic objects without energy consumption in the space environment is feasible. Compared with other confinement methods, such as ultrasound and electrostatic confinement methods, the method proposed in this study is simple, efficient and inexpensive. Most importantly, the confined objects are restricted in a region with a low magnetic field. These advantages enable the method a potentially useful alternative for studying objects under containerless and weightless condition in space.

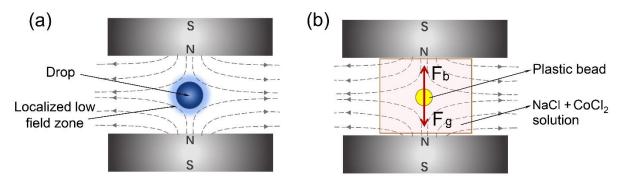


Fig. 1 Schematic illustration of diamagnetic confinement. (a) Diamagnetic confinement of a liquid drop in a localized low magnetic field under microgravity environment, (b) a mimic experiment of diamagnetic confinement using a plastic bead placed in the localized low magnetic field under a neutral buoyancy force environment created using CoCl₂ solution.

References

- [1] D. Grimm, M. Egli, M. Kruger, et al, Can. Med. Assoc. J. 27 (2018) 787-804.
- [2] M. Durante, F.A. Cucinotta, Nat. Rev. Cancer 8 (2008) 465-472.
- [3] K. Li, B.Q. Li, H.C. de Groh, Int. J. Heat Mass Tran. 46 (2003) 4799-4811.
- [4] J. Baumgartl, G. Muller, J. Cryst. Growth 169 (1996) 582-586.

New detection method for diagnosis of cancer metastasis by using pulsed magnetic field

Mikihide Hirota^{*}, Ryota Motoki, Ryuichi Fujikawa, and Isao Yamamoto
Department of Physics, Graduate School of Engineering Science, Yokohama National University
79-5 Tokiwadai, Hodogaya-ku, Yokohama 240-8501, Japan
*Corresponding author: hirota-mikihide-pn@ynu.jp

Breast cancer is known to metastasize via lymph vessels and lymph nodes. Sentinel lymph node (SLN) biopsy is useful for determining the presence or absence of metastasis of breast cancer by extracting several SLNs and performing pathological examination. The SLN is the first metastasis lymph node. In order to perform biopsy, it is necessary to locate SLNs. Conventionally, the method of

locating the SLN by using radioisotope and blue dye has mainly been performed. Radiation exposure to medical workers, however, is viewed as problems. In recent years, new methods using magnetic tracers and magnetic probes have attracted attention. Magnetic nanoparticles are injected near the breast cancer. After flowing into the SLN using the flow of lymph, SLN is located by detecting the magnetic nanoparticles from outside the body. Previous studies have reported using permanent magnets [1] and successfully detected up to 10 mm from the surface of the magnetic probe. However, the accuracy is poor for patients with large body mass index. On the other hand, pulsed magnetic field is expected for detection in deeper position since relatively large magnetic field can be generated. In this study, we

aimed to establish locating the SLN by using pulsed magnetic field.

The small pulsed magnetic field generator (1 m³), which generated maximum magnetic field B_{max} of 7 T in center of the exciting coil, was developed. The position of a search coil was changed on the central axis of exciting coil and electromotive force EMF at charging voltage $E_c = 500 \,\text{V}$ was measured. The B was calculated from EMF using Eq. (1) and B distribution of exciting coil was shown in Fig. 1. The $B_{max} = 6.8 \text{ T}$ was estimated at $E_c = 1 \text{ kV}$ since E_c and B are in proportional relationship and $B_{max} = 3.4 \text{ T}$ was generated at $E_c = 500 \text{ V}$. A search coil was made as a magnetic probe and fixed on the surface of the exciting coil. Magnetic tracer used was magnetite powder with the saturation magnetic field of 0.4 T and the saturation magnetization of 71 emu/g which value was measured previously. The EMF was measured as a function of sample amount m or the distance from surface of the exciting coil h at constant $E_c =$ 200 V. The detection was estimated by the S/N ratio of EMF as shown in Fig. 2, where the S and N were defined the apparent magnetization measured and systematic error, respectively. The symbols O, Δ , and \times represented the S/N > 1, S/N = 1, and S/N < 1, respectively. The solid curve on the triangles described S/N = 1 and the limit of detection of the tracer. The detection of the tracer was succeeded in upper left region of the curve. Therefore, 47.4 mg of magnetite was successfully detected at 8 mm from surface of exciting coil.

$$B = -\frac{1}{NS} \int V dt. \quad (1)$$

In addition, Resovist® Inj. (Fuji Film Co. Ltd) was detected as another tracer, which included

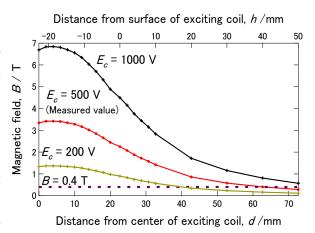


Fig. 1 Magnetic field distribution.

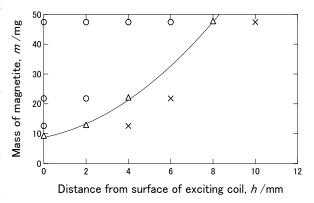


Fig. 2 Performance estimation of distance and mass of magnetite.

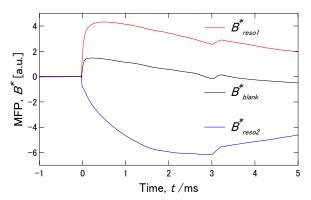


Fig. 3 MFP comparison of blank and inserting resovist one of the two search coils.

superparamagnetic fine powder of iron oxide and is used in actual medical practice. The saturated magnetization of 2 emu/g for Resovist was very small compared to magnetite [2]. It is necessary to minimize the signal of blank because of the small magnetic signal from Resovist.

A circuit that combines two search coils, the fixed resistors, and the potentiometer was fabricated. Magnetic field parameter (MFP) was defined by Eq. (2). Fig. 3 shows comparison of blank (B^*_{blank}) and inserting Resovist in one of the two search coils $(B^*_{reso1}, B^*_{reso2})$. From each MFP differences, the direction of Resovist was identified.

$$B^* = -\int V dt. \quad (2)$$

As a result, magnetite 47.4 mg was detected at 8 mm from surface of exciting coil using one search coil. The direction of Resovist was identified by improving the magnetic probe. In the future, after the optimal arrangement of search coil by changing the outer diameter and the number of turns, detection of Resovist in deep position will be performed.

Acknowledgments This work was supported partially by JSPS KAKENHI Grant No.16K04946 and The Watanabe Foundation.

References

- [1] Masaki Sekino et al., Scientific Reports 8 (2018) 1195.
- [2] M. Hirota et al., The 66th JSAP Spring Meeting, 10p-M113-3 (2019).

Effects of different frequency repetitive transcranial magnetic stimulation on memory ability and excitability of hippocampal DG neuronal in mice

Fu Rui, Xu Guizhi, Zhu Haijun, Yin Xiaonan, Xu Baohong and Ding Chong*
State Key Laboratory of Reliability and Intelligence of Electrical Equipment, Hebei University of Technology, Tianjin, 300130, China

*Corresponding author: dingchong@hebut.edu.cn

As the most commonly used non-invasive brain stimulation technology, TMS has shown great potential in the treatment of neurological diseases. TMS can promote the cognitive process of healthy people and enhance the connectivity of cortical hippocampal network ^[1]. The learning ability related to hippocampal activity and the ability of new memory formation were affected ^[2]. Some studies have shown that low-frequency rTMS can reduce the excitability of local cortex, while high-frequency rTMS can increase the excitability of local cortex ^[3]. But there are different opinions about the effects of different frequencies on memory and neuronal excitability.

Methods

- (1) Laboratory Animals and Groups
- (2) New Object Recognition Experiment
- (3) Platform jumping experiment
- (4) Patch clamp recording

Compared with Ctrl group, the cognitive index of 5Hz and 10Hz group increased significantly, but there was no significant difference at 1Hz (Fig. 1).

The number of shocks: The number of errors in 5Hz and 10Hz groups was significantly lower than that in Ctrl group and 1Hz group. The percentage of platform jumping increased significantly. There was no significant difference between 1Hz group and Ctrl group (Fig. 2a).

Avoidance latency: Compared with Ctrl group, the escape latency of 5Hz and 10Hz group increased significantly, the number of errors decreased significantly, and the

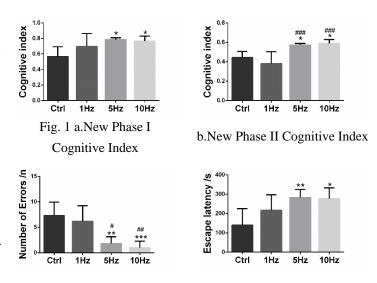
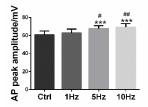


Fig. 2 a.Error times

b.Escape latency

percentage of jumping platform increased significantly. There was no significant difference at 1Hz (Fig. 2b).

Single action potential: On the peak value, compared with Ctrl group and 1Hz group, the 5Hz and 10Hz groups increased significantly(Fig. 3a), while the threshold and maximum rise slope did not change significantly. There was no significant difference between 1Hz group and Ctrl group.



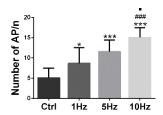


Fig. 3 a.Single action potential peak b.Number of action potentials

Action potential frequency: Compared with Ctrl group, the number of action potential increased significantly in 1Hz, 5Hz and 10Hz groups, but the difference was higher in 5Hz and 10Hz groups. The 10Hz group also increased significantly compared with 1Hz and 5Hz groups(Fig. 3b).

To explore the effects of different stimulus frequencies of rTMS on neuronal excitability. Combining new object recognition, platform jumping and electrophysiological experiments, the results show that high frequency (5Hz, 10Hz) rTMS improves the memory ability and neuronal excitability of mice, while low frequency (1Hz) rTMS has no obvious effect.

References

[1]Luber B, McClintock SM, Lisanby SH. Applications of transcranial magnetic stimulation and magnetic seizure therapy in the study and treatment of disorders related to cerebral aging[J]. Dialogues in Clinical Neuroscience. 2013, 15(1): 87-98.

[2]Francisco José Fernández-Gómez, Ana González-Cuello,Régis Bordet, et al. Cognitive impairment after sleep deprivation rescued by transcranial magnetic stimulation(TMS) application in octodon degus[J]. Neurotoxicity Research. 2015, 28(2): 95-184.

[3] Abrahamyan A, Clifford C, Arabzadeh E, et al. Low intensity TMS enhances perception of visual stimuli[J]. Brain Stimulation, 2015, 8(6): 1175-1182.

Cell biological effects of high static magnetic field and mechanism study

<u>Lei Zhang</u>^{1#}, Yubin Hou^{1#}, Qingping Tao^{1, 2}, Timothy J. Mitchison^{3*}, Qingyou Lu^{1, 2, 4*}, Xin Zhang^{1*}

¹High Magnetic Field Laboratory, Chinese Academy of Sciences, Hefei, Anhui, 230031, China;
²University of Science and Technology of China, Hefei, Anhui, 230026, China; ³Department of Systems
Biology, Harvard Medicine School, Boston, MA, 02115, USA; ⁴Collaborative Innovation Center of
Advanced Microstructure, Nanjing University, Nanjing, Jiangsu, 210093, China
*Corresponding authors: timothy_mitchison@hms.harvard.edu; qxl@ustc.edu.cn;
xinzhang@hmfl.ac.cn

1. Cell-type and density-dependent effect of 1 T static magnetic field on cell proliferation.

Increasing evidence shows that static magnetic fields (SMFs) can affect cell proliferation [1-3] but mixed results have been reported. Here we systematically examined the effects of 1 T (Tesla) SMF, for its effect on 15 different cell lines, including 12 human and 3 rodent cell lines. Our results show that 1 T SMF does not have apparent impact on cell cycle or cell death. However, at higher cell density, it reduced cell numbers in six out of seven solid human cancer cell lines. We found that both cell type and cell density had evident impacts on SMF effects. Moreover, the EGFR-Akt-mTOR pathway, which varies significantly between different cell types and densities, contributes to the differential effects of SMF. In addition, SMF also increases the efficacy of Akt inhibitors on cancer cell growth inhibition[4].

2. Moderate and strong static magnetic fields directly affect EGFR kinase domain orientation to inhibit cancer cell proliferation.

Static magnetic fields (SMFs) can affect cell proliferation in a cell-type and intensity-dependent way[4] but the mechanism remains unclear. At the same time, although the diamagnetic anisotropy of proteins has been proposed decades ago[5-7], the behavior of isolated proteins in magnetic fields has not been directly observed. Here we show that SMFs can affect isolated proteins at the single molecular level in an intensity-dependent manner. Using Liquid-phase Scanning Tunneling Microscopy (STM) to examine pure EGFR kinase domain proteins at the single molecule level in solution, we observed orientation changes of these proteins in response to SMFs. A superconducting ultrastrong 9T magnet reduced proliferation of CHO-EGFR cells (Chinese Hamster Ovary cells with EGFR overexpression) and EGFR-expressing cancer cell lines by ~35%, but minimally affected CHO cells[8].

3. 27 T ultra-high static magnetic field changes orientation and morphology of mitotic spindles in human cells.

Purified microtubules have been shown to align along the static magnetic field (SMF) in vitro because of their diamagnetic anisotropy[9, 10]. However, whether mitotic spindle in cells can be aligned by magnetic field has not been experimentally proved. In particular, the biological effects of SMF of above 20 T (Tesla) have never been reported. Here we found that in both CNE-2Z and RPE1 human cells spindle orients in 27 T SMF. The direction of spindle alignment depended on the extent to which chromosomes were aligned to form a planar metaphase plate. Our results show that the magnetic torque acts on both microtubules and chromosomes, and the preferred direction of spindle alignment relative to the field depends more on chromosome alignment than microtubules. In addition, spindle morphology was also perturbed by 27 T SMF. This is the first reported study that investigated the cellular responses to ultra-high magnetic field of above 20 T. Our study not only found that ultra-high magnetic field can change the orientation and morphology of mitotic spindles, but also provided a tool to probe the role of

spindle orientation and perturbation in developmental and cancer biology[11].

References

- [1] C. Aldinucci, J.B. Garcia, M. Palmi, G. Sgaragli, A. Benocci, A. Meini, F. Pessina, C. Rossi, C. Bonechi and G.P. Pessina, Bioelectromagnetics, 24 (2003) 109-117.
- [2] R.R. Raylman, A.C. Clavo and R.L. Wahl, Bioelectromagnetics, 17 (1996) 358-363.
- [3] T. Nakahara, H. Yaguchi, M. Yoshida and J. Miyakoshi, Radiology, 224 (2002) 817-822.
- [4] L. Zhang, X. Ji, X. Yang and X. Zhang, Oncotarget, 8 (2017) 13126-13141.
- [5] J. Torbet, M.C. Ronziere, Biochemical Journal, 219 (1984) 1057-1059.
- [6] P.M. Vassilev, R.T. Dronzine, M.P. Vassileva and G.A. Georgiev, Bioscience Reports, 2 (1982) 1025-1029.
- [7] C. Guo, L.J. Kaufman, Biomaterials, 28 (2007) 1105-1114.
- [8] L. Zhang, J. Wang, H. Wang, W. Wang, Z. Li, J. Liu, X. Yang, X. Ji, Y. Luo, C. Hu, Y. Hou, Q. He, J. Fang, J. Wang, Q. Liu, G. Li, Q. Lu and X. Zhang, Oncotarget, 7 (2016) 41527-41539.
- [9] W. Bras, G.P. Diakun, J.F. Diaz, G. Maret, H. Kramer, J. Bordas, F.J. Medrano and Biophys J, 74 (1998) 1509-1521.
- [10] W. Bras, J. Torbet, G.P. Diakun, G.L. Rikken and J.F. Diaz, J Biophys, 2014 (2014) 985082.
- [11] L. Zhang, Y. Hou, Z. Li, X. Ji, Z. Wang, H. Wang, X. Tian, F. Yu, Z. Yang, L. Pi, T.J. Mitchison, Q. Lu and X. Zhang, Elife, 6 (2017).

Magnetic susceptibility difference-induced nucleus positioning in gradient ultra-high magnetic field

Qingping Tao^{1, 2#}, Lei Zhang^{1#*}, Xuyao Han³, Hanxiao Chen^{1,2}, Xinmiao Ji¹, Xin Zhang^{1,2,4*}

¹High Magnetic Field Laboratory, Key Laboratory of High Magnetic Field and Ion Beam Physical Biology, Hefei Institutes of Physical Science, Chinese Academy of Sciences, Hefei 230031, China;

²Science Island Branch of Graduate School, University of Science and Technology of China, Hefei 230026, China; ³School of Pharmacy, Anhui Medical University, Mei Shan Road, Hefei 230032, Anhui Province, China; ⁴Institutes of Physical Science and Information Technology, Anhui University, Hefei 230601, China;

Despite the importance of magnetic properties of biological samples for biomagnetism and related fields, the exact magnetic susceptibilities of most biological samples in their physiological conditions are still unknown. Here we used SQUID (Superconducting Quantum Interferometer Device) to detect the magnetic properties of non-fixed non-dehydrated live mice tissues, bacteria, proteins, as well as cell fractions, at a physiological temperature of 37 °C (310 K). Although most biological samples are diamagnetic, their magnetic susceptibilities are different, which depend on their composition and conditions. More importantly, within a single cell, although the magnetic susceptibility difference between cellular fractions (nucleus and cytoplasm) could only cause ~41-130 pN forces to nucleus by gradient ultra-high magnetic fields, these forces are enough to cause a relative position shift of the nucleus within the cell. This not only demonstrates the importance of magnetic susceptibility in the biological effects of magnetic field, but also illustrates the potential application of high magnetic fields in biomedicine.

Effects of 3.5–23.0 T static magnetic fields on mice: A safety study

Xiaofei Tian ^{1,2,#}, Dongmei Wang ^{1,3,#}, Shuang Feng ^{1,3}, Lei Zhang ¹, Xinmiao Ji ¹,

Ze Wang ^{1,4},Qingyou Lu ^{1,4,5}, Chuanying Xi ¹, Li Pi ¹, Xin Zhang ^{1,2,3,*}

¹ High Magnetic Field Laboratory, Key Laboratory of High Magnetic Field and Ion Beam Physical Biology, Hefei Institutes of Physical Science, Chinese Academy of Sciences, Hefei, Anhui, 230031, PR China; ² Institutes of Physical Science and Information Technology, Anhui University, Hefei, Anhui, 230601, PR China; ³ Science Island Branch of Graduate School, University of Science and Technology of China, Hefei, Anhui, 230026, PR China; ⁴ Hefei National Laboratory for Physical Sciences at Microscale, University of Science and Technology of China, Hefei, 230026, PR China; ⁵ Anhui Province Key Laboratory of Condensed Matter Physics at Extreme Conditions, Hefei, Anhui, 230031, PR China

*Corresponding author: xinzhang@hmfl.ac.cn (X. Zhang).

#These authors contributed equally to this work

People are exposed to various magnetic fields, including the high static/steady magnetic field (SMF) of MRI, which has been increased to 9.4 T in preclinical investigations. However, relevant safety studies about high SMF are deficient. Here we examined whether $3.5-23.0\,\mathrm{T}$ SMF exposure for 2 h has severe long-term effects on mice using $112\,\mathrm{C57BL/6J}$ mice. The food/water consumption, blood glucose levels, blood routine, blood biochemistry, as well as organ weight and HE stains were all examined. The food consumption and body weight were slightly decreased for $23.0\,\mathrm{T}$ -exposed mice (14.6%, P < 0.01, and 1.75-5.57%, P < 0.05, respectively), but not the other groups. While total bilirubin (TBIL), white blood cells, platelet and lymphocyte numbers were affected by some magnetic conditions, most of them were still within normal reference range. Although $13.5\,\mathrm{T}$ magnetic fields with the highest gradient ($117.2\,\mathrm{T/m}$) caused spleen weight increase, the blood count and biochemistry results were still within the control reference range. Moreover, the highest field $23.0\,\mathrm{T}$ with no gradient did not cause organ weight or blood biochemistry abnormality, which indicates that field gradient is a key parameter. Collectively, these data suggest $3.5-23.0\,\mathrm{T}$ static magnetic field exposure for $2\,\mathrm{h}$ do not have severe long-term effects on mice.

1 T Static Magnetic Field Regulated Serotonin Secretion and Behavior in Caenorhabditis elegans via TRPV1 Receptor

Lei Cheng 1, 2, An Xu 1, 2'*

¹ University of Science and Technology of China, Hefei, Anhui 230026, PR China
² Key Laboratory of High Magnetic Field and Ion Beam Physical Biology, Chinese Academy of Sciences, Anhui Province Key Laboratory of Environmental Toxicology and Pollution Control Technology, Hefei Institutes of Physical Science, Chinese Academy of Sciences, Hefei, Anhui 230031, PR China

Email: anxu@ipp.ac.cn

Static magnetic field (SMF) is a ubiquitous environmental factor for all living organisms during the evolution process. Acute and chronic exposure of organisms to SMFs, which are often ten and more times greater than geomagnetic field, have been investigated for decades. However, the exact mechanism(s) underlying the influence of SMF on living systems are still largely unknown. The nematode Caenorhabditis elegans (C. elegans) as a well-established model system has many unique characteristics and distinct advantages in the discovery of fundamental biological responses in development, neurobiology and aging. We found that SMFs at either 0.5 T or 1 T had no significant effects on the movement behaviors, including body bends and head thrashes, in C. elegans; however, the avoidance behavior of the pathogenic Pseudomonas aeruginosa was greatly decreased in exposed worms. Since behavioral changes are affected by the level of neurotransmitter secretion, we further examined the secretion of five classical neurotransmitters including GABA, serotonin, acetylcholine, dopamine and glutamate in C. elegans. Exposure to 1T SMF dramatically increased the secretion of serotonin via TRPV1 receptor and receptor SRE-1 and MOD-1. There were minimal effects of SMF on the secretion of other four neurotransmitters. Our results showed that long term exposure to 1T SMF increased the serotonin secretion via the activation of TRPV1 receptor, which in turn induced avoidance behavior deficit in C. elegans. This study provides novel insights into safe application of SMF as a neurotransmitter regulator to prevent related diseases in the presence or absence of drugs.

Key words: SMF, behavior, serotonin, neural response, TRPV1 receptor, C. elegans

Acknowledgements

Thanks for the Major/Innovative Program of the Development Foundation of the Hefei Center for Physical Science and Technology (2017FXZY005).

Rotating Magnetic Field Ameliorates Experimental Autoimmune Encephalomyelitis by Promoting T cell Peripheral Accumulation and Regulating the Balance of Treg and TH1/TH17

Tianying Zhan¹*, Xiaomei Wang¹*, Zijun Ouyang¹, Youli Yao¹, Jiangyao Xu¹, Shikang Liu¹, Kan Liu¹, Qiyu Deng¹, Yushu Wang¹, Yingying Zhao¹#.

¹ Base for International Science & Technology Cooperation: Carson Cancer Stem Cell Vaccines R&D Center, Department of Physiology, School of Basic Medical Sciences, Xili campus of Shenzhen University, Keyuan Ave 1066, Shenzhen, Guangdong, China.

Multiple sclerosis (MS) is an autoimmune disease characterized by T cell infiltration and demyelination of the central nervous system (CNS). Experimental autoimmune encephalomyelitis (EAE) is the classic preclinical animal model of MS. In this study, we found that RMF treatment has potential preventive effects on the discovery of EAE, including reducing the severity of the disease and delaying the onset of the disease. The results indicate that RMF (0.2 T, 4 Hz) treatment increases the accumulation of CD4⁺ cells in the spleen and lymph nodes by down-regulating the expression of CCL-2, CCL-3 and CCL-5, but has no significant effect on MOG-specific T cell responses. Simultaneously, RMF treatment adjusted the imbalance between treg cell and Th1/Th17 cell by increasing the proportion of regulatory

T (Treg) cells and inhibiting the ratio of T helper 1 (Th1) and T helper 17 (Th17) cell subsets. These findings suggest that exposure to RMF may improve EAE disease by promoting CD4⁺ cells to peripheral lymphoid tissue accumulation and improving the imbalance between treg and Th1/Th17, and as a mild physical therapy approach, RMF, is likely to be a potential way to change the development of EAE.

Effects on longevity extension and mechanism of action of 4 Hz rotating magnetic field in C. elegans and HUVEC

Jiangyao Xu¹, Xiaoyun Zhang², Xiaomei Wang¹*

¹ Department of Physiology, School of Basic Medical Sciences, Shenzhen University, Shenzhen 518060, P. R. China; ² College of Life Science and Oceanography, Shenzhen University, Shenzhen 518060, People's Republic of China.

*Corresponding email address: xmwang@szu.edu.cn

Magnetic biological effects are a research hotspot in the field of biomedical engineering. This study will further investigate the effects of rotating magnetic field RMF (0.2 t, 4 Hz) on the growth of *C. elegans* and human umbilical vein endothelial cells (HUVEC). In the present study, RMF prolonged the lifespan of *C. elegans* and slowed the aging of HUVEC cells. RMF treatment of HUVEC cells showed that activation of Adenosine 5'-monophosphate (AMP)-activated protein kinase (AMPK) was associated with decreased mitochondrial membrane potential due to increased intracellular Ca2+ concentration induced by endoplasmic reticulum stress in anti-aging mechanisms. At the same time, RMF promotes the health of *C. elegans* by improving activity, reducing the accumulation of age pigments, delaying Aβ-induced paralysis and increasing resistance to heat and oxidative stress. The prolonged lifespan of C. elegans is associated with decreased levels of daf-16-associated insulin/insulin-like growth factor signaling pathway (IIS) and reactive oxygen species (ROS), whereas the heat shock transcription factor-1 (hsf-1) pathway is not participate. At the same time, the level of autophagy was increased after RMF treatment. These findings will help us expand our understanding of the potential RMF mechanisms during life extension.

Vascular Remodeling of Veins is Suppressed by Low Frequency Rotating Magnetic Field

Kan Liu ^{1†}, Jiangyao Xu¹, Peng Zhai¹, Xiaoyun Zhang², Xiaomei Wang^{1*}

¹ Department of Physiology, School of Basic Medical Sciences, Shenzhen University, Shenzhen 518060, P. R. China; ² College of Life Science and Oceanography, Shenzhen University, Shenzhen 518060, People's Republic of China.

*Corresponding email address: <u>xmwang@szu.edu.cn</u>

The chronic increase in venous wall stress or biomechanical stretch is sufficient to cause

development of varicose veins. The term chronic venous insufficiency (CVI) is often used to functionally describe the full spectrum of venous diseases such as development of varicose veins, suitable non interventional therapies for these venous diseases have not been explored to date. In this study, we treated mouse auricle models with low frequency rotating magnetic field (LFRMF, 0.2t, 4Hz) and evaluated therapeutic effect by laser speckle contrast imaging. We found that daily imaging of vasculature of the mouse auricle for 3 days after ligation of a central vein revealed increased tortuosity and growth of connected small collateral veins. At the same time, laser speckle contrast imaging showed that blood flowing decreased by systemic administration by LFRMF. These findings imply that low frequency rotating magnetic field effectively inhibit the development of varicose veins.



北京原力辰超导技术有限公司,简称**原力超导**,始建于2014年,是国家高新技术企业。原力超导在高温超导器件设计制造、低频电磁场计算仿真方面有强大的技术力量,致力于超导技术在新材料、电力、生物医疗等领域的创新应用。



QML 超导量子悬浮



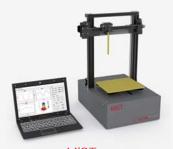
Tesla-Shielding 磁场屏蔽系统



MCorder 高温超导带材临界电流 均匀性测试系统



MTS-HT 可视化77K力电耦合测试系统



MIST 磁场时空成像系统



MCFF 磁控编队地面模拟器平台



MagT 超导材料、磁性材料 低温相变检测系统



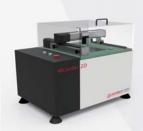
CCwin 智能绕线机



EF-721 数据采集卡



M4 磁性材料综合测试仪



MCorder 2D 扫描磁探针显微镜



MACF 超导交流测试平台



Beijing Eastforce Superconducting Technology Co., Ltd.

地址:北京市海淀区安宁庄西路15号院20号楼116 电话: +86-10-82833850

传真: +86-10-82833850 网站: http://www.eastfs.com Email: contactus@eastfs.com

MAGVISION KERR SYSTEM

高分辨率磁光克尔显微镜

High resolution imager

高分辨率成像

- 6.4 megapixels @ 60 FPS
- 78% quantum efficiency
- Real-time differential imaging with noise suppression

Patented electromagnet design

专利电磁铁设计

- 0.5% field uniformity over 4 mm
- Up to 1 T without chiller
- 8X reduced Faraday effect

Piezo actuated 5-axis stage

压电驱动5轴位移台

- Fully automatic sample stabilization for long exposures
- Software-controlled piezo actuation for remote control

Ultrabright 2200 lumens LED

超亮2200流明LED

- Narrow bandwidth for high sensitivity 50 nm FWHM
- Enables fast exposures for real-time domain viewing

Graphic User Interface

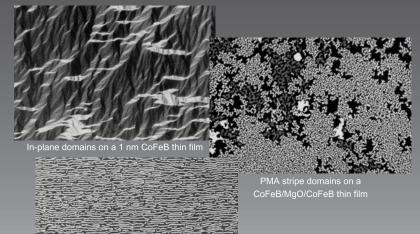
图形用户界面

- Fully automated measurements
- Integrated interfacing with SCPI instruments for *in situ* electrical measurements

3D Image Stabilization

3D影像稳定

- Fully automatic real-time image stabilization
- Both hardware and software corrections
- Reduces drift to less than 0.2 pixel (8 nm)





Sample excitation

样品激发

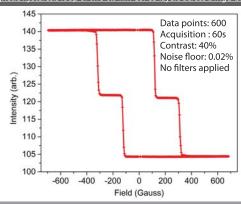
- Compatible with micromanipulators for DC/ RF probing
- Interchangeable 10-pad chip carrier stage for wire bonding

Extreme Sensitivity

极度敏感

- · Optimized light path design
- Exhaustively tested optical components ensure clean magnetic signal

Magnetic hysteresis loop of two 0.9 nm CoFeB layers across a MgO barrier



销售及售后咨询 Vertisis Technology Pte Ltd www.vertisis.com.sq



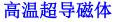


西安聚能超导磁体科技有限公司

高端特种异形超导磁体顶级设计制造商

加速器用超导磁体













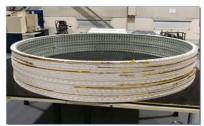










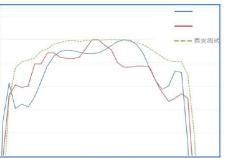




制冷机直接冷却超导磁体(1-16T)



磁体外观图



磁场数据比较

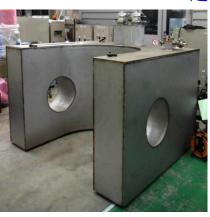








MCZ超导磁体





www.c-xsmt.com

lichao029@c-wst.com

18710781512 Tel:

029-83662840 Fax:

凝聚 自信 拼搏 创新

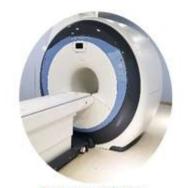
Shanghai Yuanxi Medical Technology Co,. Ltd



强磁场生命科学的探索者

Explorer of High magnetic field life sciences

我们的产品 **Products**



紹导强磁场 Superconducting magnet



旋磁治疗系统 Gyromagnetic system



专业产后康复 Postpartum rehabilitation



肛肠治疗系统 Anorectal treatment

为生命科学研究提供强磁场实验环境及强磁场医疗设备

Providing high magnetic fields environment and medical equipment for life sciences research

> 探索的领域 Research Field

强磁场生物学效应

新型强磁体

疾病治疗

Biological effects

Superconducting magnet Disease treatment

渊兮医疗 上海市奉贤区仁齐路159号3号楼101室

Room 101, Building 3, No. 159, Rengi Road, Fengxian District, Shanghai For more information contact with +86 13661642846 or huaiguotht@163.com

严重失眠 Severe insomnia

心脑血管疾病 Cardiovascular disease

高原反应 Altitude sickness

肿瘤 Tumor

骨质疏松 Osteoporosis

Fatigue syndrome

Nervous system disease





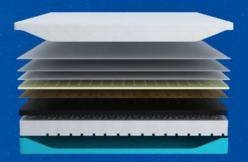
HEYE BEALTH TECHNOLOGY

磁生物学研究

MAGNETIC BIOLOGY RESEARCH

公司先后与中科院上海生命科学研究院、中科院上海生化细胞研究所、中科院合肥物质科学研究院强磁场中心、浙江大学、四川大学华西第四医院、天津医科大学、上海师范大学、纳米技术及应用国家工程研究中心、西北工业大学深圳研究院、浙江省医学科学院等高校院所开展了20余项磁生物学研究。

The company has successively carried out more than 20 magnetic biology researches with Shanghai Institutes for Biological Sciences, Shanghai Institute of Biochemistry and Cell Biology, High Magnetic Field Center of Hefei Institute of Physical Sciences, Zhejiang University, West China Fourth Hospital of Sichuan University, Tianjin Medical University, Shanghai Normal University, National Engineering Research Center for Nanotechnology and Applications, Shenzhen Institute of Northwestern Polytechnical University, Zhejiang Academy of Medical Sciences and other colleges and universities.



科技创新

TECHNOLOGICAL INNOVATION

截止2019年9月17日

- 授权专利 339 项
- 其中授权发明专利 87 项
- 实用新型专利 180 项
- 外观专利 62 项
- 国际专利 10 项
- 发表和也署名单位的论文 23 篇
- 参与专著编撰 1 部

As Of September 17, 2019

- Granted 339 patents
- Among them, <mark>87</mark> invention patents were authorized
- 180 Patents for utility models
- 62 Design patents
- 10 International Patents.
- Has published and signed 23 papers
- Participated in compiling 1 monograph



